UMS
UNIVERSITI MALAYSIA SABAH

BORNEO SCIENCE

The Journal of Science and Technology

ONLINE ISSN : 2231-9085 | ISSN : 1394- 4339

BORNEO SCIENCE

A JOURNAL OF SCIENCE AND TECHNOLOGY

BORNEO SCIENCE is a journal of science and technology published twice a year. It publishes original articles on all aspects of research in science and technology of general or regional interest particularly related to Borneo. Manuscripts submitted must not have been published, accepted for publication, or be under consideration elsewhere. Borneo Science welcomes all categories of papers: full research papers, short communications, papers describing novel methods, review papers and book reviews. Views expressed in the articles do not represent those of the Editorial Board and the University.

BORNEO *SCIENCE* *merupakan jurnal sains dan teknologi yang diterbitkan dwitahunan. Jurnal ini menerbitkan artikel asli dalam kesemua bidang sains dan teknologi secara umum mahupun dalam kepentingan serantau, terutamanya yang berkaitan dengan Borneo. Manuskrip yang dihantar bukan yang telah diterbitkan, telah diterima untuk diterbitkan, atau sedang dipertimbangkan untuk diterbitkan. Borneo Science mengalu-alukan semua jenis kertas kerja sama ada hasil penyelidikan, komunikasi pendek, penjelasan suatu kaedah, ulasan kertas kerja atau ulasan buku. Pandangan yang ditulis dalam artikel Borneo Science tidak menggambarkan pendapat Sidang Editor dan Universiti.*

DOI: https://doi.org/10.51200/bsj.v45i2.5877

BORNEO SCIENCE
A JOURNAL OF SCIENCE AND TECHNOLOGY

BORNEO SCIENCE

A JOURNAL OF SCIENCE AND TECHNOLOGY

ONLINE ISSN 2231-9085 | ISSN 1394-4339

BORNEO SCIENCE

A JOURNAL OF SCIENCE AND TECHNOLOGY
JURNAL SAINS DAN TELNOLOGI

Volume 45 Issue 2

Disember 2024

CONTENT
KANDUNGAN

Page
Muka
Surat

ORIGINAL ARTICLES

BorneoScience
The Journal of Science & Technology
Volume 45 Issue 2 : Sept 2024
Online ISSN : 2231-9085 | ISSN : 1394-4339

UNLOCKING THE POTENTIAL OF JUNIOR RANGERS: STRENGTHENING CAPACITIES FOR EFFECTIVE FOREST BIODIVERSITY CONSERVATION AND NATURE-BASED COMMUNICATION

Huda Farhana Mohamad Muslim[1], Norliyana Adnan[1] & Mohd Parid Mamat[1]

[1] Social Forestry Programme,
Forest Research Institute Malaysia, 52109 Kepong, Selangor

**Corresponding author E-mail: hudafarhana@frim.gov.my*

Received 24th April 2024; Accepted 28th Nov 2024
Available online: 31st December 2024
Doi: https://doi.org/10.51200/bsj.v45i2.6009

ABSTRACT. *Forests are vital for our well-being, providing shelter, livelihoods, water, and food, while also promoting environmental stability, conserving biodiversity, and enhancing quality of life. Effective management of tropical rainforests is crucial for maximizing benefits to local communities, which depends significantly on their socio-economic conditions. In Asia, many forested areas operate under informal customary tenure systems, leading to increased pressure to formalize these arrangements in response to growing demands for secure forest management. Community forestry, or social forestry as it is known in Malaysia, has demonstrated that local communities can sustainably manage forests and reap significant benefits when enabled. An exemplary initiative is the Sahabat Alam Tampik Janda Baik Association in Pahang, which established the Tampik Junior Rangers, a program that empowers youth as nature guides and promotes conservation. Additionally, community-based ecotourism (CBET) balances local needs with environmental preservation and enhances the quality of life for hosts. By fostering early experiences in nature, particularly through programs like the Junior Rangers, children develop a stronger connection to their environment, which is essential for future conservation efforts. This research focuses on educating and empowering rural school children in natural resource conservation through hands-on training and community engagement, enriching their skills and knowledge in forest survival and responsible stewardship.*

KEYWORDS. Human-nature interactions, junior rangers, local community, community-based ecotourism, extinction of experience.

INTRODUCTION

Forests play a crucial role in providing shelter, livelihoods, water, and food, significantly contributing to our overall well-being both directly and indirectly. Their indirect functions include ensuring environmental stability and quality, safeguarding soil and water resources, preserving biodiversity, and enhancing the quality of life for individuals. Effective management of tropical rainforests is vital to maximize benefits for local communities and rural populations, as their socio-economic conditions heavily influence sustainable forest management outcomes. In Asia, large forested regions are mainly governed by informal customary tenure systems, widely accepted in local contexts. The rising demand for secure and reliable management of forests and traditional lands has intensified calls for many countries to formalize these informal tenures within legal frameworks. Community forestry, often referred to as social forestry in Malaysia, has yielded valuable insights, demonstrating that local communities can sustainably manage forests and reap significant rewards when given the right conditions. Increasing attention is being given to the role of local communities in forest conservation, as forests and their resources remain essential for sustaining livelihoods (Mukul et al., 2016), serving not only those who inhabit them but also individuals living in surrounding areas. Various initiatives have been developed to combat habitat destruction in forest ecosystems, including empowering community participation.

The ecotourism and travel sector must adopt more environmentally sustainable practices, such as protecting tropical rainforests, preserving cultural heritage at travel destinations, and actively fostering the economic growth of local communities. These initiatives can create a balanced relationship between tourism and the environment, ensuring the long-term health of both. Community-based ecotourism (CBET) presents a groundbreaking approach that reduces the environmental impact of tourism while aligning the interests of local populations with those of nature. Involving young children in the benefits of CBET is crucial, as community engagement is closely linked to conservation efforts. A significant example in Malaysia is the Sahabat Alam Tampik Janda Baik Association in Pahang, which has initiated the Tampik Junior Rangers, a group of young nature guides committed to conservation in their area. This project illustrates the positive results that can arise when local communities are empowered to participate in sustainable forest management.

Regrettably, many individuals, especially children, are increasingly losing their connection with nature, a trend termed "the extinction of experience." For many in today's world, traditional outdoor activities are being replaced by virtual options (Clements, 2004; Pergams & Zaradic, 2006; Hofferth, 2009; Ballouard et al., 2011). The primary cause of this disconnect is the decline in opportunities for authentic nature experiences (Soga et al., 2016; Sun et al., 2023). Early encounters

with nature play a crucial role in shaping environmental perceptions and directing people towards conservation initiatives. In light of the potential risks associated with detachment from the natural world, the Tampik Junior Rangers program at Ulu Tampik Waterfall effectively promotes strong, enduring bonds between local communities and their protected environments. This study aims to (i) educate and empower the public—particularly rural school children—to actively engage in natural resource conservation and (ii) elevate public awareness and participation in conservation efforts through initiatives like the Tampik Junior Rangers (TJR).

MATERIALS AND METHODS

This research was conducted at Ulu Tampik Waterfall (UTW), located in Compartment 51 of the Lentang Forest Reserve in Malaysia, with active involvement from children aged seven to fourteen who reside in or near the protected area (Figure 1). UTW and its surroundings constitute a conserved region, being one of the protected forests in Peninsular Malaysia. This area is home to a key species of local endemic trees, which are vital for the ecosystem's floral and faunal diversity, as well as for various bird species that depend on it. The environment offers a unique and exciting recreational space, highlighted by the distinctive features of the waterfall and its pristine waters (Amirnodin, 2020). The UTW and its vicinity are popular leisure destinations for residents of Janda Baik, as well as visitors and tourists from other regions and countries.

Ecotourism is a conservation strategy that can be employed to sustainably protect the diversity of biological resources; it aims to minimize its environmental impact and is ecologically responsible, avoiding the detrimental effects associated with large-scale tourism developments. The junior rangers program actively engages young children aged seven to fourteen living in or near the protected area. Research teams carried out a rapid rural appraisal (RRA), conducted focus group discussions with scientists and experts to develop an appropriate module, and implemented hands-on capacity building through short courses in environmental interpretation. Additionally, they provided on-site training in nature communication and arranged study tours to other protected or ecotourism areas.

As of April 2020, this area was within the Use Permit area, operated by the local society, an association known as Persatuan Sahabat Alam Tampik Janda Baik (SATJB). The society was the official registered society under The Registry of Societies Malaysia (ROS), managed by the local communities, and the land was a protected water catchment area. The SATJB initiated the establishment of TJR to enhance the support for the environmental conservation of UTW.

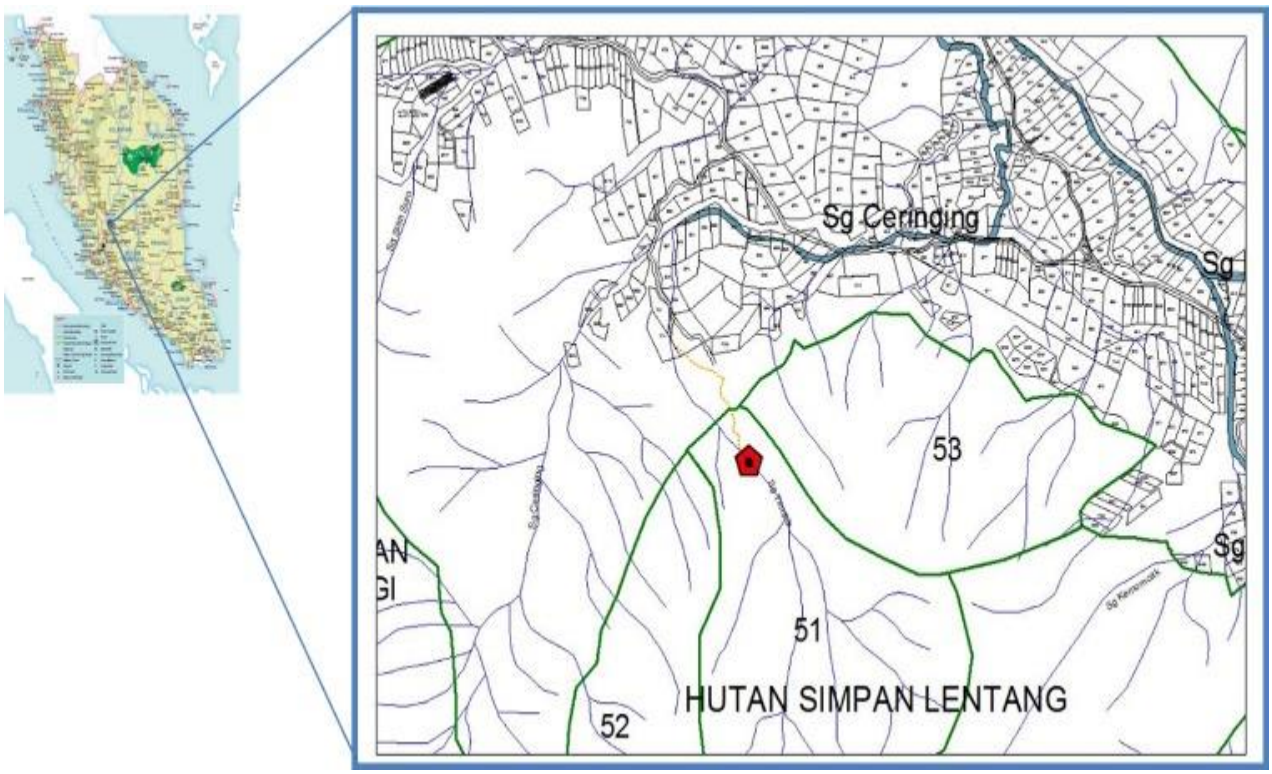

Figure 1. Map of Ulu Tampik Waterfall (UTW) indicating the project's site location.

RESULTS AND DISCUSSION

Junior rangers have been trained and gained experience as skilled young nature guides and environmental interpreters. This initiative has familiarized these young participants with the importance of preserving natural resources. The program is available to schoolchildren and operates on a voluntary basis. They underwent training on-site as local nature guides, fostering connections with their communities while learning new skills, as well as gaining knowledge in risk management and emergency procedures, all of which contributed to their understanding of forest survival. The training and capacity-building module consisted of three distinct series, each with a specific focus. Figure 2 illustrates the capacity-building series that involved children aged seven to fourteen living in or near the protected area. By 2023, the program had reached a total of twenty-five (25) junior members (see Figure 3).

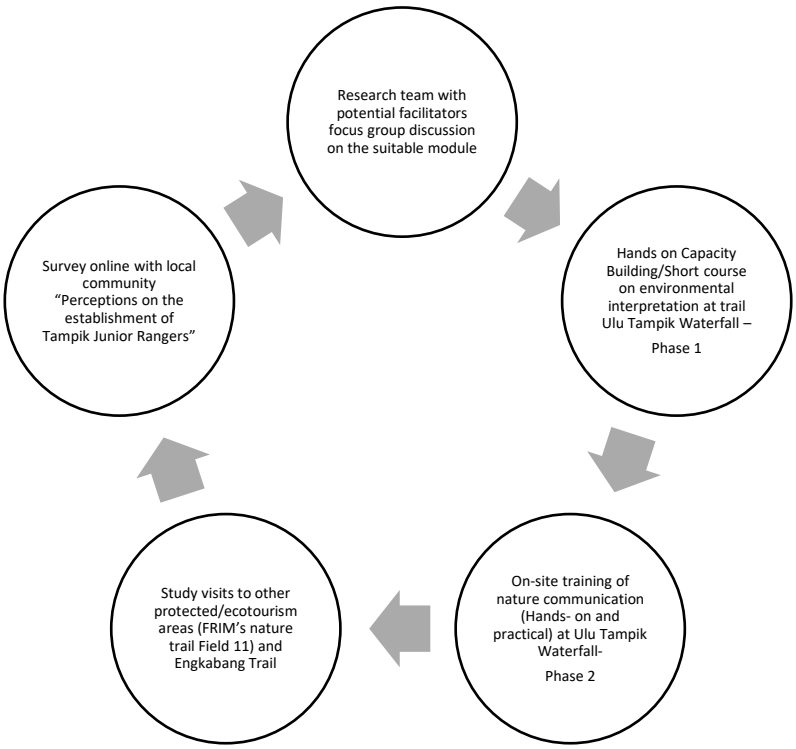

Figure 2: The community development via the Tampik Junior Rangers (TJR) from 2022 to 2023.

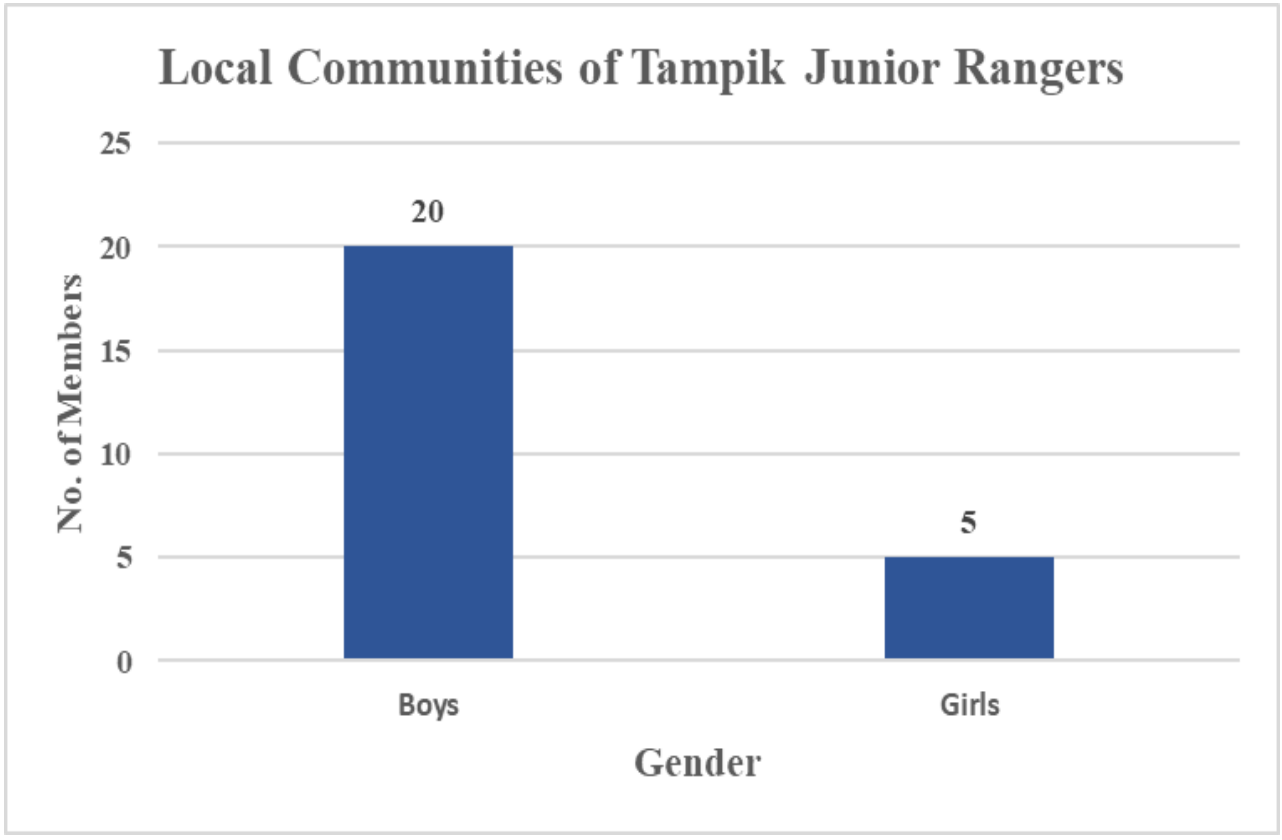

Figure 3: Number of members in the Tampik Junior Ranger for 2023.

The initial series consisted of a workshop aimed at training the TJR in environmental interpretation. This workshop took place from August 6 to 7, 2022, in Kampung Janda Baik and was organized in collaboration with the local community and the SATJB- Tampik Janda Baik Friends of Nature Association. During this first series, the junior rangers were given group tasks aligned with four different storytelling themes. In the "Oh My Trees!" activity, participants planted five trees, which were subsequently monitored according to the guidelines in the Tree Planting Eco Kit. Each junior ranger was also assigned specific practical tasks tailored to hands-on training in the field. This practical session was conducted along the Ulu Tampik Waterfall trail in the Lentang Forest Reserve. Instructors and facilitators provided participants with information about selected forest trees, including bamboo, as they trekked to the peak of the waterfall at Tier Five. Utilizing the knowledge gained, particularly about five specific species of forest trees, the junior rangers interpreted and presented their findings during the closing session in the "Let's Hear My Stories" segment.

The community development program "Oh My Forests" (Series 2), held on December 3, 2023, introduced junior rangers to two key components. The first component focused on educating the junior rangers about the ethics of being a tourist nature guide. The second element was the “What and Who is the Trees” segment, which trained the junior rangers to identify tree species such as Meranti Bukit, Perah, and Pulai, as well as various types of bamboo. Their understanding and skills were assessed through a presentation at the end of the series themed "Listen to...Trees, Nature, and Us."

Series 3 of community development included a learning visit to the FRIM campus on March 7, 2023, where participants explored attractions like the Keruing trail, crown shyness, and Field 11. This series featured 13 junior rangers and two FRIM nature guides, providing an opportunity for knowledge exchange regarding the dos and don’ts of being a nature guide and the ethical responsibilities that come with it. The visits also offered insights into forest tree species along the Engkabang trail and crown shyness, which are among FRIM’s main attractions.

The efforts of TJR have been gathered and published in a module centred on forest conservation. This module is specifically tailored to engage and educate young participants through a variety of interactive and informative sections. It comprises six main modules, starting with Module 1, titled “Who Am I,” which serves as an interactive game for introductions and ice-breaking among participants. Next, "Storytelling on the Forest and Local Traditions of My Villages" delves into the rich heritage and ecological significance of forests. Module 2 introduces a quiz and an environmental game called "Magic Bag, What Is That..." to make learning enjoyable and engaging. In Module 3, "Let's Story," themed "Story with Nature," participants are encouraged to creatively express themselves while gaining a deeper appreciation of natural ecosystems. Module 4 centres around

practical activities at the UTW trail, titled "Woody Walk and Hunt," which includes field-based storytelling activities and environmental interpretation concerning trees, natural resources, and their relationship with the local community. Module 5 focuses on training junior rangers to become nature guides for trail activities, which involves practical instruction and interactive information sharing with visitors. This segment includes jungle trekking to the UTW, allowing junior rangers to learn about key tree species and flora habitats along the trails. Finally, Module 6, "Oh My Trees," emphasizes tree planting strategies, highlighting the significance of reforestation and hands-on conservation efforts.

CONCLUSION

Tampik Junior Rangers (TJR) is a volunteer-based program designed for young schoolchildren. Founded as part of a local community initiative in Kampung Janda Baik, Bentong, Pahang, this guide group operates under the mentorship of FRIM researchers to involve the local community in preserving and conserving forest resources. The formation of the TJR initiative aims to bolster support for environmental conservation at UTW and to educate juniors and schoolchildren about the importance of safeguarding natural resources.

With ongoing backing from the Forest Research Institute Malaysia (FRIM) as a technical advisor for the community-based ecotourism project (CBET), a variety of activities have been organized. This exposure is intended to positively influence young schoolchildren's attitudes toward nature conservation and help them develop engaging conservation messages that connect them with local ecosystems.

The establishment of the junior rangers has enhanced their communication skills regarding forests and natural resources through a series of three distinct community development programs. The training journey of the junior rangers—as well as their capacity building and site visits—has been compiled into published guideline materials. This initiative represents a best practice for merging science and forestry to promote sustainability. The guidelines offer an updated framework and measurable steps for establishing junior ranger groups in other forests and protected areas. Participating in the program gives participants a sense of purpose, highlighting their role and the impact of their actions on their environment.

Additionally, it facilitates the development of strong interpersonal skills, which are valuable in various aspects of life, including education, recreation, business, and community relations. Overall, the junior rangers' program serves to close the communication gap between scientists and the public, particularly within forest communities, contributing to a more sustainable future.

ACKNOWLEDGEMENTS

The research discussed in this paper received funding from The Habitat Foundation of Sustainable Tourism Grants (Grant No. STG-20220525/23). The first author would like to express heartfelt gratitude to the local community of Kampung Janda Baik, particularly the members of Sahabat Alam Tampik Janda Baik (SATJB), as well as the scientists, researchers, and support staff including Faten Naseha Tuan Hussain, Muhammad Al Amin, and Ridzuan A Rahman; the Social Forestry Program (SFP) team members Nik Azyyati Abdul Kadir, Azahari Mohd Yusof, Naimah Che Long, and Siti Suhaila Abd Rahman; and the Environmental Education Branch at FRIM for their invaluable assistance and support throughout the fieldwork for this study.

REFERENCES

Amirnordin. (2020, October 2021). *Sahabat Alam Tampik pelopor pelancongan komuniti*. Retrieved from https://sahih.com.my/sahabat-alam-tampik-pelopor-pelancongan-komuniti/. accessed on 10th October 2023.

Ballouard, J. M., Brischoux, F., & Bonnet, X. (2011). Children prioritize virtual exotic biodiversity over local biodiversity. *PloS one*, *6*(8), e23152.

Clements, R. (2004). An investigation of the status of outdoor play. *Contemporary issues in early childhood*, *5*(1), 68-80.

Hofferth, S. L. (2009). Changes in American children's time–1997 to 2003. *Electronic international journal of time use research*, *6*(1), 26.

Mukul, S. A., Rashid, A. M., Uddin, M. B., & Khan, N. A. (2016). Role of non-timber forest products in sustaining forest-based livelihoods and rural households' resilience capacity in and around protected area: a Bangladesh study. *Journal of Environmental Planning and Management*, *59*(4), 628-642.

Pergams, O. R., & Zaradic, P. A. (2006). Is love of nature in the US becoming love of electronic media? 16-year downtrend in national park visits explained by watching movies, playing video games, internet use, and oil prices. *Journal of environmental Management*, *80*(4), 387-393.

Soga, M., Gaston, K. J., Yamaura, Y., Kurisu, K., & Hanaki, K. (2016). Both direct and vicarious experiences of nature affect children's willingness to conserve biodiversity. *International journal of environmental research and public health*, *13*(6), 529.

Sun, Y., Lu, X., Cui, J., Du, K., & Xie, S. (2024). Effects of vicarious experiences of nature, environmental beliefs, and attitudes on adolescents' environmental behavior. *Environmental Education Research*, *30*(6), 926-940.

BorneoScience
The Journal of Science & Technology
Volume 45 Issue 2 : Sept 2024
Online ISSN : 2231-9085 | ISSN : 1394-4339

FOREST FOR DOMESTIC WATER CATCHMENT OF GUNUNG TEBU FOREST RESERVES, TERENGGANU

Norliyana Adnan and Mohd Parid Mamat

[1]Social Forestry Programme, Research Planning Division
Forest Research Institute Malaysia (FRIM), 52109 Kepong, Selangor.

Received 24th April 2024; Accepted 28th Nov 2024
Available online: 31st December 2024
Doi: https://doi.org/10.51200/bsj.v45i2.5877

ABSTRACT. *Forests play an important role as water catchments for all downstream demands, such as domestic, industrial, and agricultural use. They provide not only quantity of water but also good-quality clean water. Forests help prevent impurities from entering streams, lakes, and groundwater in several ways. This process is called water purification but occurs naturally. The objective of this paper is to evaluate the importance of forest reserves, specifically the Gunung Tebu Forest Reserve (FR) in Besut, Terengganu, as a water catchment, especially for domestic use. Data on Bukit Bunga Water Treatment Plants (WTP) intakes, cost information, and forest land uses from the National Forest Inventory V (NFI V) are the main inputs for the analysis. Results show that the overall average marginal value for Gunung Tebu FR is RM297.24/ha/year. This value can be used to consider the operational cost implications of WTPs for the water purification services provided by the FR. A comparative analysis of the water catchment for Bukit Bunga WTP covers an area of 6,456.4 ha, of which approximately 88.6% is the Gunung Tebu FR. Therefore, the conservation of forest reserves as water catchment areas is important to ensure the availability of clean water, especially for domestic use.*

KEYWORDS. Watershed, domestic water used, ecosystem services

INTRODUCTION

Forests are recognized as an important source of water supply for industry, agriculture, households, and recreational purposes. Most of the clean water supply comes from rain that is filtered through forests and ends up in rivers. Forests help prevent contaminants from entering rivers, lakes, and groundwater in a number of ways. This process is called water purification. Forested areas and landscapes with trees also act as natural filters, reducing soil erosion and water sedimentation, thus providing high-quality water for human consumption and industry (Unasylva, 2019). The benefit is that clear water from forests in water catchment areas tends to reduce the cost of water treatment. Water purification ecosystem services are one of the natural services provided by ecosystems, especially forest ecosystems. It is categorized as a regulating service. The Millennium Ecosystem

Assessment (2005) also explains the role and function of this ecosystem for life. This service has a strong connection to the balance of human well-being, especially concerning issues of safety (the safety of clean water), disasters, sufficient resources, and life and health needs.

Among the earliest economic studies in the 1980s confirmed that the operating costs of water treatment plants are low when the water source is clean (Foster ***et al***., 1987; Moore and McCarl, 1987). Other studies show that improving the quality of the water source allows the utility to use a simpler treatment process to avoid large costs (Spiller *et al*., 2013). A prime example is the City of New York, which states that the utility can save multi-billion costs for a new treatment plant by utilizing the Catskills basin ecosystem (Chichilnisky and Heal, 1998). A study conducted in tropical regions, which considered the environmental impact and changes in forests related to water treatment costs, was carried out in Thailand (Sthiannopkao *et al*. 2007) and focused on samples from just one treatment plant. Another study by Abdul Rahim and Mohd Shahwahid (2011) examined the effects on six water treatment facilities in Kelantan. Furthermore, Vincent *et al*. (2015) analyzed panel data from 21 plants in Perak, with a follow-up study in Pahang in 2016.

The essential contribution of these services, along with other primary ecosystem services, lies in the continuous provision of clean water resources. Therefore, the aim of this paper is to evaluate the role of Gunung Tebu Forest Reserve (FR) as a water catchment area for domestic use.

MATERIALS AND METHODS

Data

The data utilized for the analysis were obtained from various agencies. Coordinates for the Water Treatment Plant (WTP) and the intake points, along with information on raw water sources, were sourced from the local water operator in Terengganu. Only one Water Treatment Plant, the Bukit Bunga WTP, was selected from the Gunung Tebu watershed. A Digitized Elevation Model (DEM) with a spatial resolution of 90 meters was employed, which is available for free download from https://earthexplorer.usgs.gov. The DEM data serves as a representation of the earth's surface elevation. Additionally, data from the National Forest Inventory V (NFI V) were used as the foundational information on forest land use types within the study area. This NFI V data was published by the Forestry Department of Peninsular Malaysia as part of its fifth series. Information regarding Terengganu's forest land use, specifically the gazetted forests for water catchment, was obtained from the Terengganu Forestry Department.

Methodology

Data from the relevant plant were sourced from the state water supply management agency, Syarikat Air Terengganu Sdn Bhd (SATU). The information collected included the coordinates of the WTP intake points, the monthly total volume of treated water produced, and the monthly operational costs incurred by the WTP. Catchment boundaries for the WTP intakes were created using DEM data and the intake point coordinates, processed through the ArcSWAT module within ArcGIS software. This

module utilizes a specialized Soil and Water Assessment Tool (SWAT) model integrated with ArcGIS. The ArcSWAT module has gained global usage and is continuously updated to accommodate user analysis needs. The ArcSWAT extension and additional SWAT modules are available for free download at https://swat.tamu.edu/.

A GIS analysis was performed to determine the percentage of forest land use within the water catchment area, utilizing data from the National Forest Inventory V (NFI V). To evaluate the area designated for water catchment in relation to the WTP catchment, data layers were overlaid to calculate the total matched area. The assessment of the economic benefits provided by Gunung Tebu Forest Reserve for water purification services is based on the benefit transfer approach to economic models developed in Perak (Vincent et al., 2015). The econometric analysis of water treatment costs in Perak utilizes a comprehensive panel dataset alongside an examination of forest changes. This analysis is informed by theories regarding cost functions for assessing environmental input values (McConnell and Bockstael, 2005; Vincent, 2011; Freeman et al., 2014), as follows:

$$\ln(C_{it}) = \mathbf{L}_{iy}\boldsymbol{\beta} + \alpha \ln(q_{it}) + c_i + \theta_y + \theta_m + u_{it}$$

(Equation 1)

Where;

i :WTP, t :Time (years), y :Year, m :Month, C :Operating cost (RM) or chemical quantity (kg), L :Land use (% of WTP basin), q :Volume of treated water (m3), c, θ :Fixed effects, μ :Error term. Issues: heteroskedasticity, spatial and serial correlation, Moulton problem, endogeneity of q

RESULTS AND DISCUSSION

To identify the river basin that drains into the Bukit Bunga WTP intake, a GIS analysis was conducted to establish the basin boundaries. The analysis revealed that the total area of the WTP intake basin is 9,062.91 hectares, of which 7,286.01 hectares fall within the Gunung Tebu Forest Reserve area (Figure 1). Sungai Angga, located within the Gunung Tebu FR, flows into Sungai Besut and subsequently reaches the Bukit Bunga WTP intake.

The water treatment process necessitates the use of various chemicals, each serving a specific function to achieve the desired water quality prior to distribution for domestic use. These chemicals include lime, liquid chlorine, sodium fluoride, liquid alum, and other reagents. Typically, the treatment process begins with filtering raw water at the intake to remove initial solid impurities. The water then moves to an aeration tank (aerator) to increase oxygen levels and eliminate any undesirable odors and flavors before the appropriate dose of liquid alum is added to aid in subsequent treatment steps. After filtration, liquid chlorine and sodium fluoride are introduced to adjust the pH to acceptable levels. Overall, the operating costs encompass four main components: chemical expenses,

electricity, maintenance costs, and employee salaries. The average operating cost for the Bukit Bunga WTP was 14.86 sen/m^3 in 2019 and 14.53 sen/m^3 in 2020.

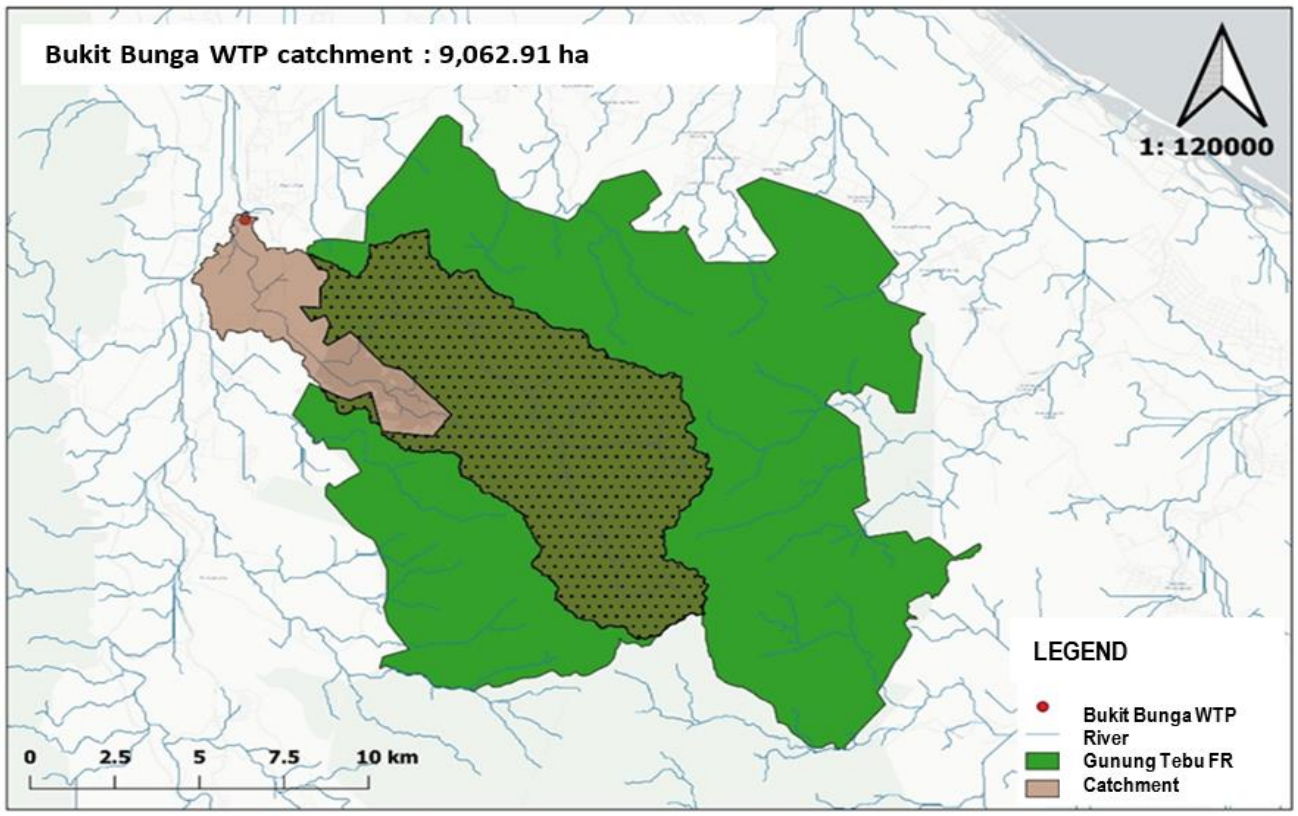

Figure 1. Delineation of the Bukit Bunga WTP catchment area within the Gunung Tebu Forest Reserve

Forest land use data from the NFI V was evaluated for the Bukit Bunga WTP catchment. This assessment is crucial as it demonstrates how forest land uses within the catchment area affect water treatment costs at the WTP. The catchment size, percentage of forest land use, and treatment costs were utilized to calculate the marginal value of water purification services. In terms of forest composition, the virgin forest occupies 3,793.33 hectares (52.5%), while logged forest covers 2,878.83 hectares (39.8%) (Table 1). Additionally, other areas, including water bodies and non-forest regions, total 560.58 hectares (7.75%).

Table 1. NFI V strata at Gunung Tebu FR

Forest Strata	Area (ha)	Percent (%)
Virgin forest	3,793.33	52.45
Logged forest	2,878.83	39.80
Others	560.58	7.75
Total	7,232.73	100.00

A comparative analysis of the water catchment area designated for Gunung Tebu FR and that for Bukit Bunga WTP indicates that the total area is 6,456.4 hectares, comprising 88.6% of the coverage (Figure 2). This demonstrates that the designated catchment zone for Gunung Tebu FR accurately encompasses the actual catchment area used for water supply. Figure 2 illustrates the water catchment area for WTP within the delineated river catchment area.

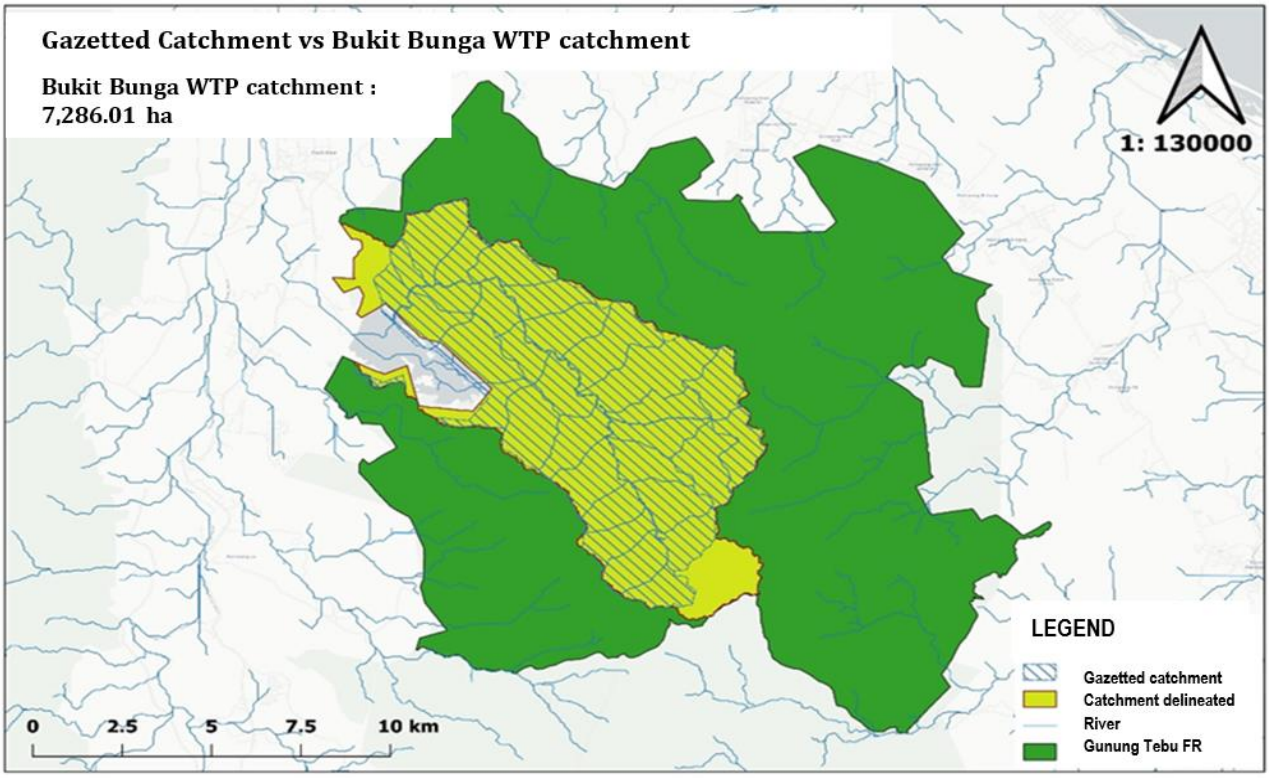

Figure 2. The catchment area for Bukit Bunga WTP within the delineated catchment zone

The analysis reveals the marginal value of water purification services provided by the forest to the Bukit Bunga WTP. Marginal value is defined as the annual benefit derived from forest reserve services in relation to the decrease in treatment costs achieved by preventing the conversion of 1 hectare of virgin forest to alternative land uses. Overall, the average marginal value for Gunung Tebu FR is RM 2,702,652 per year, which equates to approximately RM 297.24 per hectare per year. This value can be utilized to assess the operational cost implications for the WTP in financing water treatment services offered by forest reserves, similar to how other operational expenses (such as chemicals, electricity, and labor) are covered by the WTP. The findings indicate that the marginal value of forest reserve services for domestic water purification is relatively high compared to previous studies. This discrepancy may be due to the fact that this assessment focuses on a single watershed for one WTP, while earlier studies in Perak, Pahang, and Kelantan evaluated entire states or landscapes.

CONCLUSION

A comparative analysis of the water catchment area for Bukit Bunga WTP reveals that it encompasses approximately 6,456.4 hectares, with around 88.6% of this area attributed to Gunung Tebu Forest Reserve. This significant overlap indicates that the gazetted water catchment zones are closely aligned with the forest reserve areas, highlighting the importance of these zones in safeguarding water resources. To effectively protect these vital resources, it is essential to implement appropriate surveillance and enforcement measures. Such actions will ensure that the integrity of the catchment areas is maintained and that they continue to provide clean water for domestic use. Ultimately, conserving forest reserves as designated water catchment areas is crucial for securing a sustainable supply of clean water, particularly for community needs. This not only contributes to public health but also supports ecosystem balance and resilience in the face of environmental changes. The preservation of these areas will play a significant role in safeguarding water quality and availability for future generations.

REFERENCES

Chichilnisky G., Heal G.M .1998. Economic returns from the biosphere. *Nature* 391:629–630

Forster, D.L., Bardos, C.P. and Southgate, D.D. 1987. Soil Erosion and Water Treatment Costs. Journal of Soil and Water Conservation, 42, 349-352.

Freeman III, A.M., Herriges, J.A., & Kling, C.L. 2014. The Measurement of Environmental and Resource Values: Theory and Methods (3rd ed.). Routledge. https://doi.org/10.4324/9781315780917

McConnell, Kenneth E. & Bockstael, Nancy E., 2006. "Valuing the Environment as a Factor of Production," Handbook of Environmental Economics, in: K. G. Mäler & J. R. Vincent (ed.), Handbook of Environmental Economics, edition 1, volume 2, chapter 14, pages 621-669, Elsevier.

Millennium Ecosystem Assessment, 2005. *Ecosystems and Human Well-being: Synthesis*.

Moore W.B., McCarl B.A.1987. Off-site costs of soil erosion: a case study in the Willamette Valley. *West JAgric Econ* 12:42–49

Spiller M., McIntosh B.S., Seaton R.A.F., Jeffrey P. 2013. Pollution source control by water utilities – characterisation and implications for water management: research results from England and Wales. Water Environ J. 27:177–186. doi:10.1111/j.1747-6593.2012.00340.x

Sthiannopkao S .2007. Soil erosion and its impacts on water treatment in the northeastern provinces of Thailand. *Environ Int* 33:706–711

Unasylva. 2019. in Sarre A. (ed) . An International Journal of forestry and forest industries. Vol 70 2019/1

Vincent J.R .2011.Valuing the environment as a production input. In: Haque AKE et al (eds) Environmental valuation in South Asia Cambridge University Press, New Delhi, pp 36–77

Vincent J.R., Ismariah A., Norliyana A., Burwell W.B., Subrehendu P. &Tan Shoo J.S. 2015. Valuing Water Purification by Forests: An Analysis of Malaysian Panel Data. *Environ Resource Econ*. 61. DOI 10.1007/s10640-015-9934-9

https://earthexplorer.usgs.gov.

https://swat.tamu.edu/.

BorneoScience
The Journal of Science & Technology
Volume 45 Issue 2 : Sept 2024
Online ISSN : 2231-9085 | ISSN : 1394-4339

ON THE DIOPHANTINE EQUATION $P^x + Q^y = Z^2$

Izzati Izyani Japar [1, b], Siti Hasana Sapar[1, 2, a] and M Aidil M Johari [1, c]

[1]*Department of Mathematics and Statistics, Faculty of Science, Universiti Putra Malaysia, 43400 UPM Serdang, Selangor, Malaysia*
[2] *Institute for Mathematics Research, Universiti Putra Malaysia, 43400 UPM Serdang, Selangor, Malaysia*

Corresponding author : [a)] sitihas@upm.edu.my [b)] izzatiani@gmail.com [c)] mamj@upm.edu.my

Received 6th May 2024; Accepted 28th Nov 2024
Available online: 31st December 2024
Doi: https://doi.org/10.51200/bsj.v45i2.5878

ABSTRACT. *A Diophantine equation is a polynomial equation involving two or more variables for which integral solutions are sought. An exponential Diophantine equation includes additional variables that appear as exponents. This paper focuses on determining integral solutions to the Diophantine equation $px + qy = z^2$, given that $x + y = 5$, where p and q are twin primes, cousin primes, sexy primes, or any positive integers. By analyzing the solution patterns for each scenario, we aim to develop theorems and lemmas. The findings in this paper demonstrate that, for all cases where $x + y = 5$, the Diophantine equation does not have any non-trivial solutions when p and q are twin primes, cousin primes, or sexy primes, but it does have infinitely many solutions for any positive integers.*

INTRODUCTION

A Diophantine equation is a mathematical expression that involves two or more variables, where only integer solutions are desired. Over the years, extensive research has been conducted in this area, including studies by Cohn (1993), Demirci (2017), and Bennet (2017), as well as investigations into various other types of equations. Burshtein (2017) analyzed solutions to the Diophantine equation $p^x + q^y = z^4$ and demonstrated that for all primes $p \geq 2$ and $y = 1$, the equation has infinitely many solutions for every $x \geq 1$. Specifically, when x is even and q is prime, there exists a unique solution, $(p, q, x, y, z) = (2,17,6,1,3)$. In contrast, when x is even and q is composite, there are multiple solutions. For odd values of x, infinitely many solutions exist regardless of whether q is prime or composite.

Burshtein (2018a) used prime numbers to solve a new equation in the form of $p^x + (p + 4)^y = z^2$, focusing on cases where $(p, p + 4)$ are cousin primes and $x + y < 5$. He evaluated six scenarios where

the sum of x and y is less than 5 and found a solution for $x = 2$ and $y = 1$, specifically $(p, x, y, z) = (3,2,1,4)$. Burshtein (2018b) also addressed the same problem for $p^x + q^y = z^2$ with primes for $k = 3$, and the pairs $(p, p + 6)$, termed sexy primes, finding seven solutions among the first 10,000 primes *p*, where $x = y = 1$. Additionally, there was exactly one solution for $x = 2$ and $y = 1$.

Burshtein (2019) further examined two equations: $5^x + 103^y = z^2$ and $5^x + 11^y = z^2$. He concluded that the first equation has no solution while the second equation has no valid solutions when *y* is even. For all values $1 \leq x \leq 14$ and all odd values $1 \leq y \leq 9$, he identified exactly three solutions up to $5^{14} + 11^9 = 8461463316$. Further, Burshtein (2020) extended his inquiry into the equation $p^x + q^y = z^4$ and established that there are infinitely many solutions when $p = 2$ with equal values of *x* and *y*. However, he found that if *x* and *y* are distinct, there are no solutions, nor for any primes $p > 2$.

Sapar and Yow (2021) identified general forms of non-negative integral solutions to the equation $x^2 + 8(7^b) = y^{2r}$ under various conditions. Dokchan and Pakapongpun (2021) demonstrated that the Diophantine equation $p^x + (p + 20)^y = z^2$ has no positive integers solutions for *x*,*y* and *z* with both p and $(p + 20)$ are prime numbers. Borah and Dutta (2022) published findings on the exponential Diophantine equation $7^x + 32^y = z^2$, where they found discovered a unique solution $(x, y, z) = (2,1,9)$ Additionally, for the Diophantine equation $2^x + 7^y = z^2$ when $x \neq 1$, they found two solutions, which are (3,0,3) and (5,2,9). Yow et. al. (2022) provided bounds on the number of non-negative integral solutions for each *b* related to the Diophantine equation $x^2 + 16(7^b) = y^{2r}$. Burshtein (2017) suggested exploring solutions for the Diophantine equation $p^x + (p + 4)^y = z^2$ under the condition $x + y > 4$ in future research. Consequently, this paper aims to find integral solutions to the equation $p^x + q^y = z^2$ with the condition $x + y = 5$.

RESULTS

In this section, we will seek an integral solution to the Diophantine equation $p^x + q^y = z^2$ with (p, q) being twin primes and $x + y = 5$. The result is shown below:

Theorem 1: Suppose *x* and *y* are positive integers, while *p* and *q* are odd primes. There are no non-trivial solutions to the Diophantine equation $p^x + q^y = z^2$ when (p, q) are twin primes and $x + y = 5$.

Proof:
Assume p is an odd prime and (p, q) are twin primes, where $q = p + 2$ and $p < q$. Refereeing to the equation

$$p^x + q^y = z^2 \qquad (1)$$

we will examine four cases such that the sum of x and y equal to 5, as shown in Table 1.

Table 1: Possible combination of x and y for equation (1)

Case	x	y	$x + y$
I	1	4	5
II	2	3	5
III	3	2	5
IV	4	1	5

Case I: Let $x = 1$ and $y = 4$. Substituting these values into equation (1) yields:

$$p + q^4 = z^2 \qquad (2)$$

Next, let $m = q^2$. Since p and q are twin primes, with $p < q$, it follows that $p < m$. Substituting m into equation (2) gives us $p = (z + m)(z - m)$. Assuming the left-hand side (LHS) equals the righ-hand side (RHS), we set $p = z + m$ and $1 = z - m$. By solving these equations simultaneously, we find $z = \frac{p+1}{2}$. Substituting this back into equation (2), and considering that q is a twin prime, we simplify to obtain

$$4p^4 + 32p^3 + 95p^2 + 130p + 63 = 0. \qquad (3)$$

Upon solving equation (3), we conclude that there are integral solutions since p must be an odd prime such that (p,q) are twin primes. Specifically, we find two real solutions, $p \approx -0.415$ and -31.781, as well as two complex solutions. Consequently, there is no non-trivial integral solution to the equation $p^x + q^y = z^2$ for $x = 1$ and $y = 4$ when (p, q) are twin primes.

Case II: Let $x = 2$ and $y = 3$. Substituting these values into equation (1) results in

$$p^2 + q^3 = z^2. \qquad (4)$$

By substituting $q = p + 2$ into (4), we derive

$$p^3 + 7p^2 + 12p + 8 = z^2. \qquad (5)$$

Factoring equation (5), leads to

$$(p^2 + 12)(p + 7) = \left(z - \sqrt{76}\right)\left(z + \sqrt{76}\right).$$

Now, let's define $p^2 + 12 = z - \sqrt{76}$ and $p + 7 = z + \sqrt{76}$. by solving these two equations simultaneously, we orrive at;

$$p^2 - p + 5 + 2\sqrt{76} = 0.$$

Clearly, p is not an integer. Thus, there is no non-trivial solution to the equation $p^x + q^y = z^2$ for $x = 2$ and $y = 3$.

Case III: Assume $x = 3$ and $y = 2$. By substituting these values into equation (1), we obtain

$$p^3 + q^2 = z^2. \quad (6)$$

Substituting $q = p + 2$ into equation (6) and simplifying it, we get

$$(p + 1)(p^2 + 4) = z^2.$$

Since ringh-hand side (RHS) must be a perfect square, it is evident that there are no non-trivial solutions (p, q, z) to the equation $p^x + q^y = z^2$ for $(x, y) = (3, 2)$ and (p, q) are twin primes.

Case IV: Assume $x = 4$ and $y = 1$. Substituting these values into equation (1), we obtain

$$p^4 + q = z^2. \quad (7)$$

By substituting $q = p + 2$ into equation (7), we derive

$$p^4 + (p + 2) = z^2.$$

It is clear that the left-hand side cannot be expressed as a perfect square, as there is no perfect square between two consecutive squares. Therefore, there are no non-trivial solutions to the equation $p^x + q^y = z^2$ for $x = 4$ and $y = 1$.

The following theorem, will examine the equation $p^x + q^y = z^2$ when (p, q) are cousin primes and $x + y = 5$, with the result presented as follows:

Theorem 2: Let x and y be positive integers, and p and q be odd primes. There are no non-trivial solution to the equation $p^x + q^y = z^2$ when (p, q) are cousin primes and $x + y = 5$.

Proof:

Assume p is an odd prime, and let (p, q) be cousin primes such that $q = p + 4$. Based on the equation

$$p^x + q^y = z^2 \quad (8)$$

we will evaluate four cases where $x + y = 5$ as outlined in Table 1.

Case I: Let $x = 1$ and $y = 4$. Substituting x and y into equation (8) gives us:

$$p + q^4 = z^2. \quad (9)$$

Using a similar approach as in Case of Theorem 1, we conclude that there is no non-trivial solution to the Diophantine equation $p^x + q^y = z^2$ for $x = 1$ and $y = 4$.

Case II: Let $x = 2$ and $y = 3$. Substituting these values into equation (8) yields:

$$p^2 + q^3 = z^2.$$

Substituting $q = p + 4$ into equation (8) and simplifying gives:

$$p^2 + (p + 4)^3 = z^2.$$

By employing a similar method as in Case II of Theorem 1, we find there are no non-trivial solution to the equation $p^x + q^y = z^2$ for $x = 2$ and $y = 3$ when (p, q) are cousin primes.

Case III: Assume $x = 3$ and $y = 2$. Substituting these values into equation (8) and with $q = p + 4$, we derive:

$$p^3 + p^2 + 8p + 16 = z^2.$$

Using a similar argument as Case III of Theorem 1, we conclude that there is no non-trivial solution to the equation $p^x + q^y = z^2$ for $x = 3$ and $y = 2$ with (p, q) being cousin primes.

Case IV: Assume $x = 4$ and $y = 1$. Substituting these values and $q = p + 4$ into equation (8) yields:

$$p^4 + (p + 4) = z^2.$$

Employing a similar method and arguments as in Case IV in Theorem 1, we confirm that there is no non-trivial solution to the equation $p^x + q^y = z^2$ for $x = 4$ and $y = 1$ when (p, q) are cousin primes.

Having examined all cases, we have demonstrated that no non-trivial solutions exist for the Diophantine equation $p^x + q^y = z^2$ when (p, q) are cousin primes and $x + y = 5$.

Next, we will seek a solution to the equation $p^x + q^y = z^2$ where (p, q) are sexy primes and $x + y = 5$. The result is provided in the following theorem.

Theorem 3: Let x and y be positive integers, and p and q be odd primes. There are no non-trivial solutions to the equation $p^x + q^y = z^2$ when (p, q) are sexy primes and $x + y = 5$.

Proof:
Assume p is an odd prime and let (p, q) be sexy primes such that $q = p + 6$ and $p < q$. We will examined four cases where the sum of x and y equals 5:

Case I: Let $x = 1$ and $y = 4$. Substituting these values into equation (1) gives us:

$$p + q^4 = z^2 \qquad (10)$$

Using a similar approach as in Case I in Theorem 1, we arrive at the conclusion that there are no non-trivial solutions to the equation $p^x + q^y = z^2$ for $x = 1$ and $y = 4$. Thus, therefore is no non-trivial solution to $p^x + q^y = z^2$ for $(x,y)=(1, 4)$ when (p, q) are sexy primes.

Case II: Let $x = 2$ and $y = 3$. Substituting these values into equation (1) results in:

$p^2 + q^3 = z^2$.

Now, substituting $q = p + 6$ into equation (10) and simplifying, we obtain:

$p^3 + 19p^2 + 108p + 216 = z^2$.

Using a similar method as in Case II of Theorem 1, we find that there are no non-trivial integral solutions to the equation $p^x + q^y = z^2$ for $(x,y)=(2,3)$ when (p, q) are sexy primes.

Case III: Let $x = 3$ and $y = 2$. By substituting these values and $q = p + 6$ into equation (10), we get:

$p^3 + p^2 + 12p + 36 = z^2$.

As in Case III of Theorem 1, we can conclude that there is no non-trivial integral solutions to the equation $p^x + q^y = z^2$ for $(x,y)=(3,2)$ when (p, q) are sexy primes.

Case IV: Let $x = 4$ and $y = 1$. Substituting these values along with $q = p + 6$ into equation (10) gives us:

$p^4 + (p + 6) = z^2$.

By applying a similar method as in Case IV of Theorem 1, we can confirm that there is no non-trivial solutions to the Diophantine equation $p^x + q^y = z^2$ for $(x,y)=(4,1)$ when (p, q) are sexy primes.

After evaluating all cases, we have demonstrated that there are no non-trivial solutions to the Diophantine equation $p^x + q^y = z^2$ when (p, q) are sexy primes and $x + y = 5$.

In the subsequent theorem, we will seek an integral solution to the Diophantine equation $a^x + b^y = z^2$ for any $a, b \in \mathbb{Z}^+$, where the sum of x and y is fixed. The possible combination are provided in Table 2.

Table 2: Possible combination of x and y

Case	x	**Y**	$x + y$
I	1	4	5
Ii	2	3	5

To begin, we examine Case I: Let $x = 1$ and $y = 4$.

Theorem 4: Let a, b, x, y and z be positive integers. The solutions to the equation $a^x + b^y = z^2$ for $(x, y) = (1,4)$ are given by $(a, b, z) = (2m^2 + 1, m, m^2 + 1)$, where m is a positive integer.

Proof:
Consider the equation
$a^x + b^y = z^2$ (11)

where a, b, x, y and z being positive integers. Setting $(x, y) = (1,4)$ and substituting into equation (11), we have
$a + b^4 = z^2$

Let $b = m$. Then we rewrite the equation as

$a + m^4 = z^2$

Now, we can express a as:

$a = (z + m^2)(z - m^2)$.

Since right-hand side (RHS) equals the left-hand side (LHS), by comparing both sides, we derive the following equations:

$a = z + m^2$ (12)
$1 = z - m^2$. (13)

By solving equations (12) and (13) simultaneously, we obtain:

$a = 2m^2 + 1$ and $z = m^2 + 1$

Thus, we have

$(a, b, z) = (2m^2 + 1, m, m^2 + 1)$

where m is a positive integer.

Now, we will consider Case II, where $(x, y) = (2,3)$. To determine the solution, we will consider the parity of b as stated in the following theorem.

Theorem 5: Let a, b, x, y and z be positive integers. The solution to the equation $a^x + b^y = z^2$ with $(x, y) = (2,3)$ are given by:

$$(a, b, z) = \begin{cases} (2m^2 + m, 2m + 1, 2m^2 + 3m + 1) & \text{if } b \text{ odd} \\ (2m^2 - m, 2m, 2m^2 + m) & \text{if } b \text{ even.} \end{cases}$$

where m is a positive integer.

Proof:
Let $(x, y) = (2,3)$ and substitute into equation (11):

$a^2 + b^3 = z^2$.

Assuming b is an odd integer, we can set $b = 2m + 1$:

$(2m + 1)^3 = (z + a)(z - a)$.

Since right-hand side (RHS) equals left-hand side (LHS), we can let

$z + a = (2m + 1)^2$ and $z - a = (2m + 1)$.

Solving these equations simultaneously, we find:

$z = (m + 1)(2m + 1)$ and $a = m(2m + 1)$

This results in the same outcome if we reverse the assignments of $z - a$ and $z + a$. Therefore,

$(a, b, z) = (2m^2 + m, 2m + 1, 2m^2 + 3m + 1)$

where m is a positive integer.

Now, let us consider $(x, y) = (2,3)$ and substitute into equation (11), we get $a^2 + b^3 = z^2$ and the case where $b = 2m$ is an even integer. In this scenario, we have:

$(2m)^3 = (z + a)(z - a)$

Since the right-hand side (RHS) equals the left-hand side (LHS), we set:

$z + a = (2m)^2$ and $z - a = (2m)$

Solving these equations simultaneously, we get:

$z = m(2m + 1)$ and $a = m(2m - 1)$

We will arrive at the same result if we switch the values for $z - a = (2m)^2$ and $z + a = (2m)$. Thus, the solution to the equation $a^x + b^y = z^2$ with $(x, y) = (2,3)$ is:

$(a, b, z) = (m(2m - 1), 2m, m(2m + 1))$

where m is positive integer.

CONCLUSION

From this study, we established that that there are no non-trivial integral solutions to the Diophantine equation $p^x + q^y = z^2$ when (p,q) are twin, cousin, or sexy primes and $x + y = 5$. For the Diophantine equation $a^x + b^y = z^2$ where $a, b \in \mathbb{Z}^+$ and $(x, y) = (2,3)$, the solutions are given by $(a, b, z) = (2m^2 + m, 2m + 1, 2m^2 + 3m + 1)$ for odd b odd, and $(a, b, z) = (2m^2 - m, 2m, 2m^2 + m)$ for even b. For the case when $(x, y) = (1,4)$, the solution is $(a, b, z) = (2m^2 + 1, m, m^2 + 1)$, where m is a positive integer. This study could be expanded to explore integral solutions for cases involving prime triplets, prime quadruplets, or other configurations of prime number.

REFERENCES

Bennett, M. A. "The polynomial-exponential equation $1 + 2^a + 6^b = y^q$". *Period Math Hungary*, 75: 387–397 (2017).

Borah P. B. and Dutta M. "On two classes of exponential Diophantine equations". *Communications in Mathematics and Applications*. 13 (1), 137-145 (2022).

Burshtein, N. "On solutions to the diophantine equation $p^2 + q^2 = z^4$". *Annals of Pure and Applied Mathematics*, 14(1):63–68 (2017).

Burshtein, N. "All the solutions of the diophantine equation $p^x + (p + 4)^y = z^2$ when *p*, (*p*+ 4) are primes and $x + y = 2, 3, 4$". *Annals of Pure and Applied Mathematics*, 16(1):241–244 (2018a).

Burshtein, N. "Solutions of the diophantine equation $p^x + (p + 6)^y = z^2$ when p , (p + 6) are primes and $x + y = 2, 3, 4$." *Annals of Pure and Applied Mathematics*, 17(1):101–106 (2018b).

Burshtein, N. "On solutions to the diophantine equations $5^x + 103^y = z^2$ and $5^x + 11^y = z^2$ with positive integers *x, y, z*". *Annals of Pure and Applied Mathematics*, 19(1):75–77 (2019).

Burshtein, N. "All the solutions of the diophantine equation $p^x + p^y = z^4$ when *p* is prime and *x, y, z* are positive integers". *Annals of Pure and Applied Mathematics*, 21(2):125–128 (2020).

Cohn J. H. E. "The Diophantine equation $x^2 + C = y^n$". *Acta Arith.* 109 pp.205-206, (1993)

Demirci, M. "On the Diophantine Equation$x^2 + 5^a P^b = y^n$". *Filomat*, 31 (16), 5263-5269 (2017).

Dokchan, R. and Pakapongpun, A. "On the Diophantine equation $p^x + (p + 20)^y = z^2$, where *p* and *p + 20* are primes". *International Journal of Mathematics and Computer Science*, 16(1):179–183 (2021).

Sapar S H and Yow K. S, "A Generalisation of the Diophantie Equation $x^2 + 8(7^b) = y^{2r}$". *Malaysian Journal of Science*, 40(2): 151-158 (2021).

Yow K.S., Sapar S H and Low C Y, "Solution to the Diophantine Equation $x^2 + 16(7^b) = y^{2r}$", *Malaysian Journal of Fundamental and Applied Sciences*, 18(4), 489-496 (2022).[1]

BorneoScience
The Journal of Science & Technology
Volume 45 Issue 2 : Sept 2024
Online ISSN : 2231-9085 | ISSN : 1394-4339

NOTES ON BATS' DIVERSITY IN PARCEL 5 OF SEKAR IMEJ CONSERVATION AREA FROM KIBUNDU, GEROWONG AND MONJUK TRAILS

Nurul 'Ain Elias[1], Ummu 'Atiyyah Mohamed Talhah[1], Malborn Solynsem[2], Aqilah Nabihah Anuar[3], Otin Masalim[3], Yusiman Laimong[3], Raplis Kinchi[3], Ronny Ning [3] and Azniza Mahyudin[2]

[1] School of Biological Sciences, Universiti Sains Malaysia, 11800 Gelugor, PULAU PINANG,
[2] Conservation Biology Program, Faculty of Tropical Forestry, Universiti Malaysia Sabah, Jalan UMS, 88400 Kota Kinabalu, SABAH,
[3] Sekar Imej Estate, Locked Bag No.34, 90009 Sandakan, SABAH

Corresponding author: azniza@ums.edu.my

Received 23th April 2024; Accepted 28th Nov 2024
Available online: 31st December 2024
Doi:https://doi.org/10.51200/bsj.v45i2.5879

ABSTRACT. *The study on bat diversity in Sekar Imej Conservation Area (SICA) was conducted during the Sekar Imej Conservation Area Scientific Expedition from 19 September 2022 to 24 September 2022. Harp traps and mist nets were used to capture bats with placements along forest trails in Kibundu, Gerowong, and Monjuk for six consecutive nights. Species identification was performed on-site through morphological examinations of the forearm, ear, hindfoot, and tail (when available), with measurements recorded in millimeters (mm). Additionally, the bats were weighed in grams and their reproductive stages were noted. The study recorded nine bat species, belonging to four families: Pteropodidae, Rhinolophidae, Hipposideridae, and Vespertilionidae. From the Kibundu trail, Rhinolophus trifoliatus, Kerivoula intermedia and Kerivoula pellucida were collected, while Hipposideros cervinus, Kerivoula papillosa and Balionycteris maculata were recorded at Gerowong trail. At Monjuk trail, five species were recorded: Cynopterus brachyotis, Balionycteris maculata, Rhinolophus borneensis, Hipposideros cervinus and Kerivoula whiteheadi. These results will support the Sekar Imej Estate management in improving and expanding their conservation efforts and management strategies for bats and other wildlife in the landscape.*

KEYWORDS. Bat, diversity, forest trail, plantation, Sekar Imej Conservation Area

INTRODUCTION

Protected areas are viewed as vital boundaries that help conserve remaining species amid Southeast Asia's rapid deforestation (Sodhi et al., 2004; Lee et al., 2007; Fitzherbert et al., 2008). Globally, a total of 18,763,407 km² of parks and protected areas have been designated (Nagendra, 2008). However, concerns have arisen regarding habitat fragmentation and species decline when

human populations live in proximity to these areas (Nagendra, 2008). Specifically, the forests surrounding protected areas, which are intended to function as buffer or transitional zones, often experience significant degradation due to human activity (DeFries *et al*., 2005; Lee *et al*., 2007). The loss of habitat in these buffer zones can lead to the formation of isolated protected areas, ultimately diminishing their conservation effectiveness (DeFries *et al*., 2005; Lee *et al*., 2007).

As a result, the protection of natural forests within oil palm plantations has become increasingly recognized as essential for biodiversity conservation, particularly as it has become a key factor in the certification process for sustainable oil palm plantations (Fleiss *et al*., 2020). The Sekar Imej Conservation Area (SICA), which encompasses 2,469 hectares within the Sekar Imej Estate, serves as a prime example of this approach. The conservation area comprises two sections known as Parcel 4 and Parcel 5, bordered by the Paitan and Lingkabau Forest Reserves, and is potentially capable of functioning as a transitional zone. The forest ecosystem within the Sekar Imej Conservation Area is primarily characterized by lowland mixed dipterocarp forest, featuring a structure made up of young regenerating forests, abundant saplings, and a low density of established mixed dipterocarp trees.

MATERIALS AND METHODS

Study sites

Bat sampling was carried out in Parcel 5 of the Sekar Imej Conservation Area (SICA) (see Figure 1). This section of the conservation area is adjacent to the Paitan Forest Reserves. The forest vegetation in Parcel 5 is primarily composed of lowland mixed dipterocarp forest, featuring logged-over areas that are approximately 20 to 30 years old. During the Sekar Imej Conservation Area Scientific Expedition, which took place from September 19 to September 24, 2022, we explored three trails in Parcel 5 for the study of bat diversity: Kibundu, Gerowong, and Monjuk trails.

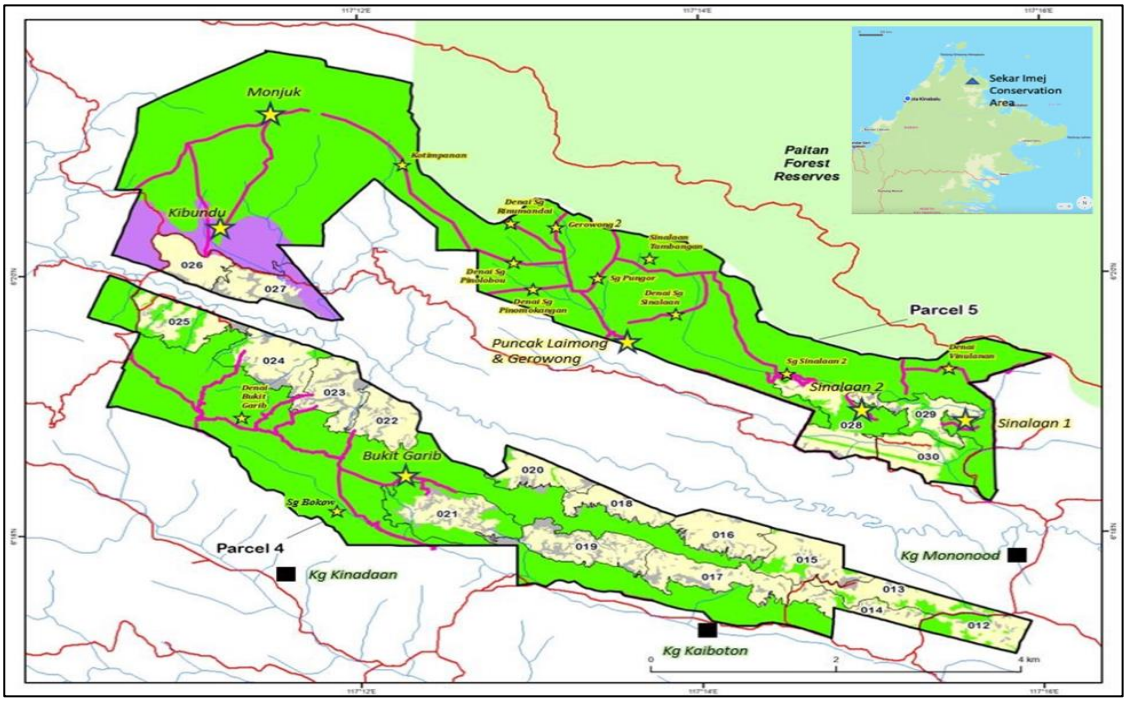

Figure 1 Sekar Imej Conservation Area (SICA), which includes Parcel 4 and Parcel 5)

Kibundu trail

The Kibundu trail is situated close to the SICA Field Base Camp and Lot 27 of the planted area, beginning at an elevation of 70 meters above sea level (m a.s.l.) and concluding at Monjuk Peak at 280 m a.s.l. A small stream runs across the trail. The vegetation in the Kibundu area is primarily composed of secondary lowland forest, featuring young regenerating plants and mixed dipterocarps.

Gerowong trail

The Gerowong trail, situated within the Sekar Imej Conservation Area, runs alongside the Gerowong River. We established three sampling locations here: S1 (N06, 19.443; E117 13.615, 63 m a.s.l.), which featured large rock boulders on the riverbed; S2 (N06, 19.516; E117 13.618, 34 m a.s.l.); and S3 (N06, 19.516; E117 13.618, 61 m a.s.l.), both of which were located on a flat sandy riverbed.

Monjuk trail

The Monjuk trail serves as the primary pathway along a ridge that ascends to Monjuk Peak, which is the tallest point in the Sekar Imej Conservation Area. Along this trail, we set up two sampling stations: M1 located at 180 meters above sea level and M2 at 260 meters above sea level. These sampling stations are surrounded by secondary forest vegetation, characterized by a plentiful presence of palms.

Bat Sampling and Handling

We adhered to the sampling protocols outlined by Kingston *et al*. (2003), utilizing a harp trap along with three mist nets set up on-site. However, we made slight adjustments to account for seasonal variations during the sampling process and to minimize lengthy operating hours to prevent any harm to the animals. Bats were collected from 30 minutes before sunset until 4 hours after sunset (5:30 PM to 10:30 PM), with the nets and traps being monitored every 30 minutes. After each collection, the traps were taken down rather than being left unmanned overnight at the locations. Bats were placed into individual cotton bags prior to undergoing morphological examination (Mahyudin *et al*., 2022).

Species Identification

The body weight of the bats was recorded in grams (g), while measurements for forearm length (FA), tibia (Tb), hindfoot (HF), ear and tragus (E-Tr), and tail (T) were taken in millimeters (mm) for species identification. Species classification was conducted in accordance with the methods of Payne *et al*. (2007), Francis (2008), and Philipps and Philipps (2016). We also assessed the age of each bat—juvenile, subadult, or adult—by examining the level of ossification in the epiphyses (Korine and Pinshow, 2004) and the color of their fur. Additionally, the reproductive stage was recorded for female bats (Korine and Pinshow, 2004).

Data Analysis

Species diversity and species distribution update

Species diversity was characterized by the species checklist generated in this study. The distribution of bats captured in the Sekar Imej Conservation Area (SICA) has been revised in light of previous findings by other researchers and specifically pertains to records from Sabah.

Foraging strategy and conservation status

We determined their guild structure based on foraging habits, following the approach of Struebig et al. (2006). The captured bats were categorized according to their conservation status as outlined in

the IUCN Red List of Threatened Species and the Sabah Wildlife Enactment (1997) (Sukiman, 2019; Mahyudin *et al*., 2022). The Sabah Wildlife Conservation Enactment of 1997 was utilized to assess conservation status at the national level, while the IUCN Red List provided the basis for determining the conservation status of each species reported internationally (Mahyudin *et al*., 2022).

RESULTS AND DISCUSSION

Species Diversity

This study identified nine bat species present at Parcel 5 of the Sekar Imej Conservation Area (SICA). The recorded species include: *Balionycteris maculata, Cynopterus brachyotis, Rhinolophus trifoliatus, Rhinolophus borneensis, Hipposideros cervinus, Kerivoula intermedia, Kerivoula pellucida, Kerivoula papillosa,* and *Kerivoula whiteheadi* (Table 1). The species assemblages in SICA consisted of four species from the Vespertilionidae family, two from Pteropodidae, one from Hipposideridae, and two from Rhinolophidae. These findings closely resemble typical palaeotropical bat assemblages, predominantly composed of insectivorous species from the families Hipposideridae, Rhinolophidae, and Vespertilionidae, particularly the subfamilies Kerivoulinae and Murininae (Struebig *et al*., 2012). The absence of Murininae species from our SICA bat checklist does not necessarily indicate that these species are completely absent from the area (Suyanto and Struebig, 2007). Expanding the surveys may lead to the discovery of additional species. Moreover, external factors such as weather conditions and trap placement may impact the sampling effort (Sedlock *et al*., 2008; Bansa *et al*., 2020).

In this study, bat sampling efforts were constrained by rainy nights. To achieve better species coverage, it is essential to sample both sub-canopy and canopy levels to prevent bias in bat sampling (Bansa *et al*., 2020). Implementing long-term monitoring, which involves sampling year-round during both wet and dry seasons, and utilizing a variety of sampling techniques—such as canopy nets and bat detectors (Bansa *et al*., 2020)—across different locations within SICA, will improve our understanding of bat diversity in the area.

Table 1: Species diversity in Parcel 5, Sekar Imej Conservation Area, Sandakan

Family	Species	Common name
Pteropodidae	*Balionycteris maculata*	Spotted-winged Fruit Bat
	Cynopterus brachyotis	Sunda Short nosed Fruit Bat
Rhinolophidae	*Rhinolophus trifoliatus*	Trefoil Horseshoe Bat
	Rhinolophus borneensis	Bornean Horseshoe Bat
Hipposideridae	*Hipposideros cervinus*	Fawn Roundleaf Bat
Vespertilionidae	*Kerivoula intermedia*	Small Woolly Bat
	Kerivoula pellucida	Clear-winged Woolly Bat
	Kerivoula papillosa	Papillose Woolly Bat
	Kerivoula whiteheadi	Whitehead's Woolly Bat

Bat Species Distribution Notes

Although all the species were recorded for the first time in the Sekar Imej Conservation Area, they have been previously documented in other regions of Sabah.

Family Rhinolophidae

Members of the Rhinolophidae family, specifically *Rhinolophus trifoliatus* (Trefoil Horseshoe Bat; Figure 2(a)), were captured in the Sekar Imej Conservation Area and are considered common in primary forests of the lowlands (Payne *et al*. 2007). This species is recognized as forest dependent. In Sabah, sightings of this bat have been recorded in various locations, including Trus Madi (Payne *et al*. 2007), Maliau Basin (Mahyudin *et al*. 2010), Sungai Rawog (Amat *et al*. 2019), Crocker Range (Yoh *et al*. 2020), and Imbak Canyon (Senawi *et al*. 2020). A male individual of this species was captured at the Kibundu trail, near a small tributary that runs alongside the trail, in an area dominated by succession species, particularly palms and *Calamus spp*.

An adult male *Rhinolophus borneensis* (Bornean Horseshoe Bat; Figure 2(b)) was caught at sampling Station 1 of the Monjuk trail (M1) in a harp trap set in an open area on the ridge of Monjuk. This species has also been reported in Sabah from locations such as Maliau Basin (Mahyudin *et al*. 2010), Imbak Canyon (Yasuma and Andau, 2000; Bansa *et al*. 2020; Senawi *et al*. 2020), and is known to be common in several cave systems across Sabah, including Gomantong, Madai, Sukau, Sapulut, and Gunung Kinabalu (Abdullah *et al*. 2007; Payne *et al*. 2007; Yasuma and Andau, 2000). Additionally, it has been documented in the Crocker Range (Yasuma and Andau 2000; Yoh *et al*. 2020), as well as in Danum Valley, Sapagaya, Sepilok, Tabin, and Ulu Tomani (Yasuma and Andau 2000).

Figure 2: The two bat species from the Rhinolophidae family that were captured in the Sekar Imej Conservation Area (SICA), a) *Rhinolophus trifoliatus*; b) *Rhinolophus borneensis* (*Photo credit: Nurul 'Ain Elias and Ummu 'Atiyyah Mohamed Talhah*)

Family Vespertilionidae, subfamily Kerivoulinae

In the subfamily Kerivoulinae, we documented four species: *Kerivoula intermedia* and *Kerivoula pellucida* were recorded at the Kibundu trail, while *Kerivoula papillosa* was found along the Gerowong trail and *Kerivoula whiteheadi* at the Monjuk trail. All these species have a strong association with primary lowland forests, although *K. intermedia* (Small Woolly Bat; Figure 3(a)) is

also known to inhabit secondary forests (Payne *et al*. 2007). The distribution of *K. intermedia* in Sabah has been observed in locations such as Sepilok, Tabin, Witti Range (Payne *et al*. 2007), Sungai Rawog (Amat *et al*. 2019), Imbak Canyon (Bansa *et al*. 2020), and Crocker Range (Yoh *et al*. 2020). During this study, a female individual was captured at the Kibundu trail with early pregnancy status, while a male was captured in a harp trap set in an open area dominated by Tarap trees and ferns at the same location.

K. pellucida (Clear-winged Woolly Bat; Figure 3(b) has been previously recorded from various locations across Sabah (Payne *et al*. 2007), including Sungai Rawog (Amat *et al*. 2019), Crocker Range (Yoh *et al*. 2020), and Imbak Canyon (Bansa *et al*. 2020; Senawi *et al*. 2020). In this study, a female *K. pellucida* in the late stage of lactation was captured at the Kibundu trail over a small tributary, along with an adult male recorded at sampling station M2 in a harp trap. Additionally, a female *K. papillosa* (Figure 3(c)) at the post-lactating stage was caught at S3 along the Gerowong trail in a harp trap set 50 meters from the Gerowong River, which is surrounded by secondary lowland forest. Previously, *K. papillosa* has been documented in Danum Valley, Gomantong, Madai, Sepilok, and Tabin (Payne *et al*. 2007), Imbak Canyon (Bansa *et al*. 2020; Senawi *et al*. 2020), and Crocker Range (Yoh *et al*. 2020). An adult male *K. papillosa* was also captured in a harp trap at M2 of the Monjuk trail, which is covered by secondary forest vegetation. Furthermore, a male *K. whiteheadi* (Whitehead's Woolly Bat; Figure (d)) was captured in the harp trap at sampling station M1 on the Monjuk trail. This species was previously reported by Payne et al. (2007) in Lower Kinabatangan, and Struebig *et al*. (2006) proposed that the genus *Kerivoula* could serve as an indicator for assessing forest disturbance, particularly for *K. papillosa*, as it is found to be less common in disturbed forests compared to natural ones.

a) *Kerivoula intermedia*

b) *Kerivoula pellucida*

c) *Kerivoula papillosa*

d) *Kerivoula whiteheadi*

Figure 3: The four bat species from the Vespertilionidae family and Kerivoulinae subfamily that were captured in the Sekar Imej Conservation Area (SICA), a) *K. interme*dia; b) *K. pellucida*; c) *K. papillosa*; d) *K. whiteheadi*. (*Photo credit: Nurul 'Ain Elias and Ummu 'Atiyyah Mohamed Talhah*)

Family Hipposideridae

Regarding the hipposiderids, a group of *Hipposideros cervinus*, comprising five females and one male (Figure 4), was captured in a harp trap. Among the females, three were observed to be in the post-lactating stage, while two were non-reproductive at sampling station M2 along the Monjuk trail. This species has also been observed at the Gerowong trail, specifically at a rock shelter adjacent to the Gerowong River (S1), where a distinct separation was noted between male and female colonies, positioned 50 meters apart. Additionally, *Hipposideros cervinus* was located at S3, which features a flat sandy riverbed along the Gerowong River. Known as the Fawn Roundleaf Bat, this species is commonly found in cave areas and has a broad distribution throughout Borneo (Suyanto & Struebig, 2007). Its presence has been documented in multiple sites including Batu Punggol, Baturong, the Crocker Range, Danum Valley, Gomantong, Gunung Kinabalu, Maliau Basin, Pulau Mantanani, Pun Batu, Sepilok, Sukau, and Tabin (Yasuma & Andau, 2000; Abdullah et al. 2007), as well as Pulau Balambangan and Pulau Banggi (Nor, 1996; Mahyudin *et al*. 2018), Imbak Canyon (Bansa *et al*., 2020; Senawi *et al*. 2020), and the Crocker Range (Yoh *et al*. 2020), along with Madai and Batu Supu (Mahyudin *et al*. 2022a; Mahyudin *et al*. 2022b).

Figure 4: *Hipposideros cervinus* from the Hipposideridae family that was captured in the Sekar Imej Conservation Area (SICA) (Photo credit: Nurul 'Ain Elias and Ummu 'Atiyyah Mohamed Talhah)

Family Pteropodidae

An intriguing sighting involved a pteropodid that flew between the trees at sampling station S2 along the Gerowong trail, where we captured a single *Balionycteris maculata* (Spotted-winged Fruit Bat) at sampling station S3 during the trapping session. The female *B. maculata* was captured while in the lactating stage. This species has also been observed at the Monjuk trail, specifically at sampling station M2, where three females were captured. Among these, two females were in the post-lactating stage and were caught in mist nets, while the other was captured in a harp trap. *B. maculata* is the

smallest fruit bat and is commonly found in the forest understory. It has been recorded in various forest types, including mangrove, primary, and secondary forests (Philipps and Philipps, 2016). The distribution of *B. maculata* includes scattered records from Kota Kinabalu, Sepilok, Madai, and Tawau (Payne et al. 2007), as well as from Imbak Canyon (Hassan, 2016; Bansa *et al*. 2020; Senawi *et al*. 2020) and the Crocker Range (Yoh *et al*. 2020).

Another fruit bat species recorded in the Sekar Imej Conservation Area is the Sunda Short-nosed Fruit Bat (*Cynopterus brachyotis*) (Figure 5(b)). At sampling station M2 along the Monjuk trail, we captured two adult males and a juvenile female of *C. brachyotis* using a mist net set in an open area surrounded by palms and shrubs. The Sunda Short-nosed Fruit Bat (*C. brachyotis*) is among the most common and widely distributed fruit bats (Payne et al. 2007). This species thrives in various landscape matrices, including orchards, oil palm plantations, secondary forests, as well as coastal and mangrove environments (Philipps and Philipps, 2016). Previous records for this species include Pulau Balambangan (Nor, 1996), Imbak Canyon (Bansa *et al*. 2020), Crocker Range (Yoh *et al*. 2020), Gomantong (Abdullah *et al.* 2007), and Madai (Mahyudin *et al*. 2022a).

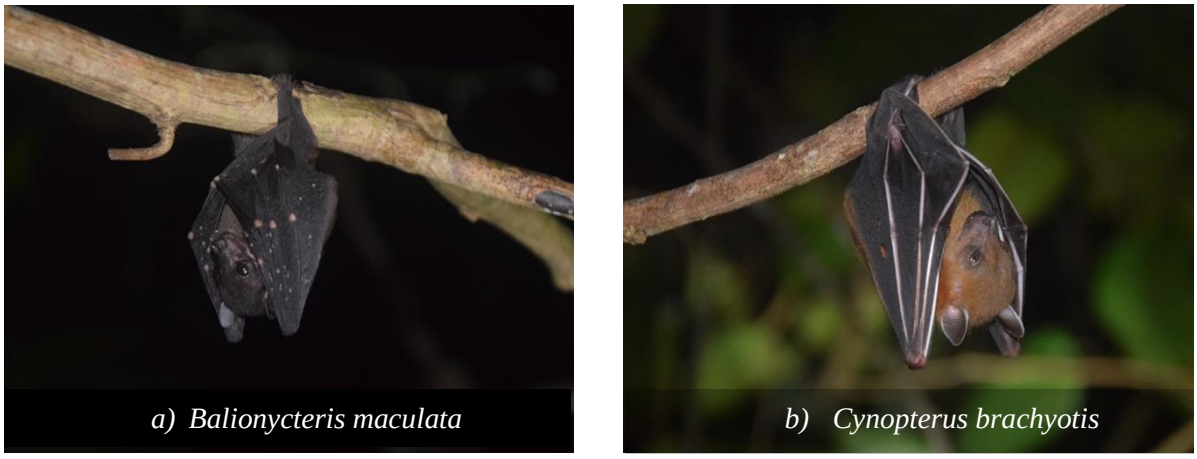

Figure 5: The four bat species from the Vespertilionidae family and Kerivoulinae subfamily that were captured in the Sekar Imej Conservation Area (SICA), a) *Balionycteris maculata* b) *Cynopterus brachyot*. (Photo credit: Nurul ‘Ain Elias and Ummu ‘Atiyyah Mohamed Talhah)

Foraging Strategy and Conservation Status

In terms of feeding guilds, insectivorous bats accounted for 88% of the species assemblages, which included six species categorized as narrow-space insectivores (Table 2). Additionally, *Hipposideros cervinus* was classified as both edge-gap and narrow-space insectivores. Meanwhile, the pteropodid *Balionycteris maculata* was designated as a narrow-space (understorey) frugivore/nectarivore, and *Cynopterus brachyotis* was classified as a below-canopy frugivore (Struebig *et al*. 2006). The assignment of each species to its respective feeding guild is influenced by habitat type and foraging behavior (Denzinger and Schnitzler, 2013). It is noteworthy that all bat species recorded from Parcel 5 of the Sekar Imej Conservation Area (SICA) are not protected under the Sabah Wildlife Conservation Enactment (1997). However, several species have been identified with high conservation value according to the IUCN Red List of Threatened Species, including *Rhinolophus trifoliatus*, *Kerivoula intermedia*, and *Kerivoula pellucida*, which are classified as Near Threatened.

The IUCN conservation status of the bats in SICA underscores the necessity for further exploratory research, as much about these species remains unknown. Additionally, the Sabah Wildlife Conservation Enactment (1997) highlights the implications of data scarcity, as none of the species listed are afforded protection under the enactment (Mahyudin *et al*., 2022a). The bat species currently protected by the Sabah Wildlife Conservation Enactment (1997) are endemic to Borneo and the Malay Peninsula and have a limited distribution range within the Sundaic region (Mahyudin *et al*., 2022a).

Table 2: Conservation status and foraging behaviours of bats in Sekar Imej Conservation Area

Species	**Sabah Wildlife Conservation Enactment (1997)**	**IUCN Red List of Conservation Status**	**Foraging strategy**
Balionycteris maculata	Not Protected	Least Concern	Nf
Cynopterus brachyotis	Not Protected	Least Concern	Bf
Rhinolophus trifoliatus	Not Protected	Near threatened	Ni
Rhinolophus borneensis	Not Protected	Least Concern	
Hipposideros cervinus	Not Protected	Least Concern	E/Ni
Kerivoula intermedia	Not Protected	Near threatened	Ni
Kerivoula pellucida	Not Protected	Near threatened	Ni
Kerivoula papillosa	Not Protected	Least Concern	Ni
Kerivoula whiteheadi	Not Protected	Least Concern	

**Note: Nf indicated narrow space (understorey) frugivore/ nectarivore; Bf indicated below canopy frugivore; Ei indicated insectivores foraging at the edges or open spaces; E/Ni indicated Insectivores foraging at the edge/open/narrow spaces, and Ni indicated insectivores foraging at narrow spaces.*

CONCLUSION

All bats captured in the Sekar Imej Conservation Area (SICA) represent new distribution records, suggesting that bat diversity in Sabah is still underrepresented and requires further survey efforts. However, existing references for bat species in Sabah do not provide accurate distribution data. The presence of several rare species with significant conservation status underscores the importance of the Sekar Imej Conservation Area ecosystem for sustaining bat diversity in the interior regions of Sabah. This highlights the urgency of improving the protection and conservation of bats in Sabah by revising and remapping their conservation status in the Sabah Wildlife Conservation Enactment of 1997. These findings will aid in the management of the Sekar Imej Estate, allowing for enhanced conservation efforts and management strategies in the landscape that support a variety of matrices for bats and other wildlife.

ACKNOWLEDGEMENT

We extend our gratitude to Sekar Imej Estate, Wilmar Oil Palm Berhad, and Universiti Sains Malaysia for organizing the expedition. We also appreciate the members of the SICA Scientific Expedition committee who assisted us throughout the expedition. Additionally, we thank the Deans of the School of Biological Sciences at Universiti Sains Malaysia and the Faculty of Tropical Forestry at Universiti Malaysia Sabah for their support of our work during the expedition.

REFERENCES

Abdullah, M. T., Hall, L.S., Tissen, O.B., Tuuga, A., Sulaiman, S and Earl of Cranbrook.2007. The large bat caves of Malaysian Borneo. *Bat Research News* **48**: 99-100.

Ag Safree, A. S. 2022. *Screening for Pathogenic Bacteria in Populations of Bats from Banggi Island and Imbak Canyon Study Centre, Sabah.* Thesis. Conservation Biology Program. Universiti Malaysia Sabah. Kota Kinabalu, Sabah.

Amat, A., Daud, U.S., Senawi, J. and Mahyudin, A. 2019. *Notes on Bat Diversity in Sungai.* Abstract presented in: Proceedings of the Seminar on Sungai Rawog Scientific Expedition. Kota Kinabalu, Sabah: 21st February 2019.

Bansa, L.A., Rosli, Q.S., Daud, U.S., Amat, A., Morni, M.A., William-Dee, J., Jinggong, E.R., Rajasegaran, R., Senawi, J., Kumaran, J.V., Azhar, I., Mahyudin, A., Hasan, N.H. and Khan, F.A.A. 2020. Survey on Small Mammals in Sg Kangkawat Research Station Imbak Canyon Conservation Area. *Journal of Tropical Biology and Conservation* **17**: 149-163.

DeFries, R., Hansen, A., Newton, A.C. and Hansen, M.C. 2005. Increasing isolation of protected areas in tropical forests over the past twenty years. *Ecological Application* **15** (**1)**: 19-26.

Denzinger, A. and Schnitzler, H.U. 2013. Bat guilds, a concept to classify the highly diverse foraging and echolocation behaviours of Microchiropteran bats. *Frontiers in Physiology* **4** (164): 1-15.

Francis, C.M. 2008. A Guide to the Mammals of South-East Asia. Princeton University Press, Princeton, United Kingdom.

Fitzherbert, E.B., Struebig, M.J. Morel, A., Danielsen, F., Brühl, C.A., Donald, P.F. and Phalan, B. 2008. How will oil palm expansion affect biodiversity? *Trends in Ecology and Evolution* **23** (10): 538-545.

Hassan, S. 2016. *Kajian Morfologi dan Kepelbagaian Parasit daripada Kelawar (Chiroptera) di Kawasan Konservasi Kanyon Imbak (ICCA), Sabah*. Thesis. Conservation Biology Program. Universiti Malaysia Sabah. Kota Kinabalu, Sabah.

Kingston, T., Francis, C. M., Akbar, Z., and Kunz, T. H. 2003. Species richness in an insectivorous bat assemblage from Malaysia. *Journal of Tropical Ecology* **19** (1).

Korine, C and Pinshow, B. 2004. Guild structure, foraging space use and distribution in a community of insectivorous bats in the Negev Desert. *Journal of Zoological London* **262**: 187-196.

Lee, M.T., Sodhi, N.S. and Prawiradilaga, D.M. 2007. The importance of protected areas for forest and endemic Avifauna of Sulawesi (Indonesia). *Ecological Application* **17** (6): 1727-1741.

Mahyudin, A., Yasuma, S., Md-Yusah, K., Abdul-Mawah, S.S., and Kho, J.M. 2010. Mammals Maliau Basin Conservation Area, Sabah, Malaysia: A Preliminary Study. *Journal of Tropical Biology and Conservation* **6**: 43-47.

Mahyudin, A., Amat, A., Daud, U.S., Robert, R., Abdul-Rani, S.N.F., Frances, F., Kuyun, S. Vijay, S.K., and Rahman, H. 2018. Characterisation of bat ectoparasite diversity in Pulau Banggi and Pulau Balambangan, Kudat, SABAH, Malaysia. *Sabah Parks Journal 2018.*

Mahyudin, A., Sukiman, S.S., Kumar, S.V and Hoque. M.Z. 2022a. Research Notes on Bats' Species Assemblage in Madai Cave of Segama Valley, Sabah, Malaysia. *I.O.P. Conference Series.: Earth Environment Science* **1053** 012017.

Mahyudin, A., Hussain, N.H.I., Rangkasan, J., Peter, C., Kuyun, S., Molius, N., Hoque. M.Z. and Kumar, S.V. 2022b. *The Diversity of Bats in Batu Supu Cave, Lower Kinabatangan Wildlife Sanctuary, Sabah, Malaysia*. Abstract presented in: Malaysian Conservation Conference. Kuching, Sarawak: 29-31 March 2022.

Nagendra, H. 2008. Do parks work? Impact of protected areas on land cover clearing. *AMBIO: A Journal of the Human Environment* **37** (5):330-337.

Nor, S. M. 1996. The mammalian fauna on the islands on the northern tip of Sabah, Borneo. *Fieldiana Zoology* **83**: 1-51.

Payne, J., Francis, C.M. and Philipps, K. 2007. *A Field Guide to Mammals of Borneo*. Sabah Society Kota Kinabalu.

Phillipps, Q., and Phillipps, K. 2016. *Phillipps' Field Guide to the Mammals of Borneo and Their Ecology: Sabah, Sarawak, Brunei, and Kalimantan*. Princeton University Press

Sedlock, J.L., Weyandt, S.E., Cororan, L., Demarow, M., Hwa, S.H. and Pauli, B. 2008. Bat diversity in tropical forest and agro-pastoral habitats within protected areas in the Philippines. *Acta Chiropterologica* **10** (2): 349-358.

Senawi, J., Mahyudin, A., Daud, U.S., Amat, A., Lagundi, S., Gondilang, E., Sutail, E., Narimin, S., and Azhar, I. 2020. Bat Diversity in Imbak Canyon Conservation Area: Note on Their

Echolocation Calls and Ectoparasites. *Journal of Tropical Biology and Conservation* **17**: 217-232.

Sodhi N.S., Koh, L.P., Brook, B.W. and Ng, P.K.L. 2004. Southeast Asia Biodiversity: an Impending disaster. *Trends in Ecology and Evolution* **19** (12): 654-660.

Struebig, M. J., Birute, M.F. G. and Suatma. 2006. Bat diversity in oligotrophic forests of southern Borneo. *Oryx* **40**(4): 447-455.

Struebig M. J., Bożek M., Hildebrand J., Rossiter S. J. and Lane D. J. W. 2012. Bat diversity in the lowland forests of the Heart of Borneo. *Biodiversity and Conservation* **21**: 3711-3727.

Sukiman, S. S. 2019. *Kajian terhadap kepelbagaian spesies kelawar di Gua Madai, Kunak, Sabah*. Thesis. Conservation Biology Program. Universiti Malaysia Sabah. Kota Kinabalu, Sabah.

Suyanto, A., and Struebig, M. J. 2007. Bats of the Sangkulirang limestone karst formations, East Kalimantan- a priority region for Bornean bat conservation. *Acta Chiropterologica*, **9** (1), 67-95.

Yasuma, S., & Andau, M. 2000. *Mammals of Sabah — part two, habitat and ecology*. Kuala Lumpur: Japan International Cooperation Agency and Sabah Wildlife Department.

Yoh, N., Azhar, I., Fitzgerald, K.V., Yu, R., Smith-Butler, T., Mahyudin, A. and Kingston, T. 2020. Bat Ensembles Differ in Response to Use Zones in Tropical Biosphere Reserves. *Diversity* **12** (60).

BorneoScience
The Journal of Science & Technology
Volume 45 Issue 2 : Sept 2024
Online ISSN : 2231-9085 | ISSN : 1394-4339

USED LUBRICATING OIL TREATMENT USING ACID ACTIVATION CLAY AS ADSORBENT FOR OIL RECOVERY

S M Anisuzzaman[1,2]*and Nurul Syufiana Jumadil[2]

[1]Energy and Materials Research Group, Universiti Malaysia Sabah,
Jalan UMS, 88400, Kota Kinabalu, Sabah, Malaysia
[2]Chemical Engineering Program, Faculty of Engineering, Universiti Malaysia Sabah, Jalan UMS,
88400, Kota Kinabalu, Sabah, Malaysia

Corresponding author: anis_zaman@ums.edu.my

Received 9th Ogos 2024; Accepted 28th Nov 2024
Available online: 31st December 2024
Doi:https://doi.org/10.51200/bsj.v45i2.5880

ABSTRACT. *The aim of this study was to assess the effectiveness of activated clay as an adsorbent in the recycling of used lubricating oil (ULO). To accomplish this, the research primarily concentrated on identifying the optimal parameters for the application of organic acids—specifically acetic acid and citric acid—in the acid activation of clay during the adsorption process. Montmorillonite K-10 clay served as the adsorbent and was activated to facilitate ULO recovery. According to the experimental findings, citric acid at a concentration of 1.0 mol/L for a reaction time of 45 minutes proved to be the most effective for ULO recovery. The optimal activated clay exhibited a viscosity of 95.10 cP and a density of 0.663 g/mL, achieving a water removal rate of 0.036% and sludge removal of up to 9.20%. Moreover, clay treated with citric acid produced a current of 1.3293 A, in comparison to 1.5721 A for acetic acid under identical conditions, as measured by Ultraviolet-visible (UV-Vis) spectrophotometry. The conditions involving citric acid at 1.0 mol/L for 45 minutes were further investigated using a scanning electron microscope (SEM) to analyze the clay before and after activation. Results indicated that the surface of the unmodified clay was smoother with fewer visible pores, whereas the activated clay displayed a more porous structure, with noticeable pores and cracks. The activated clay's average pore diameter was found to be larger, reflecting a 32.19% increase in pore size compared to the unmodified clay. Additionally, a considerable enhancement in pore area was observed, with the average pore size increasing from 1.614 µm to 2.077 µm, suggesting improved adsorption performance following activation. Fourier transform infrared spectroscopy (FTIR) was utilized to characterize and compare the recovered oil, revealing that activated clay treated with citric acid at 1.0 mol/L for 45 minutes was superior in eliminating most remaining contaminants, such as soot, water, fuel residues, carbonyl groups, discoloration, and other impurities compared to its pre-activated state.*

KEYWORDS. Used lubricating oil, adsorbent, viscosity, activated clay, Montmorillonite K-10 clay

INTRODUCTION

Lubricating oils, a diverse group of lubricants, are employed to reduce wear, heat, and friction among mechanical components in contact with one another. To enhance their properties, such as antioxidant effects, corrosion resistance, and anti-foaming capabilities, commercial base oils are often blended with various additive formulations (Moura et al., 2010). Over time, the lubricating oil undergoes changes due to oxidation, contamination, and degradation, rendering it unsuitable for further use and necessitating its replacement (Josiah & Ikiensikimama, 2010). Used lubricating oil (ULO) poses significant environmental hazards as it contains toxicants, carcinogens, and chronic aquatic toxicants. The gases emitted from waste oil can cause tissue irritation, particularly from compounds such as ketones, aldehydes, and aromatic chemicals. Additionally, elevated levels of heavy metals may adversely affect human health, particularly the prostate and respiratory systems (Vural, 2020). If ULO is not handled, treated, or disposed of properly, it can have harmful environmental consequences (Diphare *et al*., 2013). Typically, ULO contains high levels of contaminants, including carbon residues, asphaltenic materials, heavy metals, and water (Abdel-Jabbar et al., 2010). Such pollutants can significantly contribute to environmental contamination, with each volume of ULO capable of polluting at least 250,000 volumes of water (Udonne *et al*., 2016). Therefore, effective management of this hazardous waste is crucial to transform it into a valuable resource while ensuring environmental safety.

Lubricating oil degrades over time due to usage under various operating conditions. Several factors contribute to this degradation, with moisture absorption from the surrounding air being a primary cause that leads to a cloudy appearance or strong odor in the oil. The mechanisms underlying the degradation of used lubricating oil (ULO) include oxidation, thermal breakdown, micro dieseling, additive depletion, electrostatic spark discharge, and contamination. Oxidation alters the oil's viscosity, resulting in the formation of varnish, sludge, and sediment, as well as causing additive depletion, base oil breakdown, filter clogging, loss of foam properties, and increases in acid numbers, rust, and corrosion. Additionally, additive depletion can impede its ability to detect degradation levels and provide insights into specific degradation mechanisms. The contaminants found in ULO arise from both degradation processes and the operating environment. Waste components from engine oils and other lubricants—such as ash, soot, and solid metal particles resulting from wear—are examples of environment-derived contaminants (Rahman *et al*., 2008). According to Rațiu *et al*. (2020), there are four contamination mechanisms: built-in contamination, external ingression, internal generation, and mechanism-induced contamination.

According to Oladimeji *et al*. (2018), conventional treatment methods for used lubricating oil (ULO) include acid-clay treatment, solvent extraction, vacuum distillation, and hydrogenation. Solvent extraction and adsorption techniques are gaining attention due to their ability to produce high-quality products with lower costs, reduced energy consumption, minimized waste, and greater convenience (Mohammed *et al*., 2013). Despite various advanced technologies proposed for ULO recycling, such as supercritical separation, microwave pyrolysis, and catalytic processes, they are often deemed inefficient as they entail high energy demands, incomplete contaminant removal, elevated costs, and challenges for

scaled industrial application. Previous studies indicate that conventional acid-clay methods are low-cost but raise environmental concerns due to the use of inorganic acids, which can lead to corrosion of equipment and other environmental issues (Zhansheng *et al*., 2006; Opoku-Mensah *et al*., 2023). Therefore, utilizing weak acids to activate clay is preferable, as it mitigates environmental hazards by avoiding the release of harmful gases like sulfur dioxide and lessening the detrimental effects on equipment compared to stronger acids like hydrochloric and sulfuric acids (Hegazi *et al*., 2017). Key factors considered during processing include surface area and pore volume, properties influenced by the type of acid used and pore size. According to Khan *et al*. (2015), larger pore sizes facilitate more efficient removal processes. Additionally, solvent extraction combined with adsorption presents a promising approach for oil regeneration. Recent research has explored using solvent extraction followed by adsorbent activation to regenerate oil (Ani *et al*., 2023; Rosa *et al*., 2020; Velasco-Calderón *et al*., 2020). This combined method is considered more environmentally friendly, economically viable, practical, and less energy-intensive than other recycling methods. Variations in parameters during the acid activation process can enhance the physical and chemical properties of the recovered oil. Important parameters include the type and molar concentration of acids, temperature, contact time, the acid-to-clay ratio, and mixing speed, all of which influence the final adsorption properties of the clay. Table 1 presents different types of acids employed in various studies, along with comments on their usage.

Table 1. Factors influence on chosen acid for acid activation clay

Type of Acid	Findings	References
• Acetic acid • Formic acid	• Acetic acid is the best in treating used oil compare to formic acid • Have no reaction with base oil compare to sulfuric acid. • Did not emit poisonous gases to the atmosphere like sulphur dioxide. • Unlike sulfuric acid, have no adverse effects on the processing machinery. • Due to the base oil's low reactivity; fewer additives may be needed to recycle the base oil.	Hegazi *et al.*, 2017
• Oxalic acid • Acetic acid • Phosphoric acid • Citric acid	• Oil's colour, smell, and taste can be improved by rubbing it on a surface active substance that adsorbs undesirable particles from the oil. • Oxalic acid gives the best results among the other acids.	Khan *et al.*, 2015

• Acetic acid	• This process involve the addition of acetic acid and the result showed improvements on kaolin adsorbent on adsorption capacity due to separation of water content and butanol breaking contained in the ULO. • However, using glacial acetic acid show unsatisfied result as it not helping as acetic acid function.	Riyanto *et al.*, 2018

This study primarily investigates the use of acid-activated clay as an adsorbent in conjunction with the solvent extraction process for the recovery of used lubricating oil (ULO). Montmorillonite K-10 clay was selected as the adsorbent and activated for this purpose. Montmorillonite K-10 was specifically chosen due to its status as an eco-friendly solid catalyst and its unique properties, such as ion exchange capacity and swelling characteristics, which enhance its ability to adsorb other ions in its interlayers (Kumar *et al*., 2014). Its high surface area contributes to significant adsorption capabilities (Uddin, 2018). Furthermore, Montmorillonite is favored for its cost-effectiveness compared to other clays, including smectite, kaolinite, and vermiculite (Alekseeva et al., 2019). Among various solvents tested, including methyl ethyl ketone (MEK), 1-hexanol, and 2-butanol, 1-butanol demonstrated the highest efficiency in removing sludge contaminants from the oil (Kamal *et al*., 2009). Additionally, potassium hydroxide (KOH) was incorporated as it serves as a coagulant for contaminants and can be effectively absorbed by the adsorbent or eliminated during the sludge extraction process (Riyanto *et al*., 2018).

MATERIALS AND METHODS

Materials

This study utilized several key chemicals, including acetic acid, citric acid, Montmorillonite K-10 clay, 1-butanol, potassium hydroxide (KOH), used lubricating oil (ULO), virgin lubricating oil (VLO), and distilled water. The Montmorillonite K-10 was obtained from Acros Organics in Belgium, while 1-butanol and KOH were sourced from Sigma-Aldrich. The Montmorillonite K-10 clay was in granular form, and the lubricant examined was PETRONAS Syntium 3000 5W-40, which has a viscosity range of 5 at low temperatures to 40 at high temperatures. The ULO sample was gathered from a local workshop located in Menggatal, Kota Kinabalu, Malaysia.

Pretreatment of ULO

Prior to the solvent extraction, the used oil was initially subjected to a dehydration process to eliminate excess water and light hydrocarbons. This dehydration was performed at a temperature ranging from 120 to 210°C for one hour using a water bath setup on a hot plate within a fume hood. Following this, the used lubricating oil underwent the solvent extraction process.

Solvent Extraction Procedure

In this solvent extraction method, 1-butanol served as the solvent and was combined with the oil that had previously undergone a dehydration process. The solvent-to-oil ratio was set at 3:1, and the mixture was stirred for 15 minutes at a speed of 350-400 rpm, with the addition of 2 g of KOH, to ensure thorough mixing while minimizing oil loss due to sludge formation. Subsequently, the mixture was allowed to settle for 24 hours at room temperature before being filtered using oil filter paper and a vacuum pump (Riyanto et al., 2018; Mohammed *et al*., 2013). The final step of the solvent extraction involved evaporating the excess 1-butanol from the oil using a vacuum distillation column. The used lubricating oil then underwent an adsorption process utilizing clay as the adsorbent.

Adsorption Experiment

The modification of clay through an activation procedure was carried out following the method described by Salem *et al*. (2015), with some adjustments. A total of 40 g of dry Montmorillonite K-10 clay was mixed with 250 mL of various concentrations of acetic acid and citric acid, specifically 0.2, 0.3, 0.4, 0.5, and 1.0 mol/L. The mixture was then heated to a temperature range of 80 to 100°C. At this temperature, reactions were conducted for different durations of 10 and 45 minutes before the mixture was filtered and washed with distilled water to remove any excess acid and ions. In the final step, the clay filtrate underwent a drying process in an oven at 60°C for 24 hours to ensure maximum moisture removal (Khan *et al*., 2015). The activated clay was subsequently ground to achieve a fine texture. For the oil treatment, 15 g of the activated clay was added to 60 mL of oil and allowed to contact for 30 minutes at a moderate speed to optimize physical properties, after which it was left to settle for one hour at room temperature (Abdel-Jabbar et al., 2010). This was followed by a centrifugation process at 3000 rpm for 30 minutes, leading to the filtration of the final recovered oil. Table 2 provides the names of each activated clay sample.

Table 2. Naming of each samples of activated clay

Sample	Type of clay	Sample naming
1	Montmorillonite K-10, XC	Inactivated Montmorillonite K-10
2	Activated Acetic Acid, AA-1	AA 0.2 mol-1 (10 min)
3	Activated Acetic Acid, AA-2	AA 0.2 mol-1 (45 min)
4	Activated Acetic Acid, AA-3	AA 0.3 mol-1 (10 min)
5	Activated Acetic Acid, AA-4	AA 0.3 mol-1 (45 min)
6	Activated Acetic Acid, AA-5	AA 0.4 mol-1 (10 min)
7	Activated Acetic Acid, AA-6	AA 0.4 mol-1 (45 min)
8	Activated Acetic Acid, AA-7	AA 0.5 mol-1 (10 min)
9	Activated Acetic Acid, AA-8	AA 0.5 mol-1 (45 min)
10	Activated Acetic Acid, AA-9	AA 1.0 mol-1 (10 min)

11	Activated Acetic Acid, AA-10	AA 1.0 mol-1 (45 min)
12	Activated Citric Acid, CA-1	CA 0.2 mol-1 (10 min)
13	Activated Citric Acid, CA-2	CA 0.2 mol-1 (45 min)
14	Activated Citric Acid, CA-3	CA 0.3 mol-1 (10 min)
15	Activated Citric Acid, CA-4	CA 0.3 mol-1 (45 min)
16	Activated Citric Acid, CA-5	CA 0.4 mol-1 (10 min)
17	Activated Citric Acid, CA-6	CA 0.4 mol-1 (45 min)
18	Activated Citric Acid, CA-7	CA 0.5 mol-1 (10 min)
19	Activated Citric Acid, CA-8	CA 0.5 mol-1 (45 min)
20	Activated Citric Acid, CA-9	CA 1.0 mol-1 (10 min)
21	Activated Citric Acid, CA-10	CA 1.0 mol-1 (45 min)

Water content removal

The detection of water content in used lubricating oil (ULO) was conducted through a series of steps. First, the ULO was pre-treated by filtration to remove contaminants, such as small debris, using a sieve. Next, an empty 250 mL beaker was weighed on an electronic balance. Then, 100 mL of the ULO was measured using a measuring cylinder and transferred to the beaker, with the final measurement of the 100 mL of treated ULO recorded. The sample was subsequently heated in an oven at 250°C to evaporate any water residue, as described by Hamawand *et al*. (2013). After heating for an hour, the samples were allowed to cool to room temperature and then weighed again. The final weight was documented, and the weight of the dehydrated ULO was calculated. The percentage of water removal was determined using Equation (1), where the initial mass refers to the mass of the oil prior to drying, and the final mass refers to the mass of the oil after drying, measured in grams. (Zheng *et al*., 2014).

$$Water\ removal, \% = \frac{initial\ mass\ (g) - final\ mass\ (g)}{initial\ mass\ (g)} \times 100 \quad (1)$$

Sludge removal

The removal of sludge occurred during the adsorption process of the lubricant oil. In this process, 15 g of adsorbent was added to 60 mL of used lubricating oil (ULO) at a temperature of 90°C to facilitate the settling of sludge, which is a type of contamination in the oil. After 30 minutes, the mixture of adsorbent and oil was centrifuged to separate the oil from the sludge. Prior to transferring the oil, the mass of the centrifuge tube was recorded. Then, 20 mL of oil was measured with a measuring cylinder and transferred into the centrifuge tube, after which the total mass was measured again. The oil and sludge mixture were then centrifuged at 4000 rpm for one hour to achieve separation. This resulted in the formation of two layers in the centrifuge tube, with sludge at the bottom and sludge-free oil on top. The sludge-free oil was carefully transferred to a beaker with the aid of a dropper. Following this, the centrifuge bottle containing the sludge was dried in an oven to solidify it. Subsequently, the mass of the centrifuge bottle with the sludge was weighed using an electronic balance. Finally, the quantity of sludge generated per

20 mL of oil was determined by subtracting the combined mass of the tube and sludge from the mass of the tube and the 20 mL of oil. The mass of sludge produced per 20 mL of oil was calculated using Equation (2), where *W*dry refers to the mass of the sludge in grams (Daham et al., 2017).

$$Sludge\ \ removal, \% = \frac{Wdry}{Woil} \times 100 \quad (2)$$

Density

To determine the densities of the oil samples at room temperature, the density formula (density = mass/volume) was used (Abu-Elella et al., 2015). Each oil sample was carefully poured into a density bottle with a known mass and volume. The masses of both the oil and the bottle were recorded, and the mass of the oil was then calculated using the known volume of the bottle. By utilizing the recorded mass and volume, the density was subsequently calculated using Equation (3):

$$Density = \frac{Mass\ of\ the\ sample\ oil,\ \ g}{Volume\ of\ the\ sample\ oil,\ \ mL} \quad (3)$$

Viscosity

The DV-E Viscometer, a digital device, was used to measure the viscosity of the regenerated oil. The established method required choosing a suitable spindle and pouring an appropriate amount of the regenerated oil into a beaker. The beaker was placed under the spindle, and the spindle was submerged to the specified line. Consistent factors, such as temperature, spindle size, and spindle speeds, were kept uniform for all samples. Once the motor was activated, the instrument displayed the measured viscosity in centipoise (cP), and the highest value was noted for further analysis.

Recovered ULO Characterization

The lubricating oil sample obtained from the regeneration process was analyzed to determine its suitability for reuse. This sample was then compared with the characteristics of a fresh oil sample to facilitate the evaluation of the effectiveness of the treatment in restoring the properties of new oil. Additionally, the recovered oil underwent analysis using Fourier-transform infrared spectroscopy (FTIR), Ultraviolet-Visible (UV-Vis) Spectroscopy, and scanning electron microscopy (SEM) for morphological assessment.

Functional group and chemical structure analysis using FTIR

FTIR was utilized to analyze the functional groups and chemical structure of the oil. The FTIR instrument employed in this study operates within a wave number range of 400 to 4000 cm^{-1} (Salem et al., 2015). Our primary focus is on examining the structure of the treated oil and identifying the functional groups associated with fuel residue, ash, carbonyl groups, water, and other contaminants. If the clay treatment

results in an increase in unsaturated hydrocarbons and a reduction in straight-chain hydrocarbons, it suggests an enhanced adsorption capacity performance (Khan et al., 2015). Therefore, FTIR was applied to the recovered oil to assess the effectiveness of contaminant removal in the oil's chemical structures.

Recovered oil concentration analysis using UV-Vis Spectroscopy

The recovered oil was analyzed using UV-Vis spectroscopy to assess the concentrations and the UV wavelengths absorbed. The treated lubricating oil's color was evaluated at a peak wavelength of 510.02 nm for all samples to facilitate easier comparisons, as referenced in the study by Salem *et al*. (2015). Prior to this analysis, modified oil samples (1 mL) were diluted with kerosene (10 mL) because kerosene is more compatible with mass spectrometric analysis (Shigidi *et al*., 2020).

Surface analysis using SEM

The surface characteristics, including pore shape, distribution, and size, of both modified and unmodified CAC were analyzed using a Hitachi Scanning Electron Microscope (SEM). SEM enabled direct observation of microstructural changes on the surface of the modified Montmorillonite K-10 clay, allowing for a comparison with the unmodified version. Magnifications between 100x and 3000x were utilized to capture high-resolution images. The surface morphology, including pore size and porosity, of both the unactivated and activated Montmorillonite K-10 clay was evaluated using *ImageJ*, a Java-based image processing software developed by researchers at the National Institutes of Health and the Laboratory for Optical and Computational Instrumentation at the University of Wisconsin. *ImageJ* is freely available for download on Microsoft Windows and features a user-friendly interface tailored for calculating distances and areas as well as generating statistical graphs based on the results (Chilev, 2017).

RESULTS AND DISCUSSION

FTIR Analysis of ULO and VLO

Figure 1 displays the components present in both types of oil based on the peaks and transmittance observed in the FTIR analysis. VLO serves as a reference for further detailed studies. The analysis revealed that virgin lubricants primarily consist of hydrocarbons, specifically -CH and -CH_2 groups, with peaks at 1374.05 and 1374.59 cm^{-1} corresponding to -CH and peaks at 2854.26 and 2854.48 cm^{-1} associated with -CH_2, which are evident in both VLO and ULO. Additionally, a band at 968.17 cm^{-1} indicates the presence of additive compounds, particularly anti-wear additives, which were present in the existing lubricating oil but undetected in ULO (Patty and Lokollo, 2016). This may be attributed to the consumption of additives that enhance lubricating performance during use. Long-chain hydrocarbons were also confirmed, indicated by a peak at 2919 cm^{-1} (Timur, 2017). Components such as carbonyl-containing degradation products (C=O), resulting from oxidation, were not detected. In contrast, ULO contains various contaminants, including soot, carbonyl oxidation products, sulfur oxidation products,

and water. It was noted that used lubricating oils predominantly consist of paraffinic, naphthenic, and aromatic molecular structures. Paraffinic compounds are characterized by straight chains of normal alkanes, while naphthenic compounds consist of cycloalkanes, which contain at least one six-carbon ring with single or double bonds, and aromatic structures include ringed compounds (Zeng *et al*., 2016).

The FTIR analysis also identified components such as OH (3600 – 2500 cm^{-1}), C=O (1900 - 1600 cm^{-1}), and C-O (1500 – 900 cm^{-1}), indicating the presence of alcohols, ketones, aldehydes, carboxylic acids, and esters. A prominent band at 3338.79 cm^{-1} suggests the presence of hydroxyl groups from water molecules in ULO. Soot contamination was also detected, with peaks around 2000 cm^{-1} at 2074.59 cm^{-1} and 1962 cm^{-1}. The peak at 1750 cm^{-1} corresponds to carbonyl oxidation products with a C=O functional group, which may include lactones, esters, aldehydes, ketones, carboxylic acids, and salts. Moreover, sulfur oxidation products were found in both oils at 1159.75 cm^{-1}. According to Zhu *et al*. (2019), oxidation occurs over time, even if the oil is not used or stored under optimal conditions. The presence of unexpected compounds may result from exposure to high temperatures or air during storage or handling, leading to chemical modifications in the lubricant formulation. Furthermore, Adamczewska *et al*. (2005) noted that oxidation is a significant concern for lubricating oils, which is why they have a limited shelf life. Overall, ULO was confirmed to contain various contaminants, including fuel, glycol pollution, oxidation, nitration, sulfation products, soot, and water contamination, in contrast to VLO (Abu-Elella *et al*., 2015).

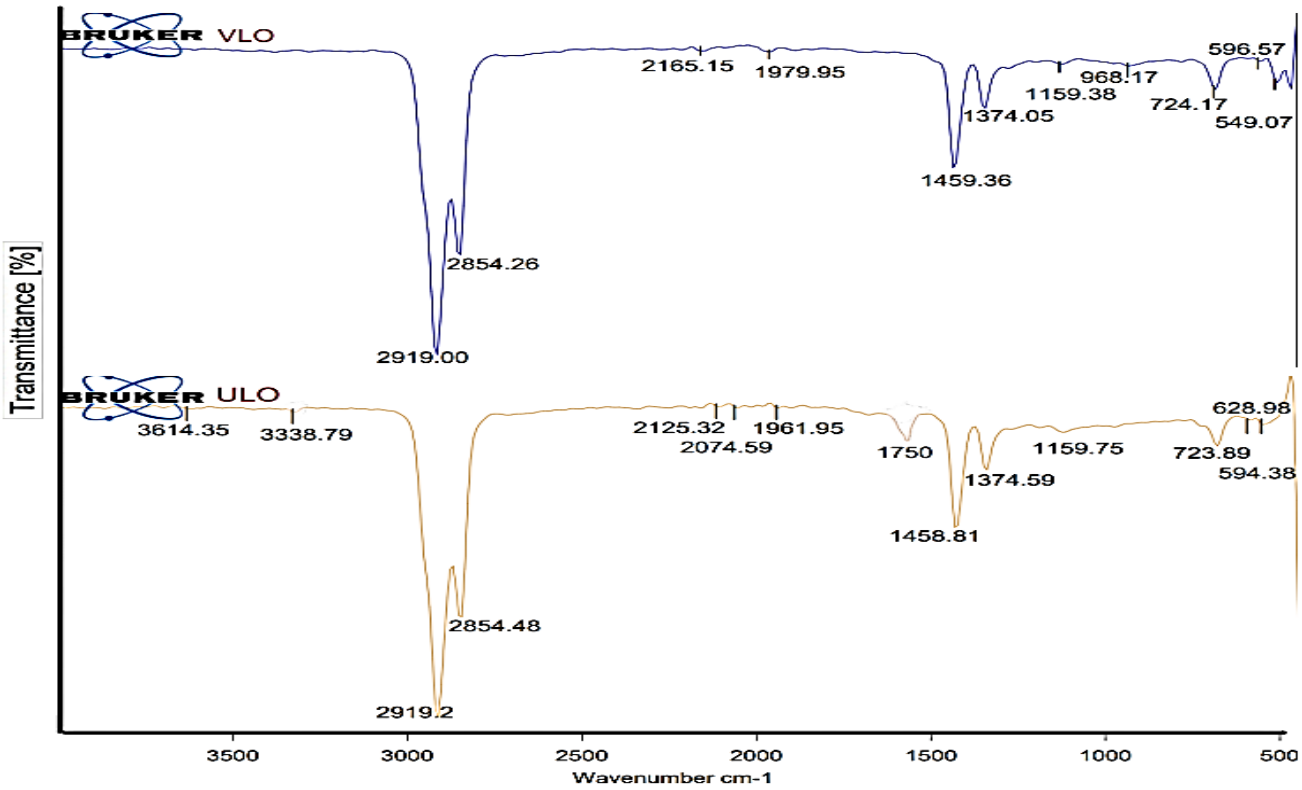

Figure 1: The comparison of wavelength signals detected in the FTIR analysis between used lubricating oil (ULO) and virgin lubricating oil (VLO).

Table 3 also presents a comparative analysis of various properties, including the effectiveness of water removal, the amount of sludge removed following the acid activation of clay, as well as the density and viscosity of the treated lubricating oil. The results highlight the differences in performance metrics, providing valuable insights into how the treatment process impacts the overall quality and characteristics of the lubricating oil.

Table 3. Water content and sludge removal in used lubricating oil (ULO) after acid activation of clay; and density and viscosity of the treated lubricating oil.

Samples	Water content removal, %	Sludge removal, %	Density, g/mL	Viscosity at room temperature, cP
AA-1	0.036	4.27	0.713	117.32
AA-2	0.024	3.82	0.879	116.54
AA-3	0.011	6.33	0.795	118.23
AA-4	0.012	5.48	0.753	115.76
AA-5	0.012	3.51	0.980	115.32
AA-6	0.012	4.95	0.708	113.50
AA-7	0.024	5.04	0.864	116.21
AA-8	0.036	8.31	0.793	113.29
AA-9	0.036	3.97	0.671	110.67
AA-10	0.036	1.90	0.711	113.25
CA-1	0.036	6.55	0.733	114.45
CA-2	0.024	6.32	0.740	115.20
CA-3	0.024	3.13	0.820	114.20
CA-4	0.036	4.96	0.812	114.80
CA-5	0.024	6.34	0.760	115.27
CA-6	0.036	4.19	0.700	116.80
CA-7	0.024	7.47	0.640	112.43
CA-8	0.024	7.77	0.703	99.95
CA-9	0.036	8.33	0.732	99.79
CA-10	0.036	9.20	0.663	95.10

Water content removal

The water content found in lubricating oil was categorized as chemical contamination. According to Hamawand *et al.* (2013), water enters the oil through moisture absorption, condensation from humid air, combustion byproducts, and neutralization as engine oil is hygroscopic in nature. Udonne (2011) states that the presence of water in engine oil was inevitable due to factors like air cooler and engine cooling system leaks causing atmospheric condensation. Table 3 presents the results of the water content levels. t was evident that all twenty samples of used lubricating oil (ULO) analyzed in this study contained water, which confirmed its presence in each sample. This finding is consistent with the data from the

FTIR analysis, indicating that complete removal of water occurred after treatment with 1.0 mol/L of citric acid for 45 minutes. According to Assunção Filho *et al*. (2010), among the methods involving (ethanol+activated carbon), (2-propanol+activated carbon), and (1-butanol+activated carbon) for determining the base oil, the combination of ethanol solvent and activated carbon achieved the highest reduction in water content, with a decrease of 58.33%.

Sludge removal

As stated by Hamawand et al. (2013), the poly-condensation and polymerization reactions that occur in used engine oil with high molecular weight result in the formation of insoluble products known as sludge. This phenomenon is linked to the secondary oxidation phase, which occurs at elevated temperatures. During this phase, the viscosity of the oil increases due to the poly-condensation of oxygenated products produced in the primary oxidation phase, such as carboxylic acids. Moreover, it has been noted that sludge formation is exacerbated as the adsorbent properties of clay improve (Devi *et al*., 2016). In this study (Table 3), clay activated with 1.0 mol/L citric acid for 45 minutes showed the highest sludge removal rate at 9.20%. This enhancement is likely attributed to the adsorbent characteristics of the clay, including its pore structure, surface area, acidity, and the effects of different concentrations, reaction times, and types of acids used in treatment. Chen *et al*. (2018) noted that effective adsorbent properties can significantly capture products resulting from oxidation, nitrification, and sulfide formation in lubricating oil. Increasing the acid concentration can enhance the surface area of the clay and decrease its hygroscopic properties (Suhdi & Wang, 2021). Additionally, the presence of ash plays a crucial role in sludge removal, as it can hinder adsorption performance by weakening the mechanical strength of the carbon (Zulkania *et al*., 2018). Furthermore, the level of purity of the carbon, indicated by the ash content, affects adsorption performance by leading to inactive sites and clogging of pores (Martínez-Mendoza *et al*., 2020; Yusufu *et al*., 2012).

Density

In this study, the densities of virgin lubricating oil (VLO) and used lubricating oil (ULO) were measured, with values recorded at 0.533 g/mL and 0.824 g/mL, respectively. The results show that ULO exhibits a higher density than VLO as well as all treated lubricating oil samples. The increased density of ULO can be attributed to the solid particles present within it. Additionally, the density of ULO rises due to contaminants such as metals and oxidation products that accumulate while the oil is in use (Hamawand et al., 2013). Consequently, the aim of recovering ULO was to restore its density properties. The CA-10 clay samples exhibited a density of 0.663 g/mL, the closest to that of VLO (Table 3). This indicates that the properties of the clay were particularly effective in removing contaminants, resulting in a lower density compared to the untreated oil. It is important to note that density is influenced by temperature, with variations occurring as temperature changes. The density of lubricating oil is significantly affected

by its composition; oils rich in aromatic compounds tend to have a higher specific density compared to those consisting predominantly of saturated compounds, which results in a lower specific gravity (Udonne, 2011).

Viscosity

The viscosity of the regenerated oil was measured using a DV-E Viscometer at 600 rpm, with the same spindle size applied across all samples for consistency in comparison. Initially, the virgin lubricating oil (VLO) and used lubricating oil (ULO) were evaluated, yielding recorded viscosities of 87.9 cP and 123.7 cP, respectively. The viscosities of VLO and ULO were thus found to be 87.9 cP and 123.7 cP, respectively (Table 3). Among the treatments, the optimal viscosity that was closest to VLO was achieved with citric acid at a concentration of 1.0 mol/L over a 45-minute activation period, resulting in a viscosity of 95.10 cP. However, this finding contrasts with results reported by Hegazi *et al*. (2017), which indicated that ULO had a lower viscosity compared to VLO when various regeneration methods were compared. The lower viscosity might be attributed to the combustion of oil, leading to a fuel mixture that dilutes the lubricants (Młynarczak & Sikora, 2014). This underscores the influence of specific contaminants on viscosity. It is crucial to understand how different contaminants affect the viscosity of lubricants since particulate matter can infiltrate the lubricants and alter their chemical properties, leading to increased viscosity. Other contributing factors include elevated temperatures during operation that can result in oxidation by-products, polymerization, and carbon deposits, all of which can further increase viscosity (Raţiu *et al*., 2021).

UV-Vis Spectrophotometry Analysis

Based on the FTIR analysis presented in Table 3, treatment with citric acid at a concentration of 1.0 mol/L for 45 minutes proved to be optimal, resulting in a density of 0.663 g/mL, a sludge removal rate of 9.20%, and a viscosity of 95.10 cP, making it nearly as refined as the recorded virgin lubricating oil (VLO). To further clarify the physical properties discussed, chemical analyses, including UV-Vis spectrophotometry, were performed to identify which clay treatment resulted in the lowest absorbance of contaminants in the treated lubricating oils. UV-Vis spectrophotometry also characterized the color changes of all refined oils based on their UV absorbance. This analysis was conducted at a peak wavelength of 510.02 nm across all samples to facilitate easier comparison, following the methodology established by Salem et al. (2015). Several factors influence the adsorption properties of clay, ultimately impacting the quality of the oil. Various investigations were carried out, exploring different molar concentrations of various types of acids at varying activation times.

Figure 2 illustrates the effect of molar concentration on the absorbance value after a 10-minute activation period. Additionally, surface morphology, pore diameter, and pore size were characterized

using SEM to examine the differences before and after the activation of Montmorillonite K-10 based on the optimal conditions. The UV-Vis spectrophotometry analysis revealed that as the molar concentration of both acids increases, their absorbance decreases. This reduction in absorbance signifies that less light is transmitted, indicating a lower concentration of oil as the colors appear lighter. The most favorable result was observed with citric acid at a concentration of 1 mol/L, yielding an absorbance of 1.5721 A. This effect may be attributed to the presence of H+ ions in the clay, which can replace cations (Kemala *et al*., 2019), thereby enhancing the adsorption properties of the clay. Additionally, Khan *et al*. (2015) reported that 1N of organic acids is optimal for the activation process. Similarly, Salem *et al*. (2015) found that a concentration of 1.0 mol/L exhibited the most significant reduction in absorbance compared to other molar concentrations.

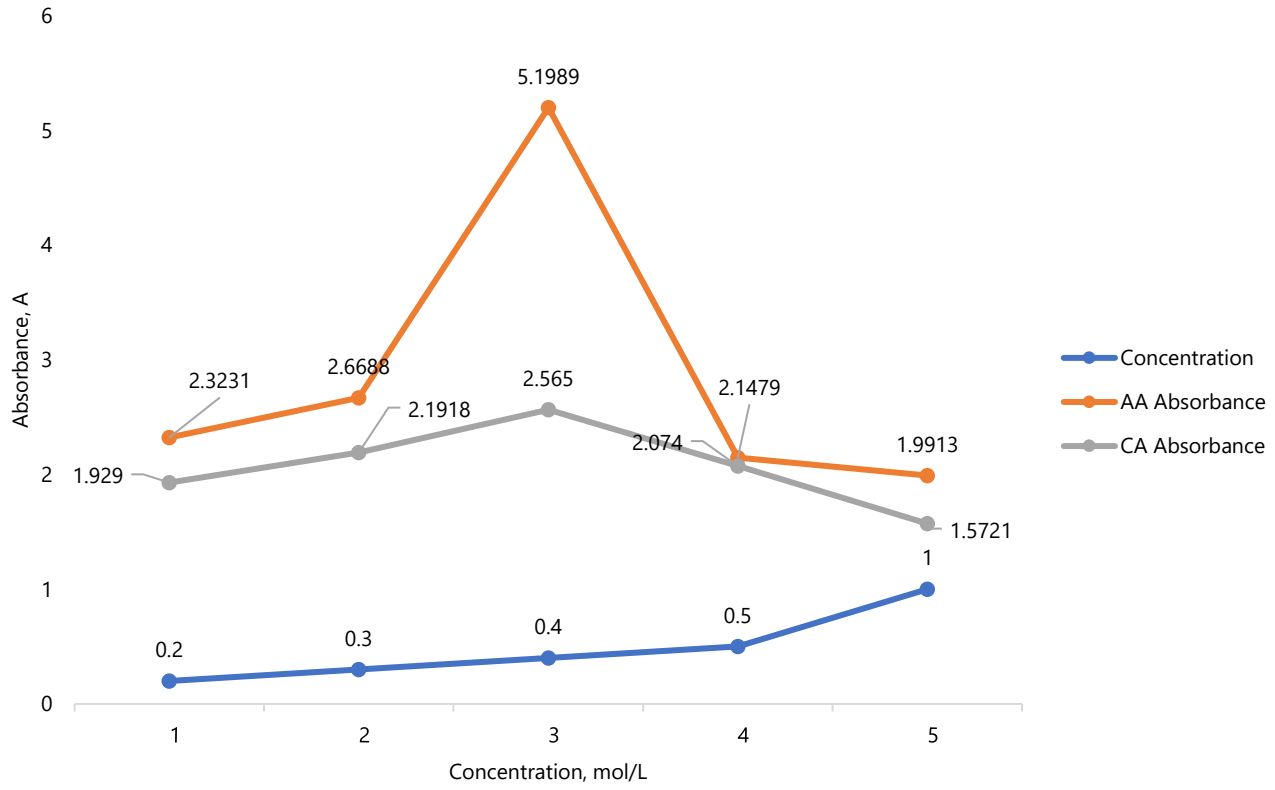

Figure 2. The effect of acid molar concentration on absorbance after a 10-minute activation period.

The second investigation aimed to compare both types of acid at varying molar concentrations, maintaining a reaction time of 45 minutes. A similar trend was observed during this reaction, where an increase in molar concentration led to an overall decrease in the absorbance of the refined oil. Figure 3 shows that citric acid provided the best absorbance, measuring 1.3293 A at a concentration of 1 mol/L. Across both investigations, citric acid demonstrated superior performance compared to acetic acid in terms of oil quality. This could be attributed to citric acid exhibiting sharp peaks in the FTIR analysis,

which indicates a strong presence of unsaturated esters and saturated aliphatic hydrocarbons (Khan *et al*., 2015). Their findings suggest that a higher concentration of these compounds enhances the adsorption capacity of the activated clay.

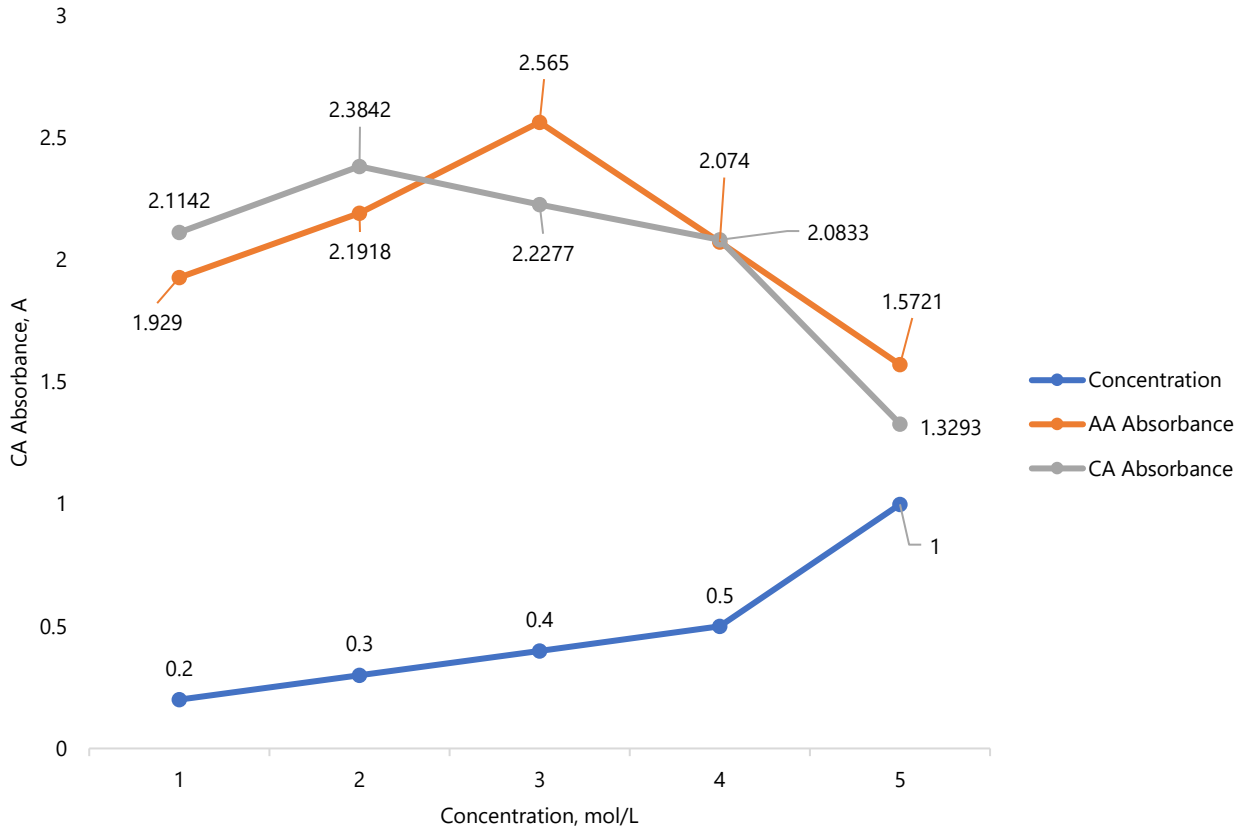

Figure 3. The effect of acid molar concentration on absorbance after a 45-minute activation period.

In comparing the activation times, it was observed that as the duration increased from 10 to 45 minutes, the absorbance of both citric acid and acetic acid at a concentration of 1 mol/L decreased (Figure 4). This indicates that a lower concentration of contaminants was being adsorbed from the oil over time, suggesting that the clay effectively removed these contaminants. Thus, the reaction time during acid activation of the clay is a critical factor in determining the quality of the refined oil. According to Kemala *et al*. (2019), the adsorption capacity of the clay improves with longer reaction times. When evaluating which acid was more effective after 45 minutes, citric acid exhibited the lowest absorbance at 1.3293 A, compared to 1.5721 A for acetic acid. This further confirms that acid activation with citric acid resulted in better refinement of the oil. In conclusion, all treated samples demonstrated lower absorbance compared to the used lubricating oil (ULO). The adsorption process effectively improved the color of the ULO, indicating that citric acid at a concentration of 1.0 mol/L for 45 minutes serves as the optimal parameter for achieving well-refined oil.

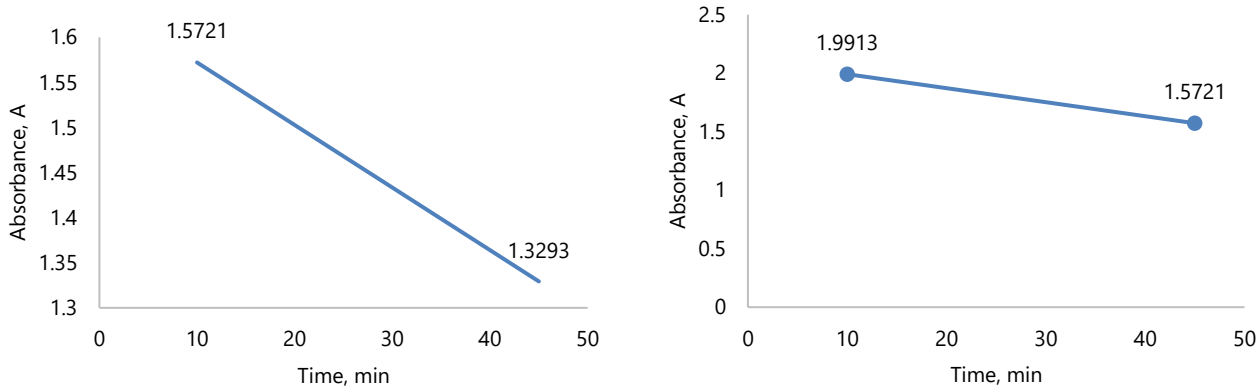

Figure 4. The obsorbance performance of various acids at different activation times

SEM Analysis on Activated Clay

Morphological Structure

To investigate the morphological structure, SEM analysis was performed based on the optimal parameters established from earlier characterizations of both activated and inactivated Montmorillonite K-10 clay. SEM images were taken at a magnification of 1500x, with an accelerating voltage of 15 kV and a pressure of 70 Pa for all samples. As shown in Figure 5, the surface of unmodified Montmorillonite K-10 appeared smoother, with less visible pores compared to the activated clay. Although the surface of the unmodified clay exhibited some scattered pores, it did not show any visible cracks (Figure 5(a)). In contrast, the surface-modified Montmorillonite K-10, depicted in Figure 5(b), displayed more distinct pore development with various shapes, sizes, and agglomerations.

Adsorption takes place because the surface particles of the adsorbent behave differently than those in the bulk. Chemical adsorption is distinguished by the stronger interactions between the adsorbate and adsorbent, resulting from covalent bonds and electrostatic forces, unlike physical adsorption (Ameri et al., 2020). Various factors have a significant impact on the effectiveness of the adsorption process. Ajemba & Onukwuli (2013) state that the efficiency of adsorption using activated clay improves with time. Additionally, temperature affects adsorption efficacy, and increasing the dosage of the adsorbent in a solution enhances the adsorption process. Zhang et al. (2017) observed that before treatment, the kaolin structure had distinct edges and a relatively smooth surface, which altered after activation. Amari et al. (2018) found that acid activation led to the formation of fine-grained aggregates of clay platelets, irregular arrangements of curved flakes, and coalesced flakes following activation.

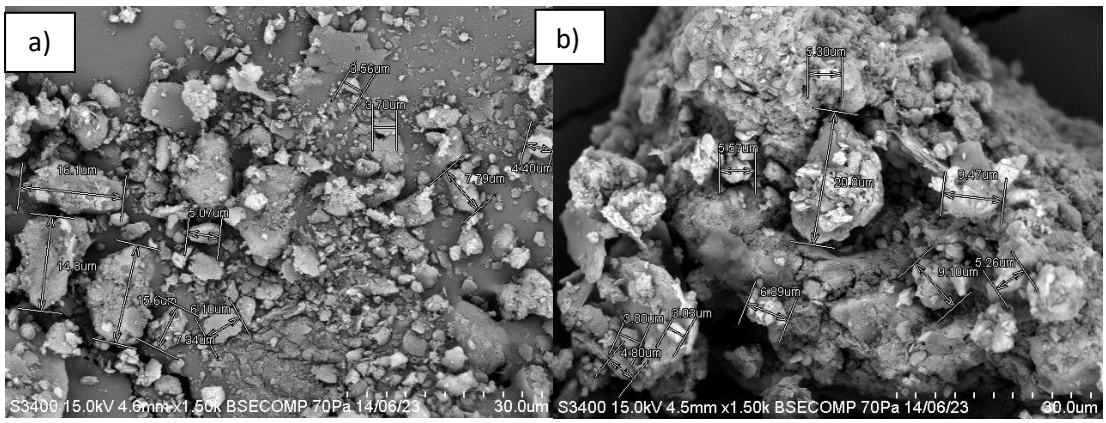

Figure 5. SEM images showing a) the clay before activation and b) the clay after activation (CA 1.0 mol/L, 45 minutes)

Surface Morphology Analysis of Modified Montmorillonite K-10 Clay

Analyzing surface morphology, including the average Feret diameter, average pore size, surface area, and porosity, is crucial for identifying enhancements on the surface that may improve the adsorption of adsorbate molecules. SEM images of both unmodified and modified Montmorillonite K-10 clay at a magnification of 1500x were examined using *ImageJ* software. The average Feret diameter and average pore size data were utilized to create a histogram reflecting the distribution of average measurements, while porosity data was obtained directly from the software.

Average Feret diameter

The Feret diameter, commonly referred to as "caliper length," represents the diameter of the circumscribed circle or the maximum distance between any two points along the perimeter of an object. The average Feret diameter was utilized to compute the pore diameter of the samples, as the pores do not have fixed shapes or sizes due to the activation process. Figure 6 indicates that the average pore diameters for unmodified and modified Montmorillonite K-10 were 5.701 µm and 7.536 µm, respectively. This demonstrates a notable increase in pore diameter in comparison to the raw material, with a 32.19% increment in pore diameter for modified Montmorillonite K-10 clay. According to the International Union of Pure and Applied Chemistry (IUPAC), all Montmorillonite samples exhibit micropores (< 2 nm) that facilitate the movement of adsorbates into mesopores (> 2 nm) (Dutta *et al.*, 2018). The enhanced pore diameter of modified Montmorillonite K-10 clay indicates that citric acid effectively expanded the pores in its carbonaceous structure. Research by Temuujin et al. (2004) showed that using acid activation, particularly leaching, on montmorillonite-rich clay from Tuulant (Mongolia) led to the production of a silica material with improved porosity. This porosity consisted of micropores ranging from 3-5 nm and mesopores ranging from 6-10 nm. Temuujin *et al*. also suggested that the formation of mesopores resulted from the delamination of the card-house structure rather than from the condensation of micropores.

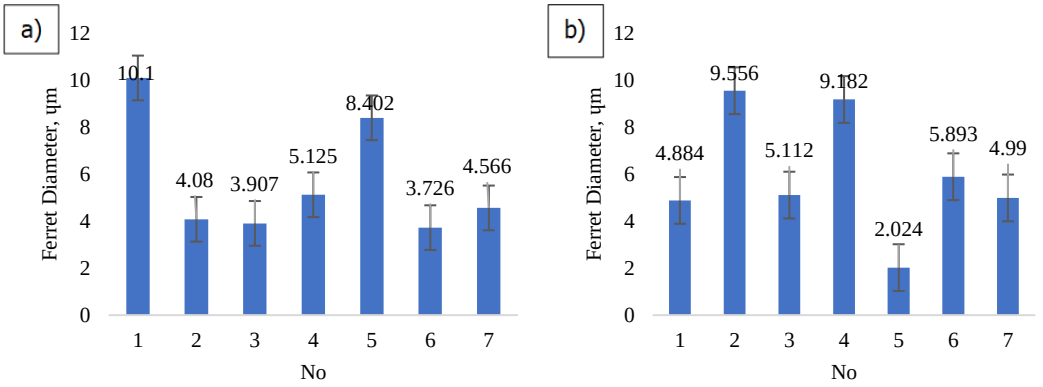

Figure 6. Ferret diameter distribution for a) before activation and b) after activation (CA 1.0 mol/L, 45 minutes)

Average pore size, surface area and porosity

Pore size is a crucial factor in the adsorption of contaminants. A larger pore size is vital as it reveals whether a pore is blocked, partially blocked, or completely open due to impurities. Increased pore size on the surface indicates that impurities were removed during the activation process, resulting in a greater number of active sites, which enhances the adsorption performance of Montmorillonite K-10 clay. Figure 7 shows the pore size distribution of both unmodified and modified Montmorillonite K-10 clay. The average pore sizes were measured at 1.614 µm for the unmodified clay and 2.077 µm for the activated version. Notably, the modified clay exhibited a considerable enhancement in pore area compared to the unmodified counterpart (Ravichandran & Sivasankar, 1997). The application of an acid, such as citric acid at a concentration of 1 mol/L, can significantly create well-defined pores that are advantageous for the adsorption process, as it makes the surface more acidic (Wahyuningsih *et al*., 2020). This indicates that acid-modified Montmorillonite K-10 clay has pronounced and uniform pore structures on its surface, suggesting that the modified clay has an increased porosity. Thus, modified Montmorillonite K-10 clay is an effective adsorbent for adsorption purposes.

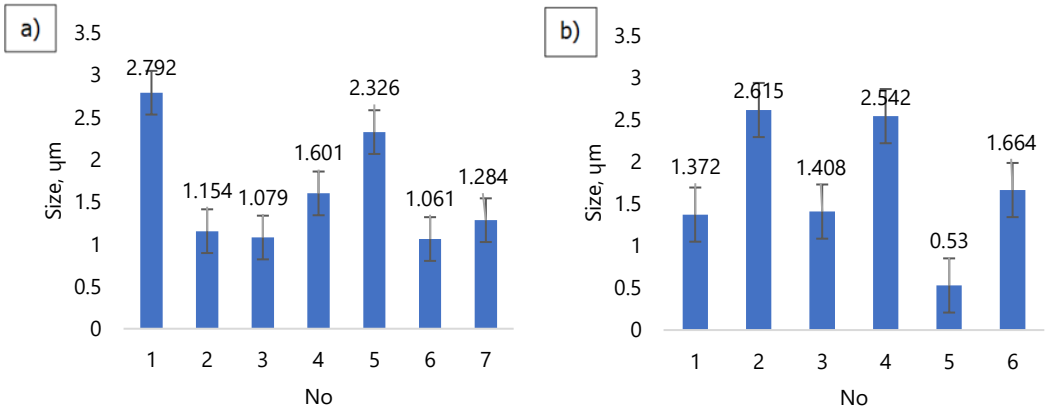

Figure 7. Pore size distribution for a) unmodified Montmorillonite K-10, b) modified Montmorillonite K-10 (CA 1.0 mol/L, 45 minutes)

Table 4 presents the pore characteristics determined using *ImageJ* software. Modified Montmorillonite K-10 clay exhibits a greater surface area than its unmodified counterpart. This increase in porosity may be attributed to the findings from previous studies, which noted that the surface area of acid-activated clay rose threefold to 93.9 m^2/g (Temuujin *et al*., 2003). Similarly, Zhang *et al*. (2017) reported that the specific surface area of kaolin increased from 8.18 m^2/g to 31.21 m^2/g following treatment with citric acid during the activation process. Furthermore, acid treatment of clays causes the replacement of exchangeable cations with H+ ions. Additionally, this activation process dissolves both organic and inorganic impurities, substituting diatomic and triatomic cations with H^+ ions. This behavior underscores the clay's role as a Bronsted-Lowry acidic active site, facilitating the adsorption of organic impurities, such as anionic dyes, through electrostatic attraction while potentially forming covalent bonds with cationic dyes (Bijang *et al*., 2019). The acid activation process also generates microporous spaces in the treated sample because of clay exfoliation. The extent of ion removal during acid activation is influenced by various factors, including the type of acid employed, the concentration of acid, the temperature during the activation reaction, the duration of contact between solid and liquid phases, the stirring rate of the mixture, the particle size of the solid, and the mass ratio of liquid to solid (Amari *et al*., 2018). These factors collectively enhance the effectiveness of the acid activation process on the clay. According to the data, all properties of ULO significantly improved after being treated with citric acid-activated clay, indicating that the activation process effectively removed contaminants through its adsorption capacity. Moreover, SEM results confirmed that the activation of clay successfully increased the surface area, which corroborates the theory that organic matter leached out from the clay upon the introduction of acid (Amari *et al*., 2018).

Table 4. Pore characteristics of unmodified and modified Mntmorillonite K-10

Type of clay	Average pore size, (μm)	Surface area, (m^2/g)	Porosity, %
Inactivated	1.614	162.25	41.36
1.0 mol/L CA, 45 minutes activation	2.077	245.76	47.18

FTIR Analysis of Treated Lubricating Oil

Figure 8 shows the components found in used lubricant oil (ULO) after treatment with clay, as indicated by the peaks and transmittance in the FTIR analysis. In this context, ULO serves as a reference for comparison. The results demonstrate that the treatment improved the removal of unwanted substances in the lubricant oil. For example, the presence of soot was highest before clay treatment, but after treatment, it was reduced from a value of 2075 cm^{-1} to an undetectable level in the activated Montmorillonite K-10 clay. This indicates that the activated clay effectively and eliminated soot from the lubricants. Additionally, the water hydroxyl group (OH) in the range of 3600 cm^{-1} – 2500 cm^{-1} was also successfully

removed during the adsorption process (Zeng et al., 2016). The results from the FTIR peaks further confirmed that activated clay achieved satisfactory removal of water.

Conversely, sulfur oxidation products showed only a minor reduction in peak absorbance, decreasing from 1160 cm^{-1} to 1157 cm^{-1}. Thus, the acid-activated clay used in this experiment was ineffective in removing sulfur oxidation products from the processed ULO. According to Abu-Elella *et al*. (2015), while sulfur oxidation products remained, nitration products were still detected at a peak of 1599.43 cm^{-1} for C=O, with the peak at 1750 cm^{-1} being effectively eliminated by citric acid-activated clay. A similar outcome was reported by Dabai *et al*. (2019), where sulfuric and oxalic acid treatments also resulted in no carbonyl compounds in used Oando Oleum Super lubricant oil. Therefore, the activation of clay using weak acids demonstrated satisfying results, like other methods. However, citric acid-activated clay did reveal the presence of fuel residue in the recovered lubricating oil. Although fuel was still present in terms of absorbance, its intensity was lower than that of the ULO (Aguilar *et al*., 2020). Thus, it can be concluded that activated Montmorillonite K-10 clay was effective in removing water, carbonyl compounds, and soot during the regeneration of ULO.

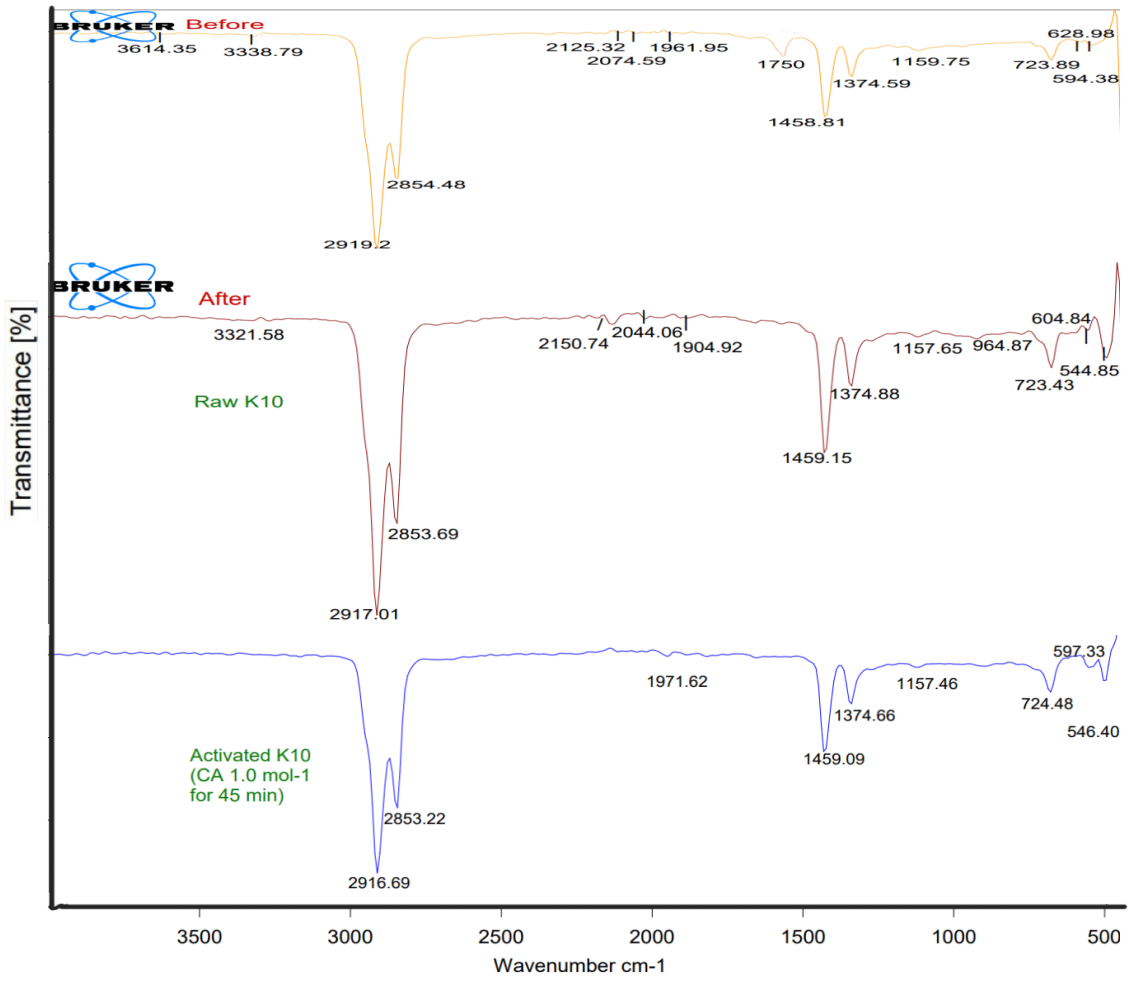

Figure 8. FTIR analysis conducted before and after treatment with clays.

CONCLUSIONS

In conclusion, the acid activation process has been shown to enhance the properties of clay, with activated Montmorillonite K-10 clay exhibiting greater adsorption capacities than its unactivated form. Following the acid activation, the recycled used lubricant oil (ULO) demonstrated both physical and chemical property improvements compared to untreated lubricating oil. The treatment with citric acid at a concentration of 1.0 mol/L for 45 minutes emerged as the optimal parameter, yielding satisfactory results, including a color change, a water content reduction of 0.036%, a sludge removal percentage of 9.20%, a density of 0.824 g/mL, and a viscosity of 95.10 cP.

The adsorption process resulted in noticeable color changes, confirmed by UV-Vis spectroscopy, which indicated a reduction in absorbance compared to ULO. The lowest absorbance value of 1.3292 A for the recycled ULO was achieved under specific operating parameters: acid type, acid concentration, and reaction time. Physical property assessments revealed that activated Montmorillonite K-10 clay effectively removed water, sludge, and viscosity. The results indicate that the activation process significantly increased the pore size, pore diameter, and overall surface area, all of which are crucial for effective adsorption.

FTIR analysis confirmed that the activated clay successfully removed carbonyl compounds and carboxylic acid components that were present in untreated oil. The unmodified clay had a smoother surface with fewer visible pores, whereas the activated clay exhibited a more porous structure with noticeable pores and cracks. The average pore diameter of the activated clay was larger, reflecting a 32.19% increase in pore size compared to the unmodified clay. Furthermore, the activated clay displayed a substantial enhancement in pore area relative to the unmodified version, with the average pore size increasing from 1.614 µm to 2.077 µm. In summary, acid activation treatment is the most effective method for recycling ULO, significantly improving its quality to a level nearly comparable to that of virgin lubricating oil (VLO).

REFERENCES

Abdel-Jabbar, N. M., Al Zubaidy, E. A. & Mehrvar, M. 2010. Waste lubricating oil treatment by adsorption process using different adsorbents. *International Journal of Chemical and Biological Engineering, 3*(2), 70-73.

Abu-Elella, R., Ossman, M. E., Farouq, R. & Abd-Elfatah, M. 2015. Used motor oil treatment: turning waste oil into valuable products. *International Journal of Chemical and Biochemical Sciences, 7*, 57-67.

Adamczewska, J. Z. & Love, C. 2005. Oxidative stability of lubricants measured by PDSC CEC L-85-T-99 test procedure. *Journal of thermal analysis and calorimetry, 80*, 753-759.

Aguilar, J., Almeida-Naranjo, C., Aldás M. B. & Víctor H. Guerrero V. H. 2020. Acid activation of bentonite clay for recycled automotive oil purification. *E3S Web of Conferences, 191*, 03002.

Ajemba, R. O. & Onukwuli, O. D. 2013. Adsorptive removal of colour pigment from palm oil using acid activated Nteje clay. Kinetics, equilibrium and thermodynamics. *Physicochemical Problems of Mineral Processing*, *49*(1), 369-381.

Alekseeva, O., Noskov, A., Grishina, E., Ramenskaya, L., Kudryakova, N., Ivanov, V., & Agafonov, A. 2019. Structural and thermal properties of montmorillonite/ionic liquid composites. *Materials*, *12*(16), 2578.

Amari, A., Gannouni, H., Khan, M. I., Almesfer, M. K., Elkhaleefa, A. M. & Gannouni, A. 2018. Effect of structure and chemical activation on the adsorption properties of green clay minerals for the removal of cationic dye. *Applied Sciences, 8*(11), 2302.

Ameri, A., Tamjidi, S., Dehghankhalili, F., Farhadi, A., & Saati, M. A. 2020. Application of algae as low cost and effective bio-adsorbent for removal of heavy metals from wastewater: A review study. *Environmental Technology Reviews*, *9*(1), 85-110.

Ani, I. J., Akpan, U. G., Hameed, B. H. and Okafor, J. O. 2023. Treatment of spent engine oil (spent SAE W50) via solvent extraction-adsorption process for the production of transfer oil: Physico-chemical properties of the adsorbents, *Scientific African, 20*, e01617. https://doi.org/10.1016/j.sciaf.2023.e01617

Assunção Filho, J. L., Moura, L. G. M. & Ramos, A. C. S. 2010. Liquid-liquid extraction and adsorption on solid surfaces applied to used lubricant oils recovery. *Brazilian Journal of Chemical Engineering, 27*(4), 687-697.

Bijang, C. M., Nurdin, M., Tehubijulluw, H., Fransina, E. G., Uyara, T. & Suarti. 2019. Application of Ouw natural clay activated acid and base as adsorbent of Rhodamine B dye, *Journal of Physics: Conference Series 1242*, 012014.

Chilev, C. 2017. A New Procedure for Porous Material Characterization. *International Journal of Science, Technology and Society*, *5*(4), 131.

Dabai, M. U. & Bello, N. 2019. Comparative study of regeneration of used lubricating oil using sulphuric and oxalic acids/clay treatment process, *International Journal of Innovative Science, Engineering & Technology, 6*(3), 13-23.

Daham, G. R., AbdulRazak, A. A., Hamadi, A. S. & Mohammed, A. A. 2017. Re-refining of used lubricant oil by solvent extraction using central composite design method. *Korean Journal of Chemical Engineering, 34*, 2435-2444.

Devi, P. & Saroha, A. K. 2016. Improvement in performance of sludge-based adsorbents by controlling key parameters by activation/modification: A critical review, *Critical Reviews in Environmental Science and Technology, 46*(21-22), 1704-1743.

Diphare, M. J., Muzenda, E., Pilusa, T. J. & Mollagee, M. 2013. A comparison of waste lubricating oil treatment techniques. *2nd International Conference on Environment, Agriculture and Food Sciences (ICEAFS'2013) August 25-26, Kuala Lumpur, Malaysia*, 106-109.

Dutta, D. K. 2018. 9 - Clay mineral catalysts. *Developments in Clay Science, 9*, 289-329.

Hamawand, I., Yusuf, T. & Rafat S. 2013. Recycling of waste engine oils using a new washing agent. *Energies 6*(2), 1023-1049.

Hegazi, S. E. F., Mohamd, Y. A., & Hassan, M. I. 2017. Recycling of waste engine oils using different acids as washing agents. *International Journal of Oil, Gas and Coal Engineering 5*(5), 69-74.

Josiah, P. N. and Ikiensikimama, S. S. 2010. Effect of desludging and adsorption ratios on recovery of low pour fuel oil (LPFO) from spent engine oil. *Chemical Engineering Research Bulletin, 14*, 25-28.

Kemala, D., Moersidik, S. S., Adityosulindro, S. and Hilwa, F. 2019. Enhancing lead adsorption in waste lubricant oil with activated clay as bleaching earth. MATEC web of conferences, 276, 06020.

Khan, A., Naqvi, S. H. J., Kazmi, A. & Ashraf, Z. 2015. Surface activation of fuller's earth (bentonite clay) using organic acids. *Science International(Lahore), 27*(1), 329-332.

Kumar, B. S., Dhakshinamoorthy, A. and Pitchumani, K. 2014. K10 montmorillonite clays as environmentally benign catalysts for organic reactions. *Catalysis Science & Technology, 4*(8), 2378-2396.

Martínez-Mendoza, K. L., Barraza-Burgos, J. M., Marriaga-Cabrales, N., Machuca-Martinez, F., Barajas, M. & Romero, M. 2020. Production and characterization of activated carbon from coal for gold adsorption in cyanide solutions. *Ingenieria E Investigacion, 40*(1), 34-44.

Młynarczak, A. & Sikora, G. 2014. Analysis of the modern oil viscosity changes during their operation in combustion engines. *Journal of KONES Powertrain and Transport, 21*, 361-368.

Mohammed, R. R., Inaam A. R. I., Alladdin H. T. & McKay, G. 2013. Waste lubricating oil treatment by extraction and adsorption. *Chemical Engineering Journal, 220*, 343-351.

Moura, L. G. M., Assunção Filho, J. L. & Ramos A. C. S. 2010. Recovery of used lubricant oils through

adsorption of residues on solid surfaces. *Brazilian Journal of Petroleum and Gas, 4*(3), 091-102.

Oladimeji, T. E., Sonibare, J. A., Omoleye, J. A., Adegbola, A. A. & Okagbue, H. I. 2018. Data on the treatment of used lubricating oil from two different sources using solvent extraction and adsorption. *Data in Brief, 19,* 2240- 2252.

Opoku-Mensah, P., Gyamfi, J. N., Domfeh, A., Awarikabey, E., & Kwao-Boateng, E. 2023. Assessment of the conventional acid-clay method in reclaiming waste Crankcase lubricating oil. *Advances in Tribology*, *2023*(6567607) 1-9.

Patty, D. J. & Lokollo, R. R. 2016. FTIR spectrum interpretation of lubricants with treatment of variation mileage. *Advances in Physics Theories and Applications, 52,* 13-20.

Rahman, M. M., T. A. Siddiquee, S. Samdani, & Kabir. K. B. 2008. Effect of operating variables on regeneration of base-oil from waste oil by conventional acid clay method. *Chemical Engineering Research Bulletin,* 12, 24-27.

Raţiu, S. Josan, A., Alexa, V., Cioată V. G. & Kiss, I. 2020. Impact of contaminants on engine oil: A review. *Journal of Physics: Conference Series, 1781*, 012051.

Ravichandran, J. & Sivasankar, B. 1997. Properties and catalytic activity of acid-modified montmorillonite and vermiculite. *Clays and Clay Minerals, 45*, 854-858.

Riyanto, Ramadhan, B. & Wiyanti. D. 2018. Treatment of waste lubricating oil by chemical and adsorption process using butanol and kaolin. *IOP Conference Series: Materials Science and Engineering*. 349(1) 012054.

Rosa, M. S. L., Knoerzer, T., Figueiredo, F. C., & dos Santos Júnior, J. R. 2020. Clarification of used lubricating oils by application of chemically-modified clays. *Cerâmica, 66,* 130-136.

Salem, S., Salem, A. & Babaei, A. A. 2015. Application of Iranian nano-porous CaBentonite for recovery of waste lubricant oil by distillation and adsorption techniques. *Journal of Industrial and Engineering Chemistry 23*,154-162.

Shigidi, I., Osman, H., Eldirderi, M., Ilyas Khan, M., Elkhaleefa, A., Dhanapal, D. & Al Mesfer, M. 2020. Waste engine oil remediation using low cost natural clay absorbent material. *International Journal of Engineering, 33*(2), 178- 185.

Suhdi & Wang, S. C. 2021. Fine activated carbon from rubber fruit shell prepared by using $ZnCl_2$ and KOH activation. *Applied Sciences, 11*(9), 3994.

Temuujin, J., Jadambaa, T., Burmaa, G., Erdenechimeg, S., Amarsanaa, J. & MacKenzie, K. J. D. 2004.

Characterisation of acid activated montmorillonite clay from Tuulant (Mongolia). *Ceramics International*, *30*(2), 251-255.

Timur A. 2017. Reclamation of used lubricating oils using magnetic nanoparticles and caustic soda, *M. Sc. thesis; Department of materials science and engineering, Graduate school of engineering and science, Bilkent university*, 1-81.

Uddin F. 2018. Montmorillonite: An introduction to properties and utilization. Current topics in the utilization of clay in industrial and medical applications. InTech. Available at: http://dx.doi.org/10.5772/intechopen.77987.

Udonne, J. D., Efeovbokhan, V. E., Ayoola, A. A., Babatunde, D. E., Ajalo Ifeoluwa A. & Ajalo l. J. 2016. Recycling used lubricating oil using untreated, activated and calcined clay methods. *Journal of Engineering and Applied Sciences*, *11*(6), 1396-1401.

Udonne, J. D. 2011. A comparative study of recycling of used lubrication oils using distillation , acid and activated charcoal with clay methods. *Journal of Petroleum and Gas Engineering*, 2(2), 12-19.

Velasco-Calderón, J. C., Garcia-Figueroa, A. A., Cervantes, J. L. L., & Gracia- Fadrique, J. 2020. Regeneration of used lubricating oil by solvent extraction and phase diagram analysis. *Current Research in Green and Sustainable Chemistry*, 3, 100010.

Vural, U. 2020. Waste mineral oils re-refining with physicochemical methods. *Turkish Journal of Engineering*. *4*(2), 62-69.

Wahyuningsih, P., Harmawan, T. & Halimatussakdiah. 2020. Synthesis and characterization of acid-activated bentonite from Aceh Tamiang. *IOP Conference Series: Materials Science and Engineering*, *725*(1), 012050.

Yusufu M. I. Ariahu C. C. & Igbabul B. D. 2012. Production and characterization of activated carbon from selected local raw materials. *African Journal of Pure and Applied Chemistry, 6*(9), 123-131.

Zeng, Q., Dong, G., Yang, Y. & Wu, T. 2016. Performance deterioration analysis of the used gear oil. *Advances in Chemical Engineering and Science*, *6*(2), 67.

Zhang, C., Zhang, Z., Tan, Y. & Zhong, M. 2017. The effect of citric acid on the kaolin activation and mullite formation. *Ceramics International*, *43*(1), 1466-1471.

Zhansheng, W. U., Chun, L. I., Xifang, S., Xiaolin, X. U., Bin, D. A. I., Jin'e, L. I. and Hongsheng, Z. H. A. O. 2006. Characterization, acid activation and bleaching performance of bentonite from

Xinjiang, *Chinese Journal of Chemical Engineering*, *14*(2), 253-258.

Zheng, X., Zhang, J., Zheng, T., Liang, C. & Wang, H. 2014. A developed technique for measuring water content in oil-contaminated porous media, *Environmental earth sciences, 71*, 1349-1356.

Zhu, Y., Zhang, Y., Shi, Z. & Li, B. 2019. Regeneration of wind power waste lubricating oil by a combination use of chitosan, sodium carbonate and silica gel. *Nature Environment and Pollution Technology*, *18*(3), 835-843.

Zulkania, A., Hanum, G. F. & Sri Rezki, A. 2018. The potential of activated carbon derived from bio-char waste of bio-oil pyrolysis as adsorbent. *MATEC Web of Conferences*, *154*, 1-6.

.

BorneoScience
The Journal of Science & Technology
Volume 45 Issue 2 : Sept 2024
Online ISSN : 2231-9085 | ISSN : 1394-4339

REDCLAW CRAYFISH (*Cherax quadricarinatus*): DISTRIBUTION, CRAYFISH PLAGUE, AND DIAGNOSTIC APPROACHES - A REVIEW

Shekinah Shamini Victor[1] and Khomaizon Abdul Kadir Pahirulzaman[1*]

[1]Faculty of AgroBased Industry, Universiti Malaysia Kelantan, Jeli campus, 17600 Jeli, Kelantan, Malaysia

*Corresponding author email: khomaizon@umk.edu.my

Received 11st June 2024; accepted 28th Nov 2024
Available online: 31st December 2024
Doi: https://doi.org/10.51200/bsj.v45i2.6010

ABSTRACT: *The crayfish plague, caused by Aphanomyces astaci, represents a serious threat to redclaw crayfish populations in Malaysia. This review examines the distribution of redclaw crayfish, the incidence of crayfish plague, and insights into its diagnosis. Previous research has established that A. astaci is the primary agent behind crayfish plague in both Asia and Europe. Gaining a comprehensive understanding of these biological threats, including A. astaci and other infections, is vital for protecting the redclaw crayfish industry. Implementing effective diagnosis and management strategies is crucial for preserving crayfish populations and ensuring the industry's sustainability. It is important to recognize that fungal plagues, like those caused by A. astaci, often show few symptoms until significant mortality occurs. Additional research is necessary to grasp the complex immune system of crayfish and to investigate potential therapeutic measures for managing inflammation. Collaboration and data sharing among researchers studying crayfish across different regions would significantly enhance progress in this field.*

KEYWORDS: *Aphanomyces astaci*, crayfish plague, crustacean disease, redclaw crayfish

INTRODUCTION

Inland fish farming has experienced significant growth, outpacing marine aquaculture, particularly in the South Asian region. In 2018, inland aquaculture yielded 51.3 million tonnes of aquatic animals, accounting for 62.5% of the global production of farmed food fish. The share of finfish in this production dropped from 97.2% in 2000 to 91.5% (47 million tonnes) in 2018, indicating the more

rapid expansion of other species, especially crustaceans like shrimps, crayfish, and crabs in Asia. Therefore, understanding the biological characteristics of *C. quadricarinatus* is essential for producing healthy redclaw crayfish (Tarun, 2021).

Over the past two decades, the dominance of finfish in inland aquaculture has diminished, giving way to other species, notably freshwater crustaceans such as redclaw crayfish (Naquiddin *et al*., 2016). *Cherax quadricarinatus*, the redclaw crayfish, is classified as a freshwater crustacean within the genus Parastacidae (Holdich, 2002; Haubrock, 2021). This species gained commercial importance following its successful cultivation in Australia in 1985, leading to its commercialization and farming worldwide, particularly in Asia, including Malaysia (Johan *et al*., 2012; Naquiddin *et al*., 2016). Overall, this species is known for its robustness, resilience to various diseases (both parasitic and non-parasitic), and its ease of cultivation. Additionally, the rapid growth rate of *C. quadricarinatus* allows for more frequent harvesting compared to other species, making it a key driver of the industry.

The growth and development of *C. quadricarinatus* are directly influenced by its lack of a larval stage. This species can adapt to various climates and reproduce in alkaline waters with a pH range of 7.0 to 8.5. Naguib *et al*. (2021) discovered that *C. quadricarinatus* can thrive in a variety of temperatures and low dissolved oxygen levels. The species exhibits a range of phenotypic variations, including size and reproduction rates, in diverse biotic and abiotic conditions, from tropical to temperate regions. Mature males are characterized by a decalcified red spot on their chelae, while both sexes feature reddish highlights on their bluish-green outer bodies (Belle & Yeo, 2010). Female redclaw crayfish have three to five distinct horizontal cervical spines along their cervical groove.

Economically, redclaw crayfish play a significant role in aquaculture and are also valued as ornamental species (Füreder, 2013). Production in Peninsular Malaysia is estimated to be around 12 tons annually (Johan et al., 2012). The price of redclaw varies based on size and quality, potentially reaching up to MYR 120 per kilogram (approximately USD 30 per kilogram), making it a lucrative industry (FAO, 2020). The sector has grown consistently, partly due to the involvement of private entrepreneurs as hotel and restaurant chains have expanded in Peninsular Malaysia. The species cultivated by local farms is imported from Australia and Indonesia, benefiting from the redclaw crayfish's ability to adapt to tropical conditions, which are conducive for reproduction.

The cultivation, harvesting, and commercial distribution of redclaw crayfish have become an increasingly important economic component of the aquaculture industry. However, the fungus *A. astaci* causes the crayfish plague, which results in high mortality rates not only among various crayfish species in Europe but also in several regions of Southeast Asia, including Malaysia.

Therefore, it is essential to understand the biological threats, such as the oomycete *A. astaci* and other infections, that could jeopardize the industry.

Redclaw crayfish (Cherax quadricarinatus) belong to the arthropod families Astacidae, Cambaridae, and Parastacidae, and are freshwater crustaceans that resemble smaller versions of marine lobsters (Holdich, 2002; Haubrock, 2021). There is a notable difference in size and growth rate between male and female *C. quadricarinatus,* with males generally being larger and growing more rapidly than females. The nutritional intake of these crustaceans often influences their sexual characteristics (Sun *et al*., 2023). As the species is harvested and consumed by humans, an entire industry has developed around them, emphasizing the need for a deeper understanding of crayfish, which encompass approximately six hundred known species (Aoki *et al*., 2018).

Like other crustaceans, crayfish possess a hard exoskeleton, or "shell," which they must molt periodically to grow. This exoskeleton serves to protect the crayfish from predators and provides structural support. Despite their armoured exterior, crayfish maintain agility and speed thanks to their flexible, jointed segments (Holdich, 2002; Louis & Robert, 2020; Haubrock, 2021). Figure 1 displays the anatomical structure of the crayfish, which consists of two main parts: the cephalothorax and the abdomen.

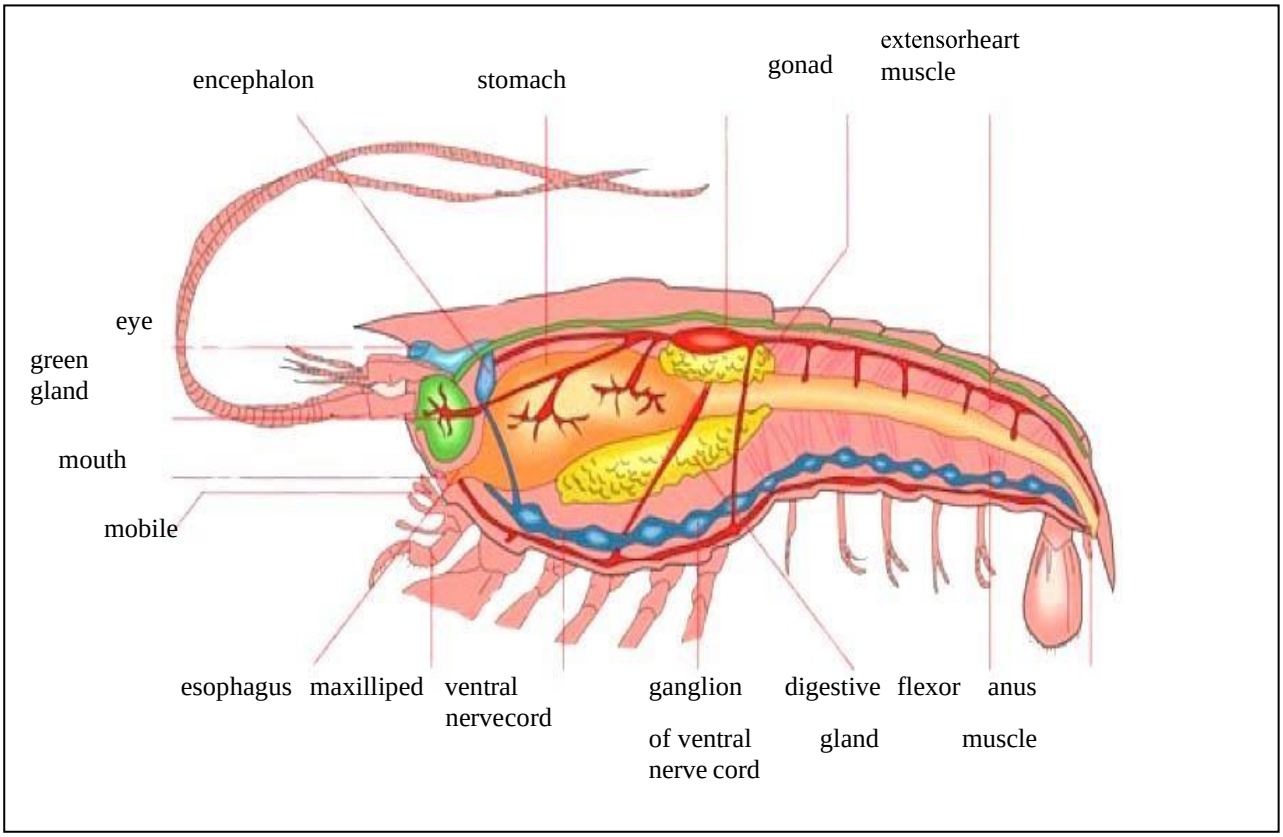

Figure 1: The internal anatomy of a crayfish. Source: www.enchantedlearning.com

The encephalon regulates the mental functions of the crayfish, while the stomach, situated in the upper region, is part of the crustacean's digestive tract, positioned between the esophagus and the intestine. The crayfish's heart is in the midsection, pumping blood to the extensor muscles and other organs, extending all the way to the tail. The gonad, which serves as the sex gland, is connected to the ventral nerve cord and the flexor muscles, which facilitate the movement of the crayfish's tail (Pliego *et al*., 1998). The cephalothorax, which includes the head and thorax, consists of 13 segments, while the abdomen is made up of six distinct segments and is located posterior to the cephalothorax. Each segment of the cephalothorax and abdomen has two appendages. In the head region, there are five pairs of appendages known as cephalic appendages. The shorter antennae, or antennules, house organs responsible for balance, touch, and taste, while the longer antennae contain organs for touch, taste, and smell (Johan *et al*., 2012; Louis & Robert, 2020; Haubrock, 2021).

Crayfish possess mandibles, or jaws, that are used for capturing and processing food. Additionally, the thoracic region has maxillipeds that help secure food during feeding, and large claws, known as chelipeds, which serve for hunting and defence. The decapod crustacean also has four pairs of walking legs and five pairs of swimmerets, or pleopods. Each leg features an attached gill to facilitate water circulation as the legs move. The gender of the crayfish can be determined by examining the first pair of swimmerets: males have larger and more robust first swimmerets for depositing sperm into the female's oviducts, whereas females have softer swimmerets to carry fertilized eggs and newly hatched young. Crayfish also utilize their tail fans, modified from a pair of uropod, to propel water forward, allowing them to move backward (Aoki *et al*., 2018)

C. quadricarinatus Habitat Conditions

Most crayfish species thrive in flowing freshwater environments, such as streams and rivers with manageable currents, rather than stagnant waters (Haubrock, 2021). This preference is due to their intolerance for high levels of ammonia and heavy metals commonly found in still water bodies (Barnett *et al*., 2017). However, certain varieties of crayfish, such as Procambarus clarkii, exhibit resilience to pollution and can survive in contaminated waters (Dorret *et al*., 2006). Additionally, crayfish favour dark, cool habitats and are frequently found hiding under rocks and vegetation. They struggle to survive in extremely cold temperatures or in aquatic environments with low oxygen levels (Belle & Yeo, 2010; Füreder, 2013). As a result, crayfish farming for industrial purposes necessitates specific temperature, pH, and salinity levels, in addition to adequate oxygen supply.

The optimal temperature range for raising healthy crayfish is between 18 °C and 25 °C, while pH levels should be maintained between 7.5 and 8.5. Lower pH levels and insufficient calcium can lead to poor molting of the crayfish shell. Adequate oxygen in the water is another crucial factor for

survival, as crayfish use gills to extract oxygen from the water (Hossain et al., 2018). If oxygen levels are insufficient, crayfish may resort to obtaining oxygen from the air above the water's surface (Holdich, 2002). Although they typically inhabit freshwater and have adapted to a stenohaline lifestyle, crayfish have demonstrated the ability to tolerate slightly elevated salinity levels (Suryanto *et al*., 2023). Hossain et al. (2018) recorded the presence of *Astacus leptodactylus* and *Astacus pachypus* in waters with salinity levels up to 14 parts per thousand (ppt) in the Caspian Sea (Yavuzcan *et al*., 2004). However, the capacity of crayfish to withstand higher salinity is directly related to their size.

Crayfish are known to be nocturnal, primarily foraging for food during the night. Most freshwater crayfish inhabit burrows, lakes, and rivers, typically seeking refuge under rocks or logs during the day and becoming more active at night (Louis & Robert, 2020; Suryanto *et al*., 2023). They are omnivorous and detritivorous, meaning they do not adhere to a specific diet but will consume a variety of plant and animal organisms, including fish, shrimp, worms, elodea, plankton, insects, and snails. Additionally, they may exhibit cannibalistic behaviour if there is an insufficient supply of food or shelter in their environment (Belle & Yeo, 2010; Neculae *et al*., 2024).

Redclaw Crayfish Distribution in Malaysia

In Malaysia, the term "freshwater lobster" is commonly used for redclaw crayfish due to their habitat and resemblance to lobsters. While it's unclear when the redclaw species was first introduced to the country, commercial-scale cultivation has been reported since 2003 in the southern region of Peninsular Malaysia (Alimon et al., 2003; Naqiuddin et al., 2016; Norshida et al., 2021). During the late 2000s, when the species was first being introduced, redclaw aquaculture thrived in southern Peninsular Malaysia, largely due to the regular importation of broodstocks from Indonesia (Naqiuddin et al., 2016). According to the FAO in 2020, Malaysia has emerged as the leading producer of redclaw, with production increasing from 2013 to 2017, driven by prices that can reach as much as MYR 120 per kilogram (Norshida et al., 2021).

Unintentional escapes or deliberate releases from aquaculture facilities and aquariums have allowed redclaw to establish themselves in natural habitats. Currently, redclaw is the only non-native crayfish species to have formed natural populations in Malaysia, a successful invasion likely due to environmental conditions that mirror their native habitat (Norshida et al., 2021). Additionally, their ability to be easily transported by humans in large quantities (Yuliana et al., 2021), alongside the country's geographical features and frequent flooding, facilitates their expansion into new areas (Mohd Dali et al., 2023). Since their introduction, wild redclaw populations have been reported not

only in Johor, in the southern part of the country, but also in Selangor along the West Coast of Peninsular Malaysia and in Sarawak on Borneo Island (Johan et al., 2012). Historical data suggest that the species was initially introduced to Malaysia in the 1980s in Johor, from where it migrated northward along the western coast of the Peninsula (Naqiuddin et al., 2016). Although no wild populations have yet been observed in states outside Johor, Melaka, and Sarawak, the spread of this species may increase with the growing number of redclaw aquaculture facilities in the country (Naqiuddin et al., 2016).

Cultivation activities for redclaw crayfish typically aim to satisfy food consumption needs, targeting sizes between 6 to 8 inches in length. However, the high demand for juveniles has shifted focus toward breeding activities, which has resulted in discoveries of the species' natural populations in East Malaysia and southern Peninsular Malaysia (Johan *et al*., 2012). The presence of wild crayfish in these areas has caught the attention of local fishermen, who have experienced losses due to crayfish damaging their catches and fishing gear.

C. quadricarinatus is the only freshwater crayfish species known to have established a population in Malaysian freshwater habitats, despite the presence of other crayfish species like the highly invasive *Cherax destructor* and *P. clarkii* in the aquarium trade. This is likely attributed to *C. quadricarinatus* demonstrating superior characteristics in terms of growth, reproduction, and size compared to the other two species (Naqiuddin *et al*., 2016). Additionally, its desirable traits for the aquaculture industry suggest that this species has been introduced in significant numbers to Malaysia for use as broodstock. Consequently, it has successfully established a wild population, as non-native species are more likely to thrive when introduced in large numbers or repeatedly (Alpert, 2006; Yuliana *et al*., 2021). Furthermore, aquaculture has historically been Malaysia's primary avenue for introducing foreign fish, accounting for 64% of all non-native fish species brought into the country (Khairul Adha *et al*., 2013).

However, invasive species are recognized as the second-largest contributor to biodiversity loss, as they disrupt ecological balance by competing for resources and shelter, spreading diseases, directly preying on native species and their eggs, and altering habitats through burrowing and grazing on macrophytes (Holdich, 1988). The invasive potential of *C. quadricarinatus* to disrupt native ecosystems in the United States has already been observed in regions where it has been introduced (Morningstar et al., 2020; Haubrock *et al*., 2021; Sanjar *et al*., 2023). Thus, redclaw crayfish exhibit characteristics typical of successful invaders, such as a broad and adaptable diet and high reproductive capacity. Nevertheless, there are currently no documented instances of *C. quadricarinatus* causing environmental harm in Malaysia. This may be due to underappreciated bio-invasion threats and the time lag between observable impacts and the establishment of the species (Othman & Hashim, 2003).

Crustacean Diseases

In 2008, the EC Council Directive 2006/88/EC created a list of three significant crustacean diseases recognized globally. These diseases are white spot disease (WSD), yellow head disease (YHD) caused by the yellow head virus (YHV), and Taura syndrome (TS) caused by the Taura syndrome virus (TSV). WSD, which was previously regarded as a "non-exotic" disease in Europe due to its documented occurrence in penaeid shrimp farms in southern Europe, has since been reclassified (Stentiford *et al*., 2009). In contrast, YHD and TS are considered exotic diseases because they are not naturally present in Europe. Their inclusion is based on their potential to spread internationally via the trade of live animals and their products, as well as their considerable economic impact worldwide (Stentiford *et al*., 2009; Morningstar *et al*., 2020).

Additionally, the International Organisation for Animal Health (OIE) has listed the crayfish plague (A. astaci) and the infectious hypodermal and hematopoietic necrosis virus (IHHNV) as other crustacean diseases that require mandatory reporting. Diagnostic techniques for detecting these diseases include traditional methods such as gross pathology, histology, classical microbiology, animal bioassay, antibody-based approaches, and molecular techniques involving DNA probes and amplification. Since shrimp aquaculture became a major commercial enterprise in the 1970s, these diseases have had a significant impact on the industry. Major diseases affecting farmed shrimp include viruses, rickettsial-like bacteria, true bacteria, protozoa, and fungi (Walker & Mohan, 2009).

Today, modern medicine employs chemotherapeutics, routine sanitation practices, and improved culture methods to combat various bacterial, fungal, and protozoan diseases. Managing these illnesses has been challenging, posing a threat to the entire industry and representing some of the most financially burdensome epizootics (Walker & Mohan, 2009). For example, the Taura syndrome outbreak from 1991 to 1992 was deemed "notorious" in the context of viral epizootics when the disease emerged in Ecuador. Likewise, white spot disease pandemics had severe repercussions for the industry in Southeast Asia during the same period. The socioeconomic importance of shrimp farming has resulted in five out of nine crustacean diseases listed by the OIE being viral diseases of shrimp (OIE, 2012), although none are as damaging as the crayfish plague.

The industry has had to adapt its practices to become more sustainable following substantial losses incurred from the crayfish plague, while the adoption of technology has opened up new opportunities. These changes have allowed the industry to recover from serious viral pandemics and resume production, ushering in a new phase of rapid growth (FAO, 2006). However, despite the implementation of new shrimp farming strategies, protocols, and technologies as well as the elimination of 'high-risk' practices, the crayfish plague caused by *A. astaci* has continued to persist. The transition away from relying on wild stocks for production has not been sufficient, as *A. astaci* has now been linked to domesticated stocks (Lightner, 2005).

Crayfish Plague

The invasive oomycete *A. astaci* is responsible for crayfish plague, posing a significant threat to freshwater crayfish populations. This pathogen is highly virulent, leading to elevated mortality rates among crayfish in Europe, Asia, Australia, and South America (Koivu-Jolma *et al*., 2023). The plague stems from the oomycete parasite *A. astaci*, a fungal-like aquatic mold that inhabits the cuticle of crayfish throughout its vegetative life stage and subsequently infects other crayfish through zoospores. While oomycetes are commonly referred to as water molds and consist of various types, some have been identified while others remain undiscovered. Regardless, these organisms can be classified as either parasites or saprophytes (Kokko *et al*., 2018). Aphanomyces belongs to the Saprolegniales group, which also includes the notorious parasitic species Saprolegnia (Leclerc *et al*., 2000). The genus Aphanomyces is associated with serious fish diseases such as mycotic granulomatosis and epizootic ulcerative syndrome (EUS), directly resulting from infections by *Aphanomyces invadans* (Viljamma *et al*., 2011).

Fungal isolation occurs upon the observation of infection symptoms, which include brownish-red melanisation, whitening of the abdomen (Figure 2), and reduced overall mobility. The non-specific melanisation seen in crayfish serves as a defensive reaction to pathogen infections (Victor & Pahirulzaman, 2020). Additional indicators of infection include the whitening of the musculature in the ventral abdomen. In advanced stages of the infection, affected crayfish may display sluggish behaviour and limb deformities (Nicky, 2008; Victor & Pahirulzaman, 2020).

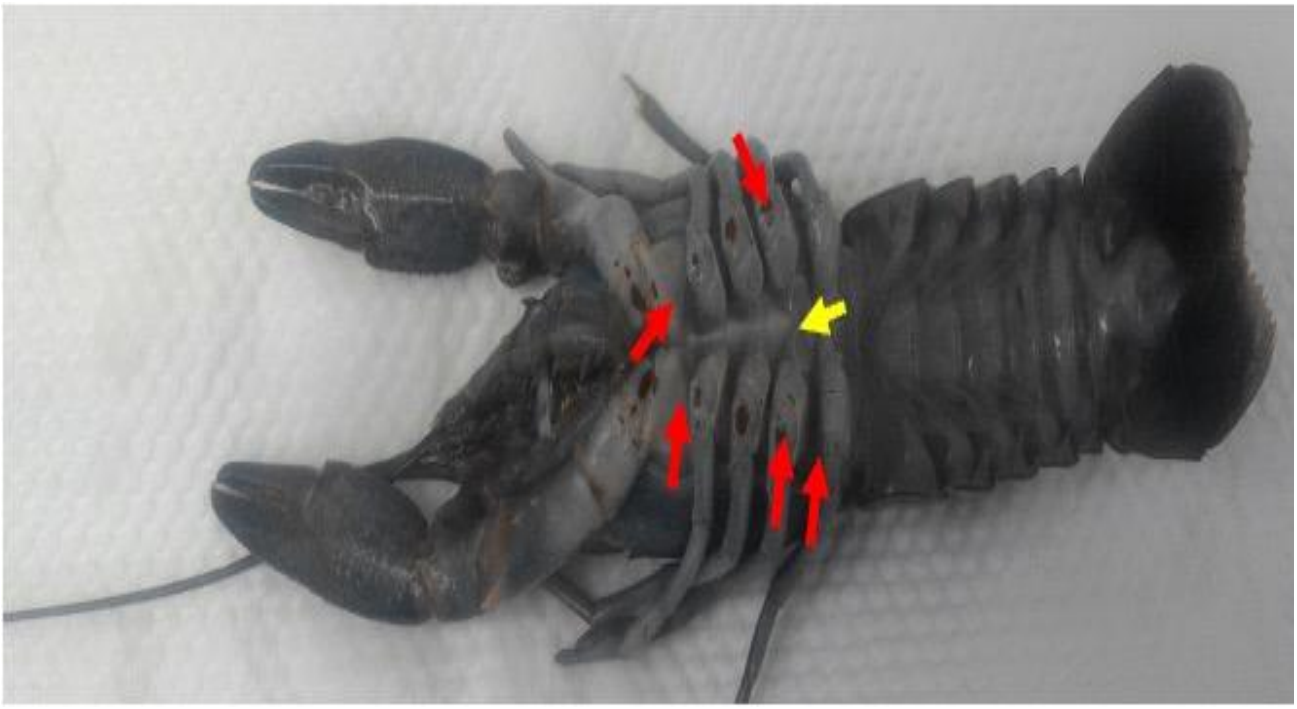

Figure 2: Signs of infection in *C. quadricarinatus* included the presence of brownish-red melanisation (red arrows) and the whitening of the abdomen (yellow arrow) (Victor & Pahirulzaman, 2020).

In addition to marine oomycetes linked to the pathology of fish and crustaceans, there are many undiscovered saprophytic species that thrive in freshwater environments, which have yet to be explored and properly classified (Vrålstad *et al*., 2009). *A. astaci*, in its somatic form, comprises a mycelium organized into structures resembling fungal hyphae (Viljamaa-Dirks & Heinikainen, 2019). These hyphae are aseptate, meaning they lack septa, and they appear turgid, colourless, and measure approximately 7.5 to 9.5 μm in width. As the life cycle progresses into the infectious stage, the spores are termed zoospores, formed in sporangia of similar size to the hyphae, separated by septa. The main spores within the sporangium aggregate into a spore ball that typically houses between 10 and 40 individual spores developed from the cytoplasm.

Following a hibernation-like phase, these cysts transform into swimming zoospores, which measure about 9-11 μm in diameter and possess two distinct flagella. The zoospores begin swimming towards nutrient sources, directing them toward crayfish (Viljamaa-Dirks, 2016). Upon contacting a crayfish, they attach to the exoskeleton, encyst, germinate, and initiate a new growth cycle. At this point, the rapidly growing hyphae invade the crayfish's tissues, and if unchecked, *A. astaci* can ultimately lead to the crustacean's death within a few weeks (Holdich, 2002; Belle & Yeo, 2010; Kokko *et al*., 2018).

The agent or agents responsible for crayfish plague are situated in the crevices of a crustacean's cuticle. The development of these agents is usually inhibited by the crustacean's immune system while being protected from competition with other organisms in the environment (Makkonen *et al*., 2013). The disease is transmitted between hosts by zoospores, which have a short lifespan but can swim for about three days, enhancing the fungi's chances of locating new hosts. The organism possesses a mechanism that allows a zoospore to encyst and produce new zoospores if the initial growth is insufficient, reinforcing the classification of these parasites as "highly specialized." While experimental replication of the survival strategy of parasitic oomycetes is possible, the exact process of generating new spores remains elusive; it is understood, however, that most spores are produced as the host is deteriorating (David *et al*., 2014).

Crayfish Plague Distribution

The crayfish plague was inadvertently introduced to Europe from North America around 1860, with *A. astaci* being recognized as a natural parasite of North American crayfish (Alderman, 1996). Despite the disease's existence since 1860, its origins remained a mystery for many years, resulting in ineffective measures to prevent its spread. The thriving crayfish trade during that time likely contributed to the propagation of the plague, which has remained a significant health issue for the

European noble crayfish, *A. astacus*. The rapid mortality caused by the disease made it virtually impossible to restore native crayfish populations to their previous levels.

The disease earned the alarming title "crayfish plague" due to its rapid and lethal nature, initially recognized through widespread crayfish die-offs. It has been shown that the native European crayfish population, which includes eastern and northern *Astacus spp*., as well as southern and western *Austropotamobius spp*., is highly susceptible to *A. astaci* infection. Laboratory studies in pathobiology indicated that these species could experience 100% mortality rates (Alderman & Polglase, 1986; Cerenius *et al*., 1988). The combination of infectious dosages of zoospores and water temperatures mimicking agricultural conditions played a crucial role in the disease's development, enhancing understanding of the mechanics of the crayfish plague.

In contrast, North American crayfish species were found to be resistant to the disease, often harbouring *A. astaci* as a latent infection without experiencing mortality unless under stress (Unestam & Weiss, 1970). Consequently, North American species were introduced to Europe to compensate for the declining native crayfish populations. The first North American crayfish, the spiny-cheek crayfish (Orconectes limosus), was introduced to Poland in 1890 (as cited in Viljamaa-Dirks, 2016). When populations of the noble crayfish, *A. astacus*, began to decline in Sweden due to the plague, the signal crayfish (*Pacifastacus leniusculus*) was introduced as a replacement. This species was considered suitable due to its size and adaptability (as cited in Viljamaa-Dirks, 2016). The signal crayfish was subsequently introduced in significant numbers into Swedish and Finnish waters during the 1960s. As predicted, the signal crayfish gradually replaced the declining noble crayfish and became a vital part of the European crayfish fishery. While the introduction of the signal crayfish has aided the recovery of European crayfish fisheries (Westman, 1991), it has complicated population management. The signal crayfish has emerged as a chronic carrier of the crayfish plague agent, spreading the disease to the already vulnerable populations of noble crayfish. Consequently, management strategies have shifted toward conserving the noble crayfish, the only native crayfish species in Europe.

Crayfish Plague in Asia

In Japan, China, Thailand, Malaysia, and Taiwan, red swamp crayfish have established populations, which are sometimes supported by ornamental fish outlets in the region (NOBANIS, 2011). This creates a risk of disease spreading across the area, either through contaminated water or via contact with live or deceased crayfish. Notably, between December 2013 and January 2014, four crayfish farms in Taiwan reported five outbreaks of an unidentified disease, resulting in moderate to high cumulative mortality among populations of freshwater redclaw crayfish, *C. quadricarinatus* (Hsieh

et al., 2016). A polymerase chain reaction (PCR) analysis identified *A. astaci* DNA in the deceased redclaw crayfish. The nucleotide sequence identities of these strains were found to be very similar to recognized *A. astaci* strains in Europe, exhibiting a sequence similarity of 99.8–100% in that genetic region. Furthermore, in situ hybridization using a digoxigenin-labelled DNA probe confirmed that *A. astaci* was responsible for the outbreaks. This represented the first documented case of a natural *A. astaci* infection in Asian freshwater redclaw crayfish. Hsieh et al. (2016) highlighted the high susceptibility of redclaw crayfish to this pathogen, noting that certain fungal strains related to crayfish plague could proliferate at temperatures as high as 29.5 °C. This raises concerns about the potential for the disease to spread throughout larger parts of Asia where it is already present, leading to devastating consequences.

Crayfish Immunology

Multicellular organisms have evolved immune systems to defend against 'non-self' substances that are foreign to them. There are two primary types of immune systems: innate immunity and adaptive immunity. Innate immunity is present in invertebrates, providing an effective defence against microbial symbionts, disease, wound repair, and responses to biotic and abiotic stimuli, while adaptive immunity is found only in vertebrates (Clark & Greenwood, 2016). The innate immune systems of invertebrates are sufficient to protect them from invasive microorganisms. Invertebrates respond to infectious pathogens through various immune cells that initially eliminate these invaders by enclosing them. The innate immune systems of invertebrates can mount both cellular responses (including phagocytosis, nodule formation, and encapsulation) and humoral responses when confronted with pathogens (Clark & Greenwood, 2016). These immune reactions are facilitated by blood cells known as hemocytes. When a disease or parasite is too large or numerous for a single phagocytic cell to handle, more complex processes, such as multicellular encapsulation or nodule formation, are required. Typically, phagocytosis is carried out by individual hemocytes (Lee, 2001). The enzyme phenoloxidase often melanises the nodules, which are aggregates of hemocytes connected by a sticky extracellular matrix. Encapsulation serves as a defensive mechanism against larger threats like fungi, nematodes, or eggs and larvae of parasitoids and is like nodule formation.

Moreover, the activation of the humoral immune system in invertebrates triggers a variety of responses, including blood clotting, melanin production, opsonization, and the temporary synthesis of potent antibacterial peptides (Lee, 2001). Therefore, extensive research on the crustacean immune system has been conducted to understand the influence of *A. astaci* on its host (Filipova *et al*., 2013). Crayfish, being invertebrates, do not possess antibodies for adaptive immunity, relying instead on innate immune response mechanisms for protection (Torrijos *et al*., 2021). The activation of the

prophenoloxidase system (proPO) in response to recognizing "non-self" patterns, such as lipopolysaccharides and peptidoglycans from bacteria, as well as -1,3-glucans from fungi, initiates a series of innate immune mechanisms, combining both humoral and cellular responses, including melanin production, cell adhesion, encapsulation, and phagocytosis (Filipova *et al*., 2013). ProPO is found in granules within the blood cells of crayfish and is released into the plasma via exocytosis triggered by the -1,3-glucan binding protein.

This response culminates in the production of melanin, which surrounds and inhibits the growth of invasive hyphae. In North American crayfish, a severe infection with A. astaci may lead to the appearance of dark brown melanized patches on the exoskeleton (Unestam & Weiss, 1970). Conversely, A. astaci can infect an individual or population without presenting obvious symptoms (Vralstad et al., 2011). Thus, both native European crayfish and their North American counterparts utilize the same crustacean immune system as their primary defense against intruders

Selecting reliable reference genes is critical for studying immune cell gene expression patterns, as various factors—including diet, changes in body size, and tissue composition—can influence the messenger ribonucleic acid (mRNA) levels of target genes, as well as gene expression control (Hibbeler *et al*., 2008). To address this, the mRNA levels of the target gene should be compared to those of a housekeeping gene, like 18S ribosomal RNA (rRNA), which is intended to reflect the health of the crayfish or a specific tissue under various conditions. One of the primary immunological effector cells in crustaceans is the hemoglobin cell. In freshwater crayfish, hemoglobin is produced from hemopoietic tissue (Hpt) located on the dorsal side of the stomach (Hai-peng *et al*., 2011). Research has shown that when noble crayfish are experimentally challenged with proPO-activating polysaccharides, there is an increase in proPO mRNA levels in the hemoglobin, indicating the crayfish's ability to respond to intruders (Cerenius *et al*., 2003)

In contrast, the signal crayfish exhibits a different response, as it was found that the proPO transcript was already maintained at a high level, and the experimental challenge did not result in any further increase. Although the crayfish plague agent has adapted to confront the effective defence mechanisms of its natural North American host, the European species has proven to be ill-prepared for this challenge. This inadequate defence response results in a critical mismatch between *A. astaci* and its new host species. Consequently, a species' ability to adapt and develop tolerance or resistance to emerging diseases caused by invasive parasites and pathogens is crucial for its survival. The genetic diversity of the host's immune system can significantly influence the development of resistance within a population. As parasites and pathogens apply intense selection pressure, some hosts manage to withstand this pressure and reproduce, promoting the emergence of resistance (Gruber *et al*., 2014). Pauwels *et al*. (2010) demonstrated that resistance to pathogens could develop in Drosophila

melanogaster within less than ten generations in laboratory conditions, and immunological protection can arise in wild populations of Daphnia magna, a planktonic crustacean, in a similar timeframe. However, there is still uncertainty regarding whether wild hosts can adapt quickly enough to counter newly emerging diseases.

Additionally, a ferritin gene (PcFer), an iron storage protein, has been identified in *P. clarkii* (Liu *et al*., 2017). The increased expression of PcFer in the hepatopancreas of crayfish after exposure to various heavy metals and lipopolysaccharides suggests its role in immune defence and protection against heavy metal stress. Similarly, the laminin receptor has also been implicated in defence against bacterial and viral infections (Rusaini *et al*., 2013; Victor & Pahirulzaman, 2024). For instance, redclaw crayfish infected with White Spot Syndrome Virus (WSSV) demonstrated an up-regulation of the laminin receptor, indicating its protective role against viral infections by binding to viral proteins and preventing them from attaching to target host cells (Liu *et al*., 2018).

Molecular Analysis for Crayfish Plague Identification

By using random oligonucleotides as primers in the amplification of deoxyribonucleic acid (DNA) through polymerase chain reaction (PCR), researchers can identify genetic differences among various isolates of organisms. This approach is known as random amplification of polymorphic DNA-PCR (RAPD-PCR) (Welsh & McClelland, 1990). The RAPD-PCR technique has been applied to *A. astaci* isolates from different sources (Huang *et al*., 1994). The study revealed two distinct groupings and an additional strain. Despite the extensive geographic and temporal isolation of these isolates, a notable degree of genetic similarity was found among these groups, largely due to the absence of sexual reproduction in *A. astaci*. The first major group included a strain from the Turkish narrow-clawed crayfish *Astacus leptodactylus* and isolates from noble crayfish populations in Sweden. These *A. astaci* strains, known as Astacus strains or group A (As), were present in European waters prior to the introduction of the signal crayfish. Consequently, it is widely believed that the As genotype represents the original genotype of *A. astaci*, which was inadvertently introduced to Europe approximately 150 years ago. However, it remains unclear which North American crayfish species initially hosted this genotype.

While there is limited information regarding the role of different genotypes in previous outbreaks of crayfish plague, the first recorded mass mortalities in European crayfish in 1859 were likely attributed to strain As (Alderman, 1996). Research utilizing RAPD-PCR has confirmed the presence of the Ps1 genotype causing the disease in native crayfish species across Sweden, Finland, England, Spain, and Germany (Filipova *et al*., 2013), as well as the Pc genotype in Spain (as cited in Viljamaa-Dirks, 2016). The As genotype, in contrast, was found to be less common and was first

identified in Sweden, Finland, and Turkey (Filipova *et al*., 2013). Nonetheless, advancements in molecular techniques have begun to enhance our understanding of the distribution of various genotypes throughout Europe (Grandjean *et al*., 2014). It is anticipated that when North American crayfish species are present or nearby, *A. astaci* strains associated with those species will cause diseases in neighbouring native populations (Kozubikova-Balcarova *et al*., 2014).

Since the first study identifying the genotypes of *A. astaci* was published in the early 1990s, there have been very few efforts to investigate the potential variability among these genotypes (Huang et al., 1994). This scarcity of research stems from the limited number of isolates available from each genotype, which hinders comparative studies. It has been established that the Pc genotype can tolerate higher water temperatures than the other three known genotypes at that time (Dorret *et al*., 2006). Variations in the chitinase gene between the As and Ps1 genotypes have also been observed, suggesting a link between these differences and the pathogenicity of the strains (as cited in Viljamaa-Dirks, 2016). Other factors that may influence virulence include the ability to produce zoospores, recognize and adhere to hosts, germinate, and penetrate the cuticle (Cerenius & Saderhall, 1984; Cerenius *et al*., 1988), as well as the capability to repeatedly generate new zoospores to pursue hosts or to produce enzymes beyond chitinases (Viljamaa-Dirks, 2016). However, these variable traits can evolve over time.

Quantitative real-time PCR (qPCR) specific to a particular species allows for the rapid identification of the pathogen. However, the *A. astaci* qPCR assay, endorsed by the World Organization for Animal Health (WOAH), also detects the recently identified *Aphanomyces fennicus*, which may lead to false-positive results. Therefore, the existing species-specific *A. astaci* qPCR assay needs refinement to prevent the amplification of *A. fennicus* when screening for *A. astaci* (Strand *et al*., 2023).

CONCLUSION

C. quadricarinatus specimens in Malaysia have been shown to be vulnerable to most diseases that also affect native Australian crayfish. This is particularly true for the redclaw crayfish, which faces threats from crayfish plague caused by *A. astaci* and other fungal pathogen variants. It is crucial to actively pursue parasitic organisms capable of decimating entire populations of specific species, like the redclaw crayfish, to ensure their protection. Fungal plagues, such as those caused by *A. astaci*, often present minimal symptoms that can be easily overlooked, with mortality being one of the first signs of infection. The immune system is a complex structure that varies among species and remains incompletely understood. A deeper understanding of their roles could lead to therapeutic interventions

aimed at controlling inflammation in affected specimens. Although cross-examination and data sharing on crayfish specimens from other regions would have been beneficial to this study, research in this area involving crustaceans is still in its early stages, and data on the subject is limited.

REFERENCES

Alderman, D. J. & Polglase, J. L. (1986). *Aphanomyces astaci*: Isolation and culture. *Journal of Fish Diseases*, 9, 367-379.

Alderman, D. J. (1996). Geographical spread of bacterial and fungal diseases of crustaceans. *Revue Scientifique Et Technique (International Office of Epizootics)*, 15, 603-632.

Alimon, A. R., Roustaian, P., Saad, C. R., & Kamarudin, M. S. (2003). Lipid content and fatty acid composition during early and late embryonic development of redclaw crayfish, *Cherax quadricarinatus (Crustacea decapoda). Journal ofApplied Ichthyology, 19*, 397-398.

Aoki, T., Reantaso, M., Jones , B., & Corsin, F. (2018). Diseases in Asian aquaculture VII. *Proceedings of the Seventh Symposium on Diseases in Asian Aquaculture*.,385.

Barnett, Z. C., Adams, S. B., & Rosamond, R. L. (2017). Habitat use and life history of the vernal crayfish, *Procambarus viaeviridis* (Faxon, 1914), a secondary burrowing crayfish in Mississippi, USA. *Journal of Crustacean Biology*, 544- 555.

Belle, C., & Yeo, D. (2010). New observations of the exotic Australian red-clawcrayfish, *Cherax quadricarinatus*. *Nature in Singapore*, 99-102.

Cerenius, L. & Soderhall, K. (1984). Chemotaxis in *Aphanomyces astaci*, an arthropod parasitic fungus. *Journal of Invertebrate Pathology*, 43, 278-281.

Cerenius, L., Soderhall, K., Persson, M., & Ajaxon, R. (1988). The crayfish plague fungus, *Aphanomyces astaci*-diagnosis, isolation and pathobiology. *Freshwater Crayfish*, 7, 131-144.

Cerenius, L., Bangyeekhun, E., Keyser, P., Söderhäll, I., & Söderhäll, K. (2003). Host prophenoloxidase expression in freshwater crayfish is linked to increased resistance to the crayfish plague fungus, *Aphanomyces astaci*. *Cellular Microbiology*, 5, 353-357.

Clark, K. F., Greenwood J., & Spencer. (2016). Next-generation sequencing and the crustacean immune system: The need for alternatives in immune gene annotation. *Integrative and Comparative Biology*, *56*(6), 1113-1130.

David, A. S., Japo, J., Stein, I. J., Satu, V., Lennart, E., Jannicke, W., Hildegunn, V., Frederik, E., & Trude, V. (2014). Detection of crayfish plague spores in large freshwater systems. *Journal of Applied Ecology*, 51, 544-553.

Dorret, A. J., Porta, G., Pedicillo, G., & Lorenzoni, M. (2006). Biology of *Procambarusclarkii*. *Bull. Fr. Pêche Piscic*, 1155-1168.

European Network On Invasive Alien Species (NOBANIS) (2011). Invasive alien species fact sheet: *Aphanomyces astaci*. www.nobanis.org. Accessed 20-4-2018.

FAO (Food and Agriculture Organization of the United Nations). (2006). The State of World Fisheries and Aquaculture. *Food and Agricultural Organization of the United Nations, Rome*.

FAO (2020). FAO Yearbook. Fishery and Aquaculture Statistics 2018, Rome, 110 pp, https://doi.org/10.4060/cb1213t

Filipova, L., Petrusek, A., Matasova, K., Delaunay, C., & Grandjean, F. (2013). Prevalence of the crayfish plague *Aphanomyces astaci* in populations of the signal crayfish *Pacifastacus leniusculus* in France: Evaluating the threat to native crayfish. *PloS ONE 8*(7).

Füreder, L. (2013). Crayfish News: Official newsletter of the International Association of Astacology. *Regional European Crayfish Meeting*, *35*(3-4), 3-4.

Grandjean, F., Vrålstad, T., Diéguez-Uribeondo, J., Jeliü, M., Mangombi, J., Delaunay, C., Filipová, L., Rezinciuc, S., Kozubiková-Balcarová, E., Guyonnet, D., Viljamaa-Dirks, S. & Petrusek, A. (2014). Microsatellite markers for direct genotyping of the crayfish plague pathogen *Aphanomyces astaci* (Oomycetes) from infected host tissues. *Veterinary Microbiology*, 170, 317-324.

Gruber, C., Kortet, R., Vainikka, A., Hyvarinen, P., Rantala, M. J., Pikkarainen, A., Jusilla, J., Makkonen, J., Kokko, H., & Hirvonen, H. (2014). Variation in resistance to the invasive crayfish plague and immune defence in the native noble crayfish. *Ann. Zool. Fennici*, 51, 371-389.

Haubrock, P.J., Oficialdegui, F.J., Zeng, Y., Patoka, J., Yeo, D.C.J. and Kouba, A. (2021), The redclaw crayfish: A prominent aquaculture species with invasive potential in tropical and subtropical biodiversity hotspots. Rev. Aquacult., 13: 1488-1530.

Hibbeler, S., Scharsack, J. P. & Becker, S. (2008). Housekeeping genes for quantitative expression studies in the three-spined stickleback *Gasterosteus aculeatus*. *BioMed Central*, 9, 18.

Holdich, D. M. (2002). Biology of freshwater crayfish. *Journal of Crustacean Biology*, *22*(4), 969.

Hossain, A. M., Monfort, J., Brugman, M. A., & Böhm, M. (2018). Assessing the vulnerability of freshwater crayfish to climate change. *Diversity and Distributions*, 1-14.

Hsieh, C-Y., Huang, C-W., & Pan, Y-C. (2016). Crayfish plague *Aphanomyces astaci* detected in redclaw crayfish, *Cherax quadricarinatus* in Taiwan. *Journal of Invertebrate Pathology*, 136, 117-123.

Huang, T., Cerenius, L., & Soderhall, K. (1994). Analysis of genetic diversity in the crayfish plague fungus, *Aphanomyces astaci*, by random amplification of polymorphic DNA. *Aquaculture*, 126, 1-9.

Johan, I., Hena, A., & Fadly, Z. (2012). Morphological characteristics of freshwater crayfish from natural habitat in Sarawak. *Malaysia International Biological Symposium, Sustainable Management of Bio-Resources 2012*.

Karplus, I., Zoran, M., Milstein, A., Harpaz, S., Eran, Y., Joseph, D. & Sagic, A. (1998). Culture of the Australian red-claw crayfish *(Cherax quadricarinatus)* in Israel: III. Survival in earthen ponds under ambient winter temperatures. *Aquaculture, 166,* 259–267.

Khairul, A. A. R., Yuzine, E., & Aziz, A. (2013) The influence of alien fish species on native fish community structure in Malaysian waters. *Kuroshio Science*. *7*(1), 81-93.

Koivu-Jolma, M., Kortet, R., Vainikka, A., & Kaitala, V. (2023). Crayfish population size under different routes of pathogen transmission. Ecology and Evolution, 13, e9647.

Kokko, H., Harlioglu, M. M., Aydin, H., Makkonen, J., Gökmen, G., Aksu, Ö., et al. (2018). Observations of crayfish plague infections in commercially important narrow-clawed crayfish populations in Turkey. *Knowledge & Management of Aquatic Ecosystems*, 419.

Kozubiková-Balcarová, E., Beran, L., Ćuriš, Z., Fischer, D., Horká, I., Svobodová, I., & Petrusek, A. (2014). Status and recovery of indigenous crayfish populations after recent plague outbreaks in the Czech Republic. *Ethology Ecology & Evolution*, 26, 299-319.

Leclerc, M. C., Guillot, J., & Deville, M. (2000). Taxonomic and phylogenetic analysis of *Saprolegniaceae* (Oomycetes) inferred from LSU rDNA and ITS sequence comparisons. *Antonie Van Leeuwenhoek*, *77*, 369-377.

Lee, S. Y. (2001). Initiation of innate immune responses in the freshwater crayfish *Pacifastacus leniusculus*. *Comprehensive Summaries of Uppsala Dissertations from the Faculty of Science and Technology*, 613.

Lightner, D. V. (2005). Biosecurity in shrimp farming: pathogen exclusion through useof SPF stock and routine surveillance. *Journal of the World Aquaculture Society*, *36*, 229-248.

Liu, Q. N., Xin, Z. Z., Liu, Y., Wang, Z. F., Chen, Y. J., Zhang, D. Z., Jiang, S. H., Chai, X. Y., Zhou, C. L. & Tang, B. P. (2017). A ferritin gene from *Procambarus clarkii*, molecular characterization and in response to heavy metal stress and lipopolysaccharide challenge. *Fish & Shellfish Immunology*, 63.

Liu, L. K., Li, W. D., Gao, Y., Chen, R. Y., Xie, X. L., Hong, H., Wang, K. J. & Liu, H. P. (2018). A laminin-receptor-like protein regulates white spot syndrome virus infection by binding to the viral envelope protein VP28 in redclaw crayfish *Cherax quadricarinatus. Developmental & Comparative Immunology*, 79.

Louis, A. H., & Robert, J. D. (2020). Sustaining America's aquatic biodiversity crayfish biodiversity and conservation. Virginia Cooperative Extension, Virginia Tech. 420-524.

Makkonen, J., Strand, D. A., Kokko, H., Vralstad, T., & Jussila, J. (2013). Timing and quantifying *Aphanomyces astaci* sporulation from the noble crayfish suffering from the crayfish plague. *Veterinary Microbiology*, 750-755.

Mohd Dali, M. Z., Mohd Nasir, M. S. A., Khaleel, A. G., Chun, L. M., Gan, H. M., Nik Wan, N. A. F., Umar, R., & Umar, Kamarudin, A. S. (2023). Predicting *Cherax quadricarinatus* habitat distribution patterns through the usage of GIS and eDNA analysis in Terengganu, Malaysia. Sains Malaysiana. 52. 343-354.

Morningstar, C. R., Daniel, W. M., Neilson, M. E., & Yazaryan, A. K. (2020). The first occurrence of the Australian redclaw crayfish *Cherax quadricarinatus* (von Martens, 1868) in the contiguous United States. BioInvasions Record 9: 120–126.

Naguib, S. S. I., Sallehuddin, A. S., Kamarudin, A. S., Dali, M. Z. M., Kassim, Z., Lokman, M. I. N. & Ismail, N. (2021). Length weight relationship and condition factor of Australian redclaw crayfish (*Cherax quadricarinatus*) from three locations in Peninsular Malaysia. Bioscience Research 18(SI-2): 413-420.

Naquiddin, A. S., Rahim, K., Long, S., & Firdaus, F. (2016). The spread of the australian redclaw crayfish (*Cherax quadricarinatus* von Martens, 1868) in Malaysia. *Journal of Sustainability Science and Management*, 31-38.

Neculae, A., Barnett, Z. C., Miok, K., Dalosto, M. M., Kuklina, I., Kawai, T., Santos, S., Furse, J. M., Sîrbu, O. I., Stoeckel, J. A., & Pârvulescu, L. (2024). Living on the edge: Crayfish as drivers to anoxification of their own shelter microenvironment. PloS one, 19(1), e0287888.

Nicky, B. (2008). Crayfish Plague. *Australia and New Zealand Standard DiagnosticProcedure.*

Norshida, I., Nasir, M.A.N., Khaleel, A.G., Sallehuddin, A., Idrus, S., Istiqomah, I. & Kamarudin, A. (2021). First wild record of Australian redclaw crayfish Cherax quadricarinatus (von Martens, 1868) in the east coast of Peninsular Malaysia. BioInvasions Records, 10(2): 360-368.

Othman, M. H. & Hashim, A. K. A. (2003). Prevention and management of invasive alien species. Proceedings of a Workshop on Forging Cooperation throughout South-Southeast Asia. *Global Invasive Species Programme, Cape Town, South Africa.*

Pauwels, Kevin, De Meester, L., Put, S., Decaestecker, E. & Stoks, R. (2010). Rapid evolution of phenoloxidase expression, a component of innate immune function, in a natural population of *Daphnia magna. Limnology and Oceanography*, 55(3).

Pliego, M. G., Falcón, J. H., Benitez, E. A., Novoa, R. G., & Pardo, B. F. (1998). Ventral nerve cord transection in crayfish: A study of functional anatomy. *Journalof Crustacean Biology, 18*(3), 449–462.

Rusaini, A. E., Burgess, G. W. & Owens, L. (2013). Investigation of an idiopathic lesion in redclaw crayfish *Cherax Quadricarinatus* using suppression subtractive hybridization. *Journal of Virology & Microbiology*. 2013, 569032.

Sanjar, A., Davis, D. R., & Kline, R. J. (2023). Evidence of an established population of *Cherax quadricarinatus* (von Martens, 1868) in south Texas, USA. BioInvasions Records 12(1): 284–291.

Stentiford, G. D., Bonami, J-R., & Alday-Sanz, V. (2009). A critical review of susceptibility of crustaceans to Taura syndrome, Yellowhead disease and White Spot Disease and implications of inclusion of these diseases in European legislation. *Elsevier*, *291*(1-2), 1-17.

Strand, D. A., Jinnerot, T., Aspán, A., Viljamaa-Dirks, S., Heinikainen, S., Rolén, E., & Vrålstad, T. (2023). Molecular detection of *Aphanomyces astaci* - An improved species specific qPCR assay. Journal of invertebrate pathology, 201, 108008.

Sun, Y., Shan, X., Li, D., Liu, X., Han, Z., Qin, J., Guan, B., Tan, L., Zheng, J., Wei, M., & Jia, Y. (2023). Analysis of the differences in muscle nutrition among individuals of different sexes in redclaw crayfish, *Cherax quadricarinatus*. Metabolites, 13(2), 190.

Suryanto, M. E., Audira, G., Roldan, M. J. M., Lai, H. T., & Hsiao, C. D. (2023). Color Perspectives in Aquatic Explorations: Unveiling Innate Color Preferences and Psychoactive Responses in Freshwater Crayfish. Toxics, 11(10), 838.

Tarun, S. (2021). The Indian Subcontinent – A Cradle of Aquaculture. Retrieved in 2022. https://planet.outlookindia.com/opinions/the-indian-subcontinent-a-cradle-of-aquaculture-news-414480

Torrijos, L. M., Ríos, M. M., Herrero, G. C., Adams, S. B., Jackson, C. R., & Uribeondo, J. D. (2021). Tracing the origin of the crayfish plague pathogen, *Aphanomyces astaci*, to the Southeastern United States. *Scientific Reports*, 11(332).

Unestam, T., & Weiss, D. W. (1970). The host-parasite relationship between freshwater crayfish and the crayfish disease fungus *Aphanomyces astaci*: Responses to infection by a susceptible and a resistant species. *Microbiology*, 77-90.

Victor, S. S., & Pahirulzaman, K. A. K. (2020.) *IOP Conf. Ser.: Earth Environ. Sci.* 596, 012092.

Viljamaa-Dirks, S., & Heinikainen, S. (2019). A tentative new species *Aphanomyces fennicus* sp. nov. interferes with molecular diagnostic methods for crayfish plague. *Journal of Fish Diseases*.

Vrålstad, T., Knutsen, A. K., Tengs, T., & Jensen, H. (2009). A quantitative TaqMan MGB real-time polymerase chain reaction based assay for detection of the causative agent of crayfish plague *Aphanomyces Astaci. Vet Mic*, 146-155.

Walker, P. J., & Mohan, C. V. (2009). Viral disease emergence in shrimp aquaculture: origins, impact and the effectiveness of health management strategies. *Reviews in Aquaculture*. *1*(2), 125-154.

Welsh, J. & McClelland, M. (1990). Fingerprinting genomes using PCR with arbitrary primers. *Nucleic Acid Research*, 18, 7213-7218.

Westman, K. (1991). The crayfish fishery in Finland-its past, present and future. *Finnish Fisheries Research*, 12, 187-216.

World Organisation of Animal Health (OIE). Chapter 2.2.01: Crayfish plague. Manual of diagnostic tests for aquatic animals. Accessed 20-4-2018.http://www.oie.int/fileadmin/Home/eng/Health_standards/aahm/2010/2.2.01_CRAYFISH.pdf

Wong, F. Y. K., Fowler, K. & Desmarchelier, P. M. (1995). Vibriosis due to *Vibrio mimicus* in Australian freshwater crayfish. *Journal of Aquatic Animal Health*, *7*, 284-291.

Yavuzcan, H., Köksal, G., & Gunal, C. (2004). Physiological response of the crayfish, *Astacus leptodactylus* to saline water. *Crustaceana, 77*(10), 1271-1276.

Yuliana, E., Yonvitner, A. S., Subing, R. A., Ritonga, S. A., Santoso, A., Kouba, A. & Patoka, J. 2021. Import, trade and culture of non-native ornamental crayfish in Java, Indonesia. Management of Biological Invasions 12(4): 846-857.

BorneoScience
The Journal of Science & Technology
Volume 45 Issue 2 : Sept 2024
Online ISSN : 2231-9085 | ISSN : 1394-4339

SOIL LOSS PREDICTION USING REVISED UNIVERSAL SOIL LOSS EQUATION (RUSLE) MODEL IN KUNDASANG, SABAH

Aiman Nabila Abdul Malik[1], Baba Musta[1], Sahibin Abd Rahim[1] & Hennie Fitria W.S.E[1]

[1]Geology Program, Faculty of Science and Natural Resources (FSSA), Universiti Malaysia Sabah (UMS), Jalan UMS, 88400 Kota Kinabalu, Sabah, Malaysia

Corresponding author: babamus@ums.edu.my

Received 22th July 2024; Accepted 28th Nov 2024
Available online: December 2024
Doi: https://doi.org/10.51200/bsj.v45i2.5881

ABSTRACT. *Soil erosion poses a significant environmental issue in Kundasang, Sabah, which is situated in the highlands and is recognized for its soil erosion challenges. The natural forces of water gradually wear away the topsoil of fields, leading to soil erosion. This phenomenon is often exacerbated by various triggering factors such as agricultural practices, deforestation, and unsustainable development. The region is particularly noted for its temperate vegetable cultivation. This study aimed to spatially estimate potential soil loss or erosion using the Revised Universal Soil Loss Equation (RUSLE) model. The RUSLE model incorporates six parameters, all expressed quantitatively in an equation to calculate soil erosion for a specific area. These parameters include rainfall erosivity (R), soil erodibility factor (K), slope length and steepness factor (LS), cultivation and management factor (C), and conservation support practice factor (P). The analysis leverages databases of soil types, topography, land use, and precipitation. The results indicate that only 3.11% (271.92 ha) and 0.72% (62.51 ha) of the study area is categorized as having high and very high erosion potential, respectively.*

KEYWORDS: Erosion, GIS, Kundasang, Soil loss, RUSLE model

INTRODUCTION

Soil erosion is a significant global issue that warrants serious attention. In highland regions, soil erosion involves the detachment and displacement of soil material. This process results in the contamination of rivers, streams, and groundwater with pesticides, fertilizers, and other harmful agricultural pollutants (Gallaher and Hawf, 1997). Erosion can occur naturally or be accelerated by human activities. The rate of erosion varies considerably based on the area's topography and prevailing weather conditions (Hagen, 1991; Nyakatawa *et al*., 2001). It is often linked to multiple triggering factors, including unsustainable agricultural practices, deforestation, and development, which lead to the depletion of natural resources and adversely impact the long-term productivity of the land (Roslee and Sharir, 2018). Furthermore, soil erosion can lead to events such as landslides and flooding, negatively affecting the environment through issues like deteriorating water quality, road damage, land degradation, and increased sedimentation in rivers (Almouctar *et al*., 2021).

Kundasang, situated in the State of Sabah at the base of Mount Kinabalu, is a prominent region in Malaysia known for its highland vegetable farming. With an elevation exceeding 1,000 meters above sea level, Kundasang is categorized as mountainous (Gasim *et al*., 2009). The area produces a variety of vegetables, with a particular focus on five key types: carrots, spring onions, tomatoes, lettuce, and cabbage. Income pattern analyses indicate that increasing the area planted and the use of fertilizers could enhance vegetable income (Fujimoto & Miyaura, 2002). Nevertheless, large-scale vegetable cultivation and the excessive application of chemicals beyond recommended levels adversely affect downstream water resources, particularly the Liwagu River and the Labuk drainage system. These adverse effects include changes in water flow, increased sediment loads, and residues from agricultural chemicals (Sinun & Douglas, 1998; Sahibin *et al*., 2020). Erosion in vegetable fields, particularly along access tracks and on newly prepared beds, worsens these problems, especially when beds are oriented parallel to slopes, contrary to optimal agricultural practices for highland farming (Malaysian Standard, 2007).

Various erosion prediction models have been developed to calculate and estimate soil erosion rates. The Universal Soil Loss Equation (USLE) determines the average soil erosion rate by taking into account factors such as soil type, rainfall patterns, crop management techniques, and topography (Fadzilah *et al*., 2019). The Revised Universal Soil Loss Equation (RUSLE) is an improved version of the USLE, which incorporates significant modifications including adjustments to rainfall data for particular locations, improvements to the soil erodibility factor, alterations to slope length and steepness, and specific updates to the cover management factor (Renard et al., 1997). In this study, the Revised Universal Soil Loss Equation (RUSLE) model was employed to estimate the average annual spatial soil loss in Kundasang area.

DESCRIPTION OF STUDY AREA

Kundasang is situated between the latitudes of 05°52'0" N and 06°5'0" N, and the longitudes of 116°33'0" E and 116°40'0" E. The primary geological composition of the study area includes ultrabasic rocks, particularly serpentinized peridotite, which forms part of the ophiolite basement. Additionally, it features sedimentary rock formations such as the Trusmadi Formation (dating back to the Paleocene and Eocene periods) and the Crocker Formation (from the Late Eocene). A significant portion of the landscape is covered by Pinousuk Gravel, which was deposited during the Pliocene to Pleistocene epochs (Colennette, 1958). The Crocker Formation is defined by four main lithological types: slumped deposits, red and dark shales, thick-bedded sandstones, and thin-bedded sandstones. It is characterized by its monotonous rock facies, alternating layers of sandstone and shale, along with isoclinal folding and faults. Statistical evaluations of various structural features and aerial photographs have highlighted these rugged textures (Kasama *et al*., 1970; Roslee, 2020).

The Trusmadi Formation, located around the Mount Kinabalu and Ranau regions, comprises four key lithological units: thick sandstones, cataclastics, interbedded sandstone and shale (turbidites), and shale. This formation is notable for its alternating layers of dark shale and sandstone that include numerous quartz veins, with some rock units showing signs of low-grade metamorphism (Jacobson, 1970). Pinousuk Gravel is a tilloid deposit made up of granite boulders embedded in a matrix of mud and sand, transported by glacial activity from Mount Kinabalu and its vicinity (Colennette, 1958). The sedimentary rocks consist of angular to rounded clasts set within a light

brown to red-brown matrix of sandy, clayey, and silty materials (Hennie *et al*., 2019; Roslee, 2020). Pinousuk Gravel is primarily found in three main locations to the south and west of Mount Kinabalu: the Pinousuk Plateau, Tohubang Valley, and near Tenompok. The outcrops along the Tawaras River, Mantaki River, Mesilau River, and Bambangan River, which flow through the Pinousuk Plateau from east to south, serve as the type section. Based on the materials' roundness, size, and sphericity, Pinousuk Gravel can be categorized into two units: the Lower Unit and the Upper Unit (Jacobson, 1970; Tjia, 1974; Liew & Gue, 2001).

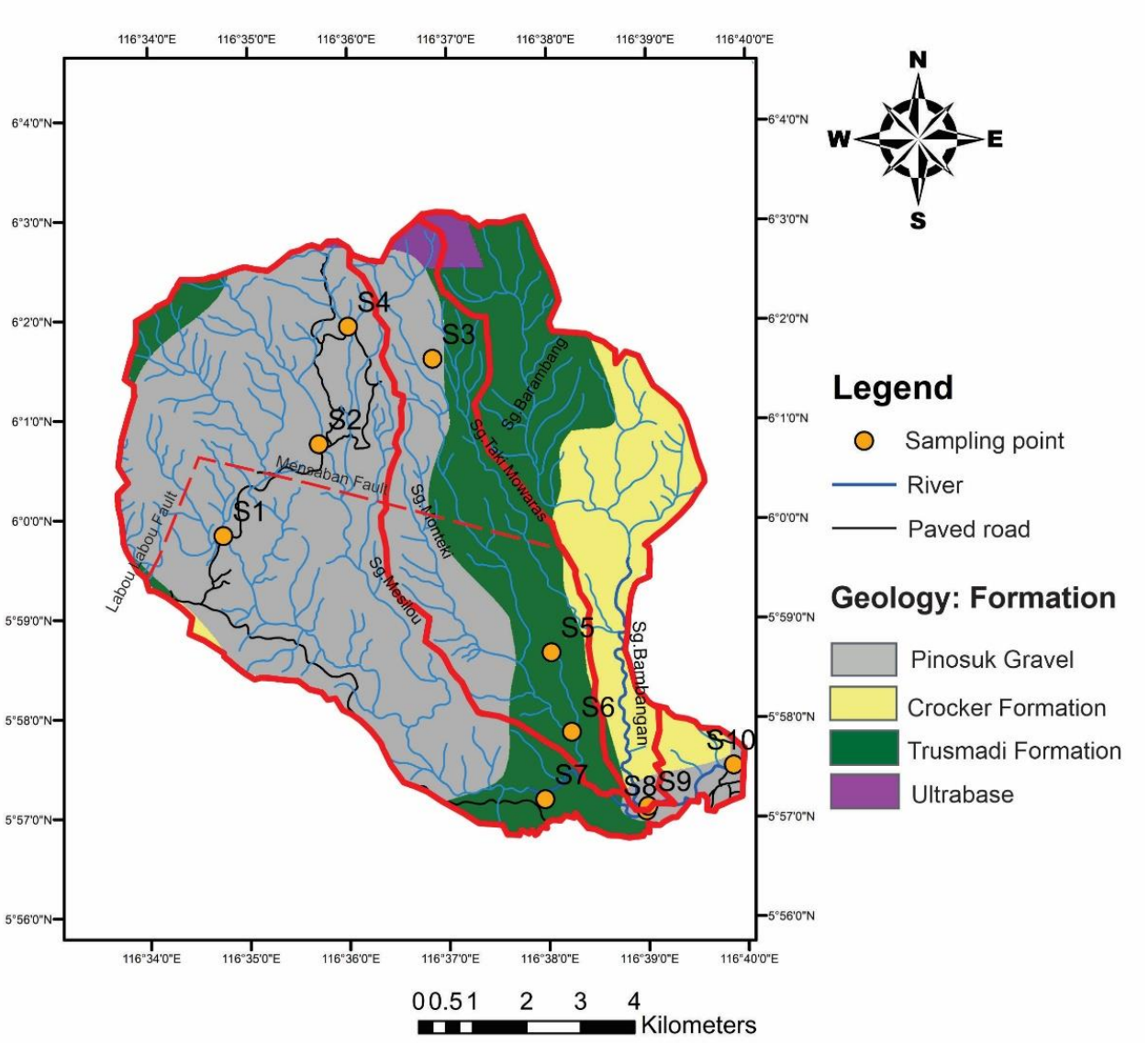

Figure 1. General geological map of the study area

MATERIALS AND METHODS

In the analysis of soil erosion, ArcGIS 10.8 software is utilized to enhance the study's accuracy. This research integrates Geographic Information System (GIS) applications with the Revised Universal Soil Loss Equation (RUSLE) model to estimate soil loss in specific locations (Yusof *et al*., 2019). The model considers five critical factors: the Rainfall Erosivity factor (R), the Soil Erodibility factor

(K), the Slope Length and Steepness factor (LS), the Cultivation and Management factor (C), and the Conservation Support Practice factor (P). These factors are combined to formulate an equation for predicting soil loss, which is presented in Equation 1 below:

$$A = R \times K \times LS \times C \times P \quad (1)$$

Where A is the mean annual soil loss per unit area (ton ha^{-1} yr^{-1}); R is the rainfall erosivity factor (MJ mm ha^{-1} h^{-1} yr^{-1}); K is the soil erodibility factor (ton h^{-1} MJ^{-1} mm^{-1}); slope length and steepness produce LS factor; C is cultivation and management factor; and P is the conservation support practices factor.

The preliminary assessment suggests that Road 1 is the most preferred choice, followed by Road 3, while Road 2 is the least preferred option. It is important to highlight that the score differences between Road 1 and Road 3 are relatively minor. The scoring provides a broad evaluation of the unmitigated environmental impacts of each alignment in relation to site-specific conditions. Consequently, any alternative can be chosen, provided that the proposed mitigation measures are considered and put into practice. These measures are designed to reduce the project's impacts and support sustainable development objectives.

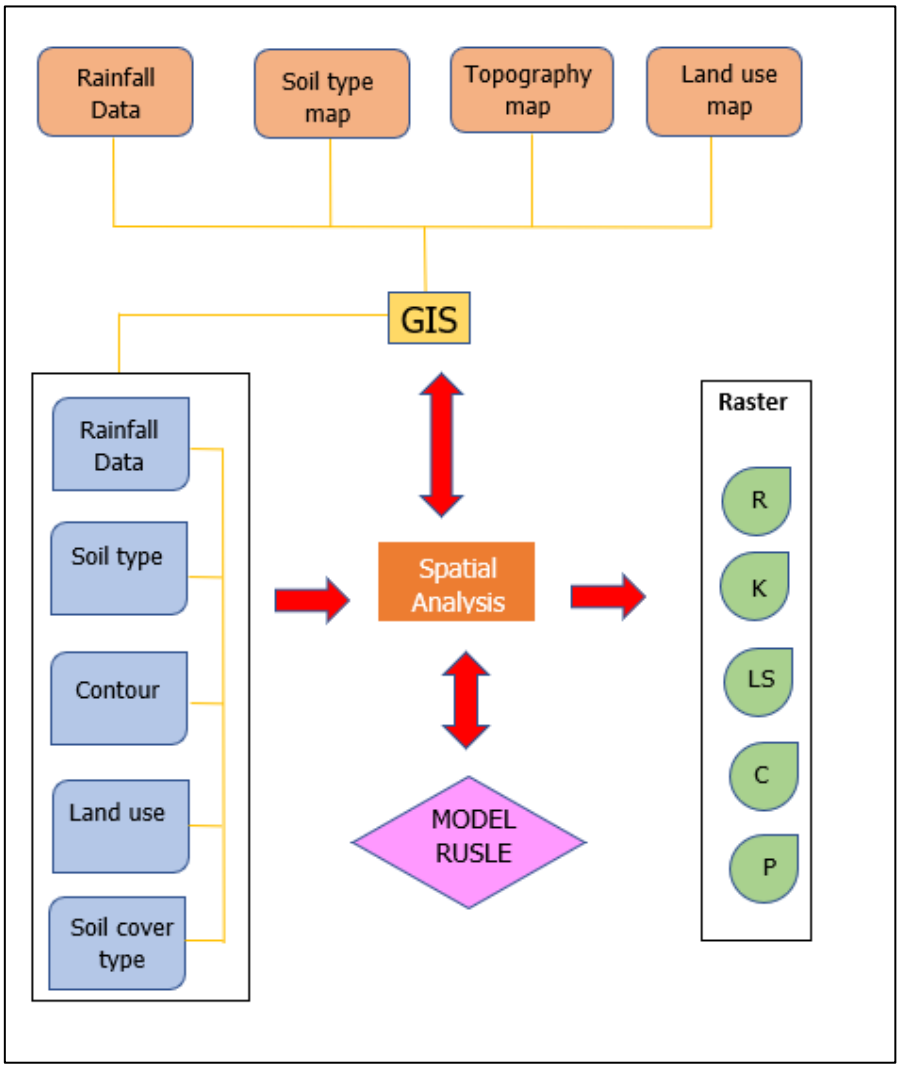

Figure 2. Flow chart for modelling soil erosion (Modified from Roslee *et al.,* 2017)

i. Rainfall Erosivity Factor (R)

Erosivity, which gauges the capability of rainfall to detach soil particles, is a crucial factor in evaluating soil erosion. It influences how rainwater penetrates the soil surface and subsequently generates surface runoff, which in turn affects the rate of soil erosion (Morgan *et al*., 1998; Rasooli, 2022). The erosivity factor is dependent on both the intensity and amount of rainfall. To assess this factor, precipitation data is utilized. Monthly rainfall data (in mm) from 2010 to 2019 was acquired from the Malaysian Meteorological Department in Sabah. The Equations 2 and 3 proposed by Roose (1977) and Morgan (2005) were employed, with the best estimates (Equation 4) taken as the final results.

$$R_M = \frac{[(9.28P - 8838.15) \times (75)]}{100} \quad (2)$$

$$R_R = 0.5\ P\ \times 17.3 \quad (3)$$

$$\text{Best estimation, } R_{MR} = \frac{(\text{Morgan} + \text{Roose})}{2} \quad (4)$$

P denotes the average annual precipitation for the study area. The mean annual rainfall recorded at each rainfall station is documented in the GIS file attributes. Subsequently, to create continuous raster rainfall data for the study area (Figure 3), the mean annual rainfall was computed using the interpolated rainfall data through the Inverse Distance Weighting (IDW) method.

ii. Soil Erodibility Factor (K)

The soil erodibility factor, K, represents both the amount and rate at which soil influences runoff, as well as its inherent susceptibility and resistance to erosion. Factors such as organic content, permeability, soil structure, and soil texture are utilized to determine the K factor. Soil maps for the study area were sourced from the Sabah Department of Agriculture. All data were documented in spatial vector format within attribute tables and subsequently converted to spatial raster format using conversion tools. The K factor was calculated in SI units using the Equation 5 below (Tew, 1999):

$$K = \frac{[1.0 \times 10^{-4}\ (12 - \%\text{OM})(\text{M})^{1.14} + 4.5\ (\text{S} - 3) + 8.0\ (\text{P} - 2)]}{100} \quad (5)$$

In this equation, K represents the soil erodibility factor (to convert it to SI units, this equation is divided by 7.59); OM denotes the percentage of organic matter; M indicates the product of the primary particle size fractions [(% modified silt or the 0.002-0.1 mm size fraction) multiplied by (% silt + % sand)]; S refers to the soil structure; and P signifies hydraulic conductivity. The calculated K factor values are presented in Table 1.

Table 1. Soil series with soil erodibility factor

Soil series	Lithology (Geological Formation)	K value (ton h^{-1} MJ^{-1} mm^{-1})
Bidu-Bidu	Ultrabasic Rock	0.019
Pinosuk	Pinousuk Gravel	0.006
Crocker	Crocker Formation	0.013
Trusmadi	Trusmadi Formation	0.032
Labau	Alluvium	0.021

(Source: Sabah Department of Agriculture, 2021)

iii. Slope Length and Steepness Factor (LS)

The contour topographical map of the Sg Liwagu basin, along with the digital elevation model (DEM) derived from a USGS satellite image at a resolution of 30 meters, is utilized to calculate the slope length and steepness, also known as the LS factor, for the study area. L represents the distance from the point where surface flow initiates to the location where runoff converges into a channel or where the slope gradient decreases, leading to the deposition of eroded sediments. S is evaluated using both percentage and angle measurements (Coote, 2002). The calculation for the LS factor is outlined in Equation 6, where L represents the slope length (in meters) and S denotes the slope angle (in percentage).

$$LS = (0.065 + 0.046S + 0.065S^2) \times \sqrt{L/22.13} \quad (6)$$

iv. Cultivation and Management Factor ©

The Cultivation and Management Factor © serves as an indicator of the effectiveness of soil and crop management practices in preventing or reducing soil erosion (Shelton, 2002). Known as the soil loss ratio, the C factor quantifies the amount of soil erosion from the surface caused by a specific plant over a continuous duration until the soil becomes exposed. This ratio directly correlates with land use type and its effects on the rate of soil erosion (Wischmeier & Smith, 1978). The C value is affected by management practices, the presence of soil cover, and protective growth during rainfall, all of which can contribute to erosion (Roslee & Sharir, 2019). The land use map was sourced from the Sabah Department of Agriculture. The C value is assessed based on the land use types within the study area, and C factors were assigned to each land use class according to recommendations from the Department of Irrigation and Drainage (DID, 2010). After the digitizing process, all data were converted from vector to raster format.

V. Conservation and Support Practices Factor (P)

The P factor measures the effectiveness of erosion control practices and is affected by the cover management factor (Vliet, 2002). It reflects the management strategies implemented in the study area. Depending on the land management activities in the region, P values range from 0 to 1. These P values are established based on the updated land use types and the variables suggested by the Department of Irrigation and Drainage (DID, 2010).

RESULTS AND DISCUSSION

The soil erosion rate in the Liwagu River basin was assessed by integrating the erosion factors from the Revised Universal Soil Loss Equation (RUSLE) model into Geographic Information System (GIS) software. The calculated R value for the Liwagu River basin falls between 19,000 and 21,000 $MJ.mm.ha^{-1}.h^{-1}.yr^{-1}$. It was found that the northwest region of the study area exhibits the highest rainfall erosivity (21,000 $MJ.mm.ha^{-1}.h^{-1}.yr^{-1}$), indicating this area receives significantly more rainfall compared to other regions in the basin.

The basin contains five distinct soil types: Bidu – Bidu (Ultrabasic Rock), Labau (Alluvium), Crocker (Crocker Formation), Trusmadi (Trusmadi Formation), and Pinousuk (Pinousuk Gravel), each with varying K factor values (Table 1). Pinousuk soil is the most prevalent, covering 67.77% (6,218.06 ha) of the total area, followed by Trusmadi at 14.61% (1,340.41 ha), Crocker at 9.49% (870.62 ha), Bidu-Bidu at 6.79% (622.82 ha), and Labau at only 1.35% (123.83 ha). The K factor values in the area range from 0.006 to 0.032 $ton.ha^{-1}.h^{-1}.MJ^{-1}.mm^{-1}$, with an average K factor of 0.018 $ton.ha^{-1}.h^{-1}.MJ^{-1}.mm^{-1}$.

The sand content in the soil varies from 26% to 67%, clay ranges from 23% to 64%, and silt is between 3% and 51%. The soil structure codes in this area range from 3 to 4, and permeability scales vary from 3 to 4. Sandy soil, due to its high infiltration rate, is less prone to transport; in contrast, silt loam soil is more easily eroded, while clay soil tends to remain cohesive (Anees *et al*., 2018). Clay soils demonstrate resistance to detachment because they form stronger structures (Roslee, 2019), resulting in lower K values that range from 0.05 to 0.15. Likewise, coarse-textured soils, like sandy soils, generally have low K values between 0.05 and 0.2. The low K values for sandy soils are attributed to the reduced surface runoff expected when good infiltration conditions exist, despite their susceptible nature. Soils with high silt content are the most erodible due to their weak structure, making them easily detached and prone to collapse, which can obstruct surface soil pore spaces and lead to surface runoff. Specifically, soil with over 40% silt is highly vulnerable to erosion, while clay soils exceeding 30% clay content show significant resistance to erosion (Morgan, 2005; Roslee, 2019). Among the four soil types, Trusmadi has the highest K value at 0.032 $ton.ha^{-1}.h^{-1}.MJ^{-1}.mm^{-1}$, while Pinousuk, with its high sand content, presents a low K value of 0.006 $ton.ha^{-1}.h^{-1}.MJ^{-1}.mm^{-1}$ (Table 1).

Overall, an increase in both slope length and steepness contributes to a higher rate of soil erosion. Consequently, the LS factor is crucial as it measures the impact of topography and terrain on erosion occurrences. The LS map (Figure 3C) demonstrates that as slope steepness decreases, the potential for soil loss diminishes. In the study area, slopes tend to increase with elevation. LS values in this region range from 0 to 416.18, with the majority falling between 0 and 12, indicating that the slopes are slightly to moderately sloped. The influence of the LS factor in the study area is evident, as a significant portion shows a low potential for soil loss. Asmamaw and Mohammed (2019) found that on steeper slopes, the velocity and volume of surface runoff increase, significantly elevating the risk of soil erosion.

The land cover factor C and the erosion management practice P are interconnected. The C factor represents the land cover in the area, while P reflects the specific erosion management strategies

employed. Factors influencing the C value include management practices, soil cover, and protective growth. The study area comprises six distinct land cover categories: urban area, scrubland, agricultural land, grassland, cleared land, and forest. Forests, which account for approximately 44% of the Liwagu River Basin, exhibit low C and P values, indicating minimal susceptibility to erosion. The dense canopy in forested areas reduces the risk of erosion, thereby protecting the soil from rapid loss. The P values depend on the land management practices within the study area and range from 0 to 1. The C and P factors were estimated following the guidelines of Morgan (2005) and the Department of Irrigation and Drainage (DID, 2010) (Table 2), with a C value of 0.39 for forests and 0.5 for agricultural areas. The P values are 0.1 for forested areas and 1 for urban areas. Practices such as contour farming and other agricultural methods can significantly mitigate soil erosion.

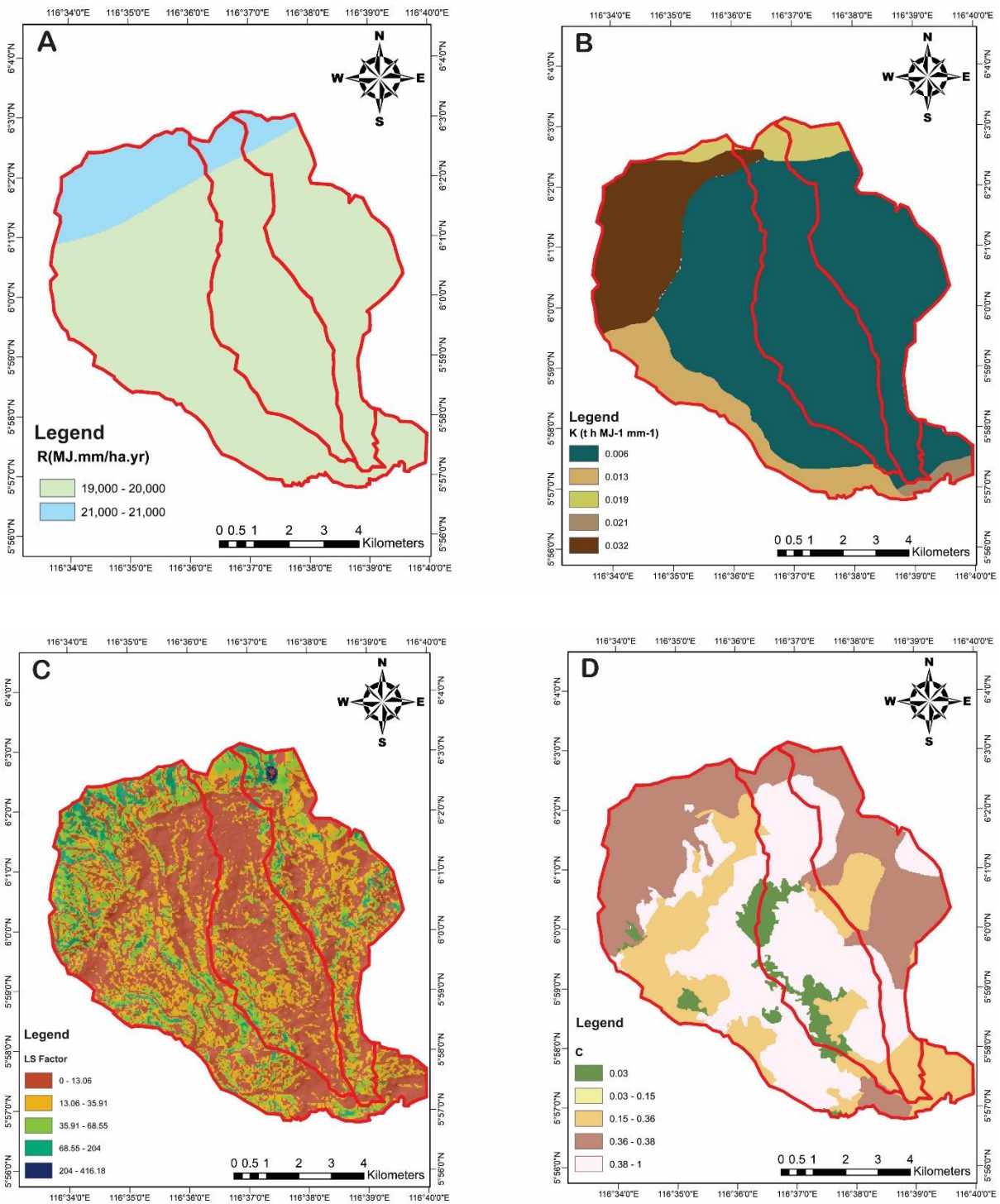

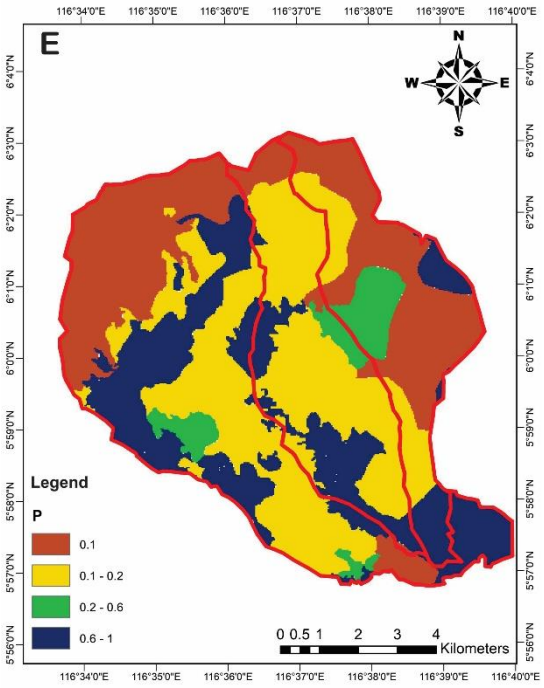

Figure 3. A) Rainfall erosivity factor (R), B) Soil erodibility factor (K), C) Slope length and steepness factor (LS), D) Cover management factor, E) Support practice factor (P)

Table 2. C and P factors for the land use map

Land Use	C factor	P factor
Urban Area	0.15	1
Scrub	0.35	0.2
Agriculture	0.38	0.14
Grassland	0.03	0.6
Cleared Land	1	1
Forest	0.01	0.1

Sources: DID (2010) and Morgan (2005)

The total value of A was calculated and categorized according to the soil erosion risk classification established by the Department of Irrigation and Drainage (DID, 2010). An assessment of potential soil erosion in the Ranau area, utilizing the RUSLE erosion model, indicated that the soil erosion risk class categorized as extremely high (>150 ton/ha/yr) accounts for approximately 4.7 – 9.66% of the Ranau area (Rendana et al., 2014; Roslee and Sharir, 2018). This finding was observed in the western part of Ranau, covering the highland regions of Tudan, Kundasang, Bundu Tuhan, and extending southward to the Nampasan area.

In this study, it was found that the Liwagu River basin has annual average soil erosion rates distributed as follows: 58.91% (5,150.71 ha) classified as very low risk, 27.63% (2,415.25 ha) as low risk, 9.63% (841.98 ha) as moderate risk, 3.11% (271.92 ha) as high risk, and 0.72% (62.51 ha) as very high risk (Table 3). The estimated annual potential soil loss for the basin ranges from 0 to 11,323.6 (ton/ha/year) (Figure 4). It is noteworthy that approximately 86.54% of the Liwagu River Basin is categorized within the very low to low erosion risk levels, indicating that the overall erosion

conditions in the basin are effectively managed. The prevalence of low to very low erosion risk can likely be attributed to the extensive forest coverage and the predominantly gentle slope topography throughout much of the area.

Table 3. Average annual soil erosion rate

Class of Average Soil Loss Risk	Risk Level	Area (ha)	Soil Loss (%)
Very Low	Very Low	5150.71	58.91
Low	Low	2415.25	27.63
Moderate	Moderate	841.98	9.63
High	High	271.92	3.11
Very High	Very High	62.51	0.72
Total		**8742.37**	**100**

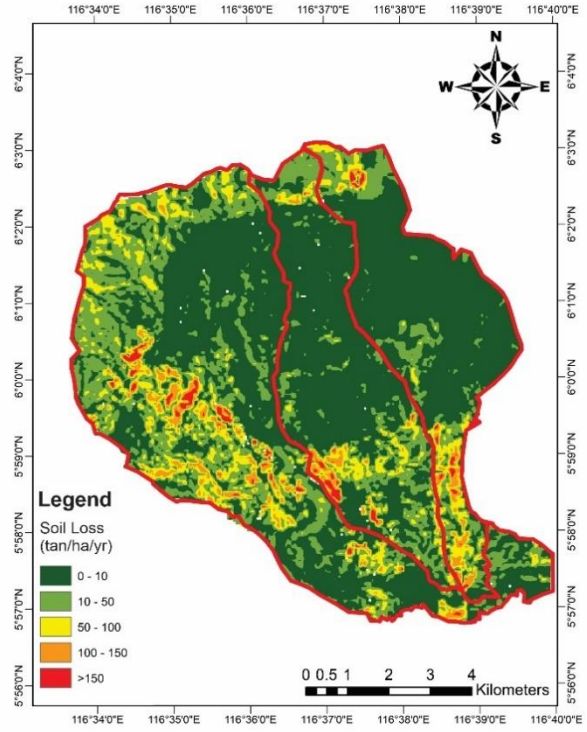

Figure 4. Average annual soil loss map (A) of the study area

CONCLUSIONS

According to the GIS-integrated RUSLE equation prediction model, the majority of the erosion potential in the Liwagu Basin is classified as very low risk and low risk, comprising 86.54% of the area, which equates to 7,565.96 ha. Conversely, only 3.83% of the basin is categorized as having a very high or high risk of erosion. The primary source of erosion in the area is attributed to newly opened agricultural land. While the potential soil loss remains low at present, any future plans for agricultural development or clearing of forested areas in the basin should take into account the potential for increased erosion. Additionally, it is crucial to conserve soil to prevent direct erosion

effects, particularly from ultrabasic soils, which could contaminate surface areas, river water, and groundwater. Further research is recommended to enhance these findings and to devise context-specific strategies for erosion mitigation in Kundasang. Effective planning can help protect the well-being of the highland agricultural area while also preserving the health of the surrounding environment.

ACKNOWLEDGEMENT

Deepest appreciation to Universiti Malaysia Sabah (UMS) for the award of research grant SDN0037-2019 and GUG0388-2/2019. All laboratory work has been done in the Faculty of Science and Natural Resource, Universiti Malaysia Sabah.

REFERENCES

Anees, M.T., Abdullah, K., Nawawi, M.N.M., Norulaini, N.A.N., Syakir, M.I. & Omar, A.K.M. 2018. Soil erosion analysis by RUSLE and sediment yield models using remote sensing and GIS in Kelantan state, Peninsular Malaysia. *Soil Research* 56(4); 356-372.

Asmamaw, L.B. & Mohammed, A.A. 2019. Identification of soil erosion hotspot areas for sustainable land management in the Gerado catchment, North-eastern Ethiopia. *Remote Sensing Applications: Society and Environment* 13: 306-317.

DID, 2010. Guideline for Erosion and Sediment Control in Malaysia, Kuala Lumpur. Department of Irrigation and Drainage.

Gassim, M.B., Surif, S., Toriman, M.E., Abd Rahim, S., Elfithri, R. & Pan, I.L. 2010. Land Use Change and Climate Change of the Cameron Highlands, Pahang, Malaysia. 4th International Congress of the Islamic World Geographers (ICIWG2010). University of Sistan and Baluchestan, Zahedan.

Fujimoto, A. & Miyaura, R. 2002. Farm Management Study of Highland Vegetable Cultivation in Sabah, Malaysia: Farm Questionnaire Survey in Kundasang Area. *Journal of Agricultural Science*, 47 (2): 111-119 - Tokyo Nogyo Daigaku (Japan). ISSN: 0375-9202.

Gallaher, R.N. & Hawf, L. 1997. Role of conservation tillage in production of a wholesome food supply. In: Gallaher, R.N. (Ed.), Proceedings of the 20th Annual Southern Conservation Tillage for Suistanable Agriculture, University of Florida, Gainesville, FL, USA, June 24-26, pp. 23-27.

I.J.P. Van Vliet. 2002. RUSLEFAC – Revised Soil Loss Equation for Application in Canada: A Handbook for Estimating Soil Loss from Water Erosion in Canada. Research Branch, Agriculture and Agri – Food Canada. Ottawa. Contribution No. AAFC/AAC2244E. 117pp.

Malaysian Standard. 2007. MS 1784-7: *Good Agricultural Practice (GAP) – Fruits and Vegetables.* Department of Standard Malaysia. Cyberjaya, Selangor.

Morgan R, Quinton J, Smith R, Govers G, Poesen J, Auerswald K, CHisci G, Torri D and Styczen M. 1998. The European Soil Erosion Model (EUROSEM): A dynamic approach for predicting sediment transport from fields and small catchments; *Earth Surf. Earth Surf. Process. Landf*. 23 527-544.

Morgan, R.P.C. 2005. Soil Erosion and Conservation. New York: Wiley.

Noor Fadzilah Yusof, Tuklimat Lihan, Wan Mohd Razi Idris, Zulfahmi Ali Rahman, Muzzneena Ahmad Mustapha & Mohd. Abdul Wahab Yusof. 2019. Prediction of Soil Erosion in Pansoon Sub-Basin, Malaysia using RUSLE integrated in Geographical Information System. Sains Malaysiana 48 (11) (2019): 2565-257.

Nyakatawa, E.Z & Reddy, K.C & Lemunyon, J.L. 2001. Predicting soil erosion in conservation tillage cotton production systems using the Revised Universal Soil Loss Equation (RUSLE). Soil and Tillage Research. 57. 213-224. 10.1016/S0167-1987(00)00178-1.

R Roslee and K Sharir. 2018. Intergration of GIS – Based RUSLE Model for Land Planning and Environmental Management in Ranau Area, Sabah, Malaysia. ASM Sc.J., 12, Special Issue 3, 2019 for ICST2018, 60 – 69.

R Roslee and K Sharir. 2019. Soil Erosion Analysis using RUSLE Model at Minitod Area, Penampang, Sabah, Malaysia. 12th Seminar on Science and Technology. *J.Phys : Conf. Ser.* 1358 012066. IOP Publishing.

Rendana, M., Sahibin, A.R., Idris, W.M.R., Zulfahmi, A.R. & Tukimat, L. 2014. GIS and NDVI Application for Soil Erosion Potential Modelling Using RUSLE Method in Ranau District, Sabah. Proceeeding of The Soil Science Conference of Malaysia 2014. Putra Palace, Kangar Perlis, 8 – 10 April. Pg 104 – 107.

Roose, E.J. 1977. *Application of the Universal Soil Loss Equation of Wischmeier and Smith in the West Africa*. London: Wiley.

Sahibin Abd Rahim, Ng Siuw Sing, Diana Demiyah Mohd Hamdan, Junaidi Asis, Hennie Fitria Wulandari Soehadi Erfen, Nur Zaida Zahari, Baba Musta. 2022. Properties of Cultivated Soil from Mesilou-Kundasang Agricultural Area. *Transactions on Science and Technology* Vol. 7, No. 4, 213 – 218.

Sidi Almouctar, M.A.; Wu, Y.; Zhao, F.; Dossou, J.F., **2021**. Soil Erosion Assessment Using the RUSLE Model and Geospatial Techniques (Remote Sensing and GIS) in South-Central Niger (Maradi Region). *Water 13*, 3511. https://doi.org/10.3390/w13243511.

Sinun, W. & Douglas, I. 1998. Impact of Conversion of Upland Forest to Tourism and Agricultural Land Uses in the Gunung Kinabalu Highlands, Sabah, Malaysia. In: Kalvoda, J., Rosenfeld, C.L. (eds) Geomorphological Hazards in High Mountain Areas. *The GeoJournal Library*, vol 46. Springer, Dordrecht. https://doi.org/10.1007/978-94-011-5228-0-7.

Tew, K.H. 1999. Production of Malaysian Soil Erodibility Nomograph In Relation to Soil Erosion Issues. Soil Erosion Research and Consultancy.

Wall. G.J., D.R. Coote, E.A. Pringle & I.J. Shelton. 2002. RUSLEFAC – Revised Soil Loss Equation for Application in Canada: A Handbook for Estimating Soil Loss from Water Erosion in Canada. Research Branch, Agriculture and Agri – Food Canada. Ottawa. Contribution No. AAFC/AAC2244E. 117pp.

Wischmeier, W.H. & Sminth, D.D. 1978. *Predicting Rainfall Erosion Losses: Guide to Conservation Planning*. Vol. 53.